ulm university universität
uulm

Abteilung Neurobiologie

Navigieren und Laufen bei *Cataglyphis* Wüstenameisen:

Virtuelle Wegintegration auf einer Laufkugelapparatur und vergleichende Kinematikanalyse der Lokomotion

Dissertation

zu Erlangung des Doktorgrades ***Dr. rer. nat.***
der Fakultät für Naturwissenschaften der Universität Ulm
vorgelegt von

Verena Luisa Wahl

aus Hechingen

Ulm 2016

Amtierender Dekan:

Prof. Dr. Peter Dürre

Gutachter:

Prof. Dr. Harald Wolf

Prof. Dr. Manfred Ayasse

Betreuer:

Dr. Matthias Wittlinger

Prof. Dr. Harald Wolf

Tag der Abgabe:

03.11.2016

Tag der Verteidigung:

20.12.2016

Inhaltsverzeichnis

Abstract

The fascinating navigation behaviour of insects has engaged scientists for several decades – particularly in the model organism *Cataglyphis. Cataglyphis* desert ants are famous for their fascinating navigational performance. They are able to navigate by means of path integration as a sort of vector navigation. For this purpose, they integrate angels steered and distances travelled of individual path segments to integrate a home vector. This allows the animals at any time of their outbound run to return directly to their nest. The heading direction is determined predominantly by the polarization pattern of the sky as a celestial compass cue. To estimate the distance, two parameters are known that are essential for path integration – the optic flow and the stride integrator that accounts for stride number and the respective length. Contrary to the well-studied compass cue, the cue that provides the path integrator with distance information is still not fully understood. Nonetheless, locomotion is a fundament of distance estimation while integrating a path. Besides, a reduction of the time spent outside the nest is indispensable for survival while foraging in the extreme and unpredictable biotope of the desert. Fast locomotion of these long-legged desert ants thus prevents them from becoming a victim of heat stress or enemies.

In the first part of this thesis (Kapitel 3) we present a newly improved spherical treadmill developed by Dr. Hansjürgen Dahmen, Tübingen. This spherical treadmill allows us to study complex naturalistic orientation behaviour in tethered animals in the laboratory and outdoors in the field. The spherical treadmill detects the motion of the animal via optical mouse sensors equipped with long focal-length lenses. We have also implemented an optimized form of tethering which allows the animals to adjust their body posture and to freely rotate around their yaw axis. This enables the treadmill to function as a natural closed loop system.

Cataglyphis desert ants, a model system for navigation research, were challenged to perform a navigation task on the spherical treadmill in the laboratory and in the field. We can show that the ants are able to perform a complex behaviour like path integration on the spherical treadmill set-up which does not differ significantly from the open field experiments. This does not only emphasizes the functionality of our improved system but in particular proves that we are for the first time able to analyse the desert ants' navigation behaviour spatially and temporally in very high resolution and along the entire walking trajectory (most runs are longer than 30m). The improved spherical treadmill system will be of broad interest, not just to the navigational communities, but to those interested in studying complex naturalistic behaviour in a sophisticated, detailed and more controllable way. In the case of navigation research in *Cataglyphis* ants, our quite simple set-up is a breakthrough that enables us to study navigation and all sorts of complex interactions such as panoramic vision, landmark navigation, the use of local and global

vectors and also the much disputed use of cognitive maps in a highly controlled way. This is a further step towards the understanding of the fascinating navigation behaviour of these ants.

The second part of this thesis (Kapitel 4-6) deals with the locomotion and inter-leg coordination of *Cataglyphis* ants as a fundament of distance estimation while integrating a path. Since the stride integrator is apposed to be the major source for errors occurring during path integration, a detailed analysis of the robust but flexible locomotion and the inter-leg coordination along the entire speed range is required.

Usually, during forward locomotion (Kapitel 4) the *Cataglyphis fortis* ants use tripod coordination almost over the entire speed range – only during slow walks, we observed that ants occasionally deviated from tripodal leg coupling. To gain high-speed, the ants commonly increase stride frequency, but mainly stride length, even above their morphological limits. This is possible because the ants perform aerial phases (complete loss of ground contact) when stride frequency reaches its maximum. Tripods and thus stride length proved to be highly constant spatial entities. Thus, the spatiotemporal constancy of this gait pattern may be a general feature used in fast-running desert ants to gauge distances. Tripod as most sufficient mode of walking may reduce odometric errors arising from the iterative process of path integration.

In contrast to this tripod coordination, we observed for the first time backward walking *Cataglyphis* desert ants (Kapitel 5) dragging a heavy food load with rearward locomotion as a natural common behaviour, where each leg acted on its own. The range of flexibility with respect to the ant's inter-leg coordination increased. Additionally, the ants improved their stability while dragging heavy food items, because more than three legs touched the ground and therefor fulfil wobbly movement. In a follow-up paper Pfeffer and Wittlinger (Pfeffer and Wittlinger, 2016) were able to show that the navigational performance of forward and backward walking ants back to the nest does not differ significantly in length. It can thus be concluded that each leg contributes independently to a total distance value for path integration and does not rely on a fairly constant stride pattern. The pedometer most likely remains unaffected by the irregular inter-leg coordination during slow walking speeds and the reversal of the environment cues.

The last part of the thesis investigates the Saharan silver ant *Cataglyphis bombycina* that lives in sand dune habitat (Kapitel 6). These ants are the fastest *Cataglyphis* desert ant species reaching speeds of up to 1 ms^{-1} (100 body length per second). We wanted to examine how these ants are able to achieve such high walking speeds although they have relatively shorter legs than other *Cataglyphis* species. Like *Cataglyphis fortis* they use tripod coordination across the entire walking speed range. Stride length and the stride amplitude increase linearly with walking speed, whereas the stride frequency levels off at a maximum of around 40 Hz. Interestingly *Cataglyphis bombycina* show aerial phases already at speeds of 120 mms^{-1} long before they reach a frequency plateau at a walking speed of 300 mms^{-1}. The ants seem well-adapted to their ecological niche, therefore, reducing stance phase to a minimum of 7 ms and lifting all three legs of one tripod off the ground simultaneously, might prevent them from sinking in the loose sand and allow them to gain higher walking speeds and economical foraging trip.

Kapitel 1

1.1 Die Wüstenameise der Gattung Cataglyphis

Bereits im Jahr 1850 wurde die langbeinige Wüstenameise als „auffälligste Erscheinung der Insektenfauna altweltlicher Trockengebiete“ (Foerster, 1850) beschrieben. Als Bewohner ausgetrockneter Sand-und Steinböden sind sie in vorder- und zentralasiatischen und nordafrikanischen Gebieten zu finden (Wehner, 1983; Lenoir et al., 2009). Ihr arabischer Name حرامي الحلة heißt übersetzt „Dieb des Kochtopfs“ (Harkness und Wehner, 1977). Es ist somit wohl schon lange bekannt, dass diese Tiere sehr gezielt ihre Futterquelle ausbeuten können. Die *Cataglyphis* Wüstenameisen sind dabei ausschließlich solitäre Futtersammler (Dietrich und Wehner, 2003). Bei hohen Temperaturen suchen die tagaktiven Aasfresser den Wüstenboden nach Futter ab, denn die Ameisen ernähren sich hauptsächlich von anderen dem Hitzetod erlegenen Insekten (Wehner, 1983; Wehner und Wehner, 2011). Besonders ist zudem, dass sie keine Pheromonspuren nutzen, um Wege zu Futterquellen anzuzeigen oder andere Ameisen zu rekrutieren – diese flüchtigen Verbindungen würden aufgrund der heißen Temperarturen schnell verdampfen oder bei Anheftung an lose Sandkörner vom Wind verweht werden (Ruano et al., 2000). Da außerdem die toten Insekten klein sind und die Futterdichte gering ist, schließt dies die Notwendigkeit von Pheromonspuren und die Kooperation mehrerer Arbeiterrinnen aus (Wolf und Wehner, 2000). Durch ihre extrem langen Beine vergrößern sie zum einen den Abstand zum Boden (Lenoir et al., 2009), zum anderen sind sie so zu enorm hohen Laufgeschwindigkeiten fähig, welche wiederum eine kühlende Luftströmung produzieren (Konvektion), die es den Tieren erlaubt selbst bei extremen Temperaturen aktiv zu sein (Sommer und Wehner, 2012).

Als thermophile Sammler gehören die Tiere zu den thermotolerantesten Ameisenarten (Cerdá und Retana, 2000; Wehner, 2003). Sie furagieren zu den heißesten Zeiten des Tages. Dabei können sie Temperaturen wiederstehen, die in Bodennähe im Sommer bis zu 50° Celsius betragen (Gehring und Wehner, 1955). Im Laufe der Evolution haben diese erstaunlichen Tiere mehrere Anpassungen an ihren heißen und trockenen Lebensraum entwickelt, denn sie zeigen sowohl physiologische, morphologische- und ethologische Anpassungen (Wehner et al, 1992, Shi et al., 2016). Besonders sind, neben den extrem langen Beinen und der Hitzetoleranz durch Hitzeschockproteine (Gehring und Wehner, 1995) aber vor allem die beeindruckenden Navigationsleistungen der Tiere. Das Überleben jedes Tieres hängt von einem Minimieren der Aufenthaltsdauer außerhalb des Nestes ab. Die Tiere können sich in dem

landmarkenarmen Steppen- und Wüstengelände hunderte von Metern weit weg von ihrem unterirdischen Nestern entfernen (Wehner, 1983), auf verschlungenen Wegen nach Beute jagen und am Ende doch zielgerichtet und geradlinig ihre unscheinbare, kleine Nestöffnung, welche nur ein kleines 1-2 cm großes Loch im Sandboden darstellt, ansteuern (Wehner 1981). Wird ein Tier nach dem Heimlauf am Nesteingang abgefangen und im freien Feld wiederum frei gelassen, so ist sie hoffnungslos verloren und findet nicht mehr heim. Denn sie ist zu jedem Zeitpunkt ihres Auslaufes mit einer Art unsichtbarem Ariadne-Faden an den Ausgangspunkt, das Nest, gekoppelt (Wehner und Wehner, 1990). Über eine Summation von Teilvektoren von Richtung und Distanz ist sie stets über ihre relative Lage zum Ausgangspunkt informiert (Drapser et al., 1960). Diese bemerkenswerte Heimlauffähigkeit minimiert die Aufenthaltsdauer außerhalb des Nestes drastisch und nennt sich Wegintegration (engl: path integration) (siehe dazu Kapitel 1.2) (Mittelstaedt, 1983; Müller und Wehner, 1988, Wehner und Srinivasan, 2003).

Die Versuchstiere *Cataglyphis bicolor*, *Cataglyphis fortis*, *Cataglyphis bombycina* und ihr Habitat

Diese erstaunliche Navigationsleistung der Wegintegration, wie sie erstmals bei Bienen entdeckt wurde (von Frisch, 1950), wurde bei den *Cataglyphis* Ameisen zuerst bei ***Cataglyphis bicolor*** (FABRICIUS, 1793) erforscht (Wehner und Menzel, 1969). Das Habitat von *Cataglyphis bicolor* liegt in ariden Gebieten Nordafrikas, Südeuropas, Asien und dem Vorderen und Mittleren Orient. Sie bevorzugen mikroklimatisch betrachtet eher feuchtere Standorte (Dietrich und Wehner, 2003). Die Tiere haben eine Alitrunklänge von 2.1-4.95 mm (berechnet nach Sommer und Wehner, 2012). Sie leben monogyn (eine Königin) und polydom (mehrere unterirdische Nester). Die Kolonie besteht folglich aus einem Hauptnest, mit Königin, und mehreren Satellitennestern (Dillier und Wehner, 2004). Dazwischen findet ein reger Austausch von Eiern, Larven, Puppen, Futter und auch von Arbeiterinnen statt (für den Transport von Arbeiterinnen möchte ich hier auch auf Pfeffer und Wittlinger, 2016 verweisen).

Aufgrund der verhältnismäßig struktur- und objektreichen Umgebung rückte später auch ***Cataglyphis fortis*** (FOREL, 1902) in den Fokus der Forschung (u.a. Wehner 1983). Denn *Cataglyphis fortis* (siehe Abb. 1) bewohnt ausschließlich die lebensfeindlichen salzigen Chotts (Salzseen, die im Sommer austrocknen) und Sebkkhas (abflusslose flache Becken) in Tunesien und Nordalgerien, die in den Wintermonaten regelmäßig mit Meer- oder Süßwasser überflutet werden. Diese häufig ebene, struktur- und objektarme Umgebung eignet sich hervorragend für Beobachtungen und Versuche, in der die Tiere in Hinblick auf die Navigation unter extremen Bedingungen agieren müssen. Auch *Cataglyphis fortis* ist monogyn. Die Tiere haben bei einer Alitrunklänge von 1.86 – 3.54 mm (berechnet nach Sommer und Wehner, 2012) eine Körpergröße von durchschnittlich 5.5-9.6 mm (Wehner, 1983;

Abb. 1: *Cataglyphis fortis* bei Menzel Chaker, Tunesien; Foto: Verena L. Wahl

Knaden und Wehner, 2003). Im Gegensatz zu *Cataglyphis bicolor* bewohnen sie aber nur ein Nest (monodom), welches mehrjährig ist. Als Bewohner dieser nur saisonal nutzbaren Umgebung, die dazu noch landmarkenarm ist, müssen die Ameisen ihre Futtersuche dahingehend optimieren, dass sie den größten Erfolg aus den einzelnen Ausläufen ziehen können (Wehner, 1983). Daher ist ihre hohe Suchmotivation und zudem ihre individuelle Navigation ideal für Verhaltensforscher.

Die Sammlerinnen von *Cataglyphis bicolor* und *Cataglyphis fortis* passen ihre Exkursionen außerhalb des Nestes an die tageszeitlichen Temperaturen an. Ist eine gewisse Temperatur erreicht, so verlassen sie ihr Nest, um die Suche zu beginnen. Bei zu hohen Temperaturen, meist in der Mittagszeit, ziehen sich die Tiere in ihr kühleres Nest zurück (Harkness und Wehner, 1977; Knaden und Wehner, 2005a).

Anders ist dies bei ***Cataglyphis bombycina*** (ROGER, 1859), denn diese Art der *Cataglyphis* Wüstenameisen furagiert bei Temperaturen über 45°C zur heißesten Zeit des Tages (Wehner et al., 1992; Review von Wehner, 1987). Sie bewohnt die sehr heißen Dünengebiete der Sahara, der Sinai und der arabischen Peninsula Wüste. Diese Tiere zeigen eine Belastungsgrenze mit einem Temperatur-maximum von bis zu 53.6 ± 0.8 °*C.* Somit gehören sie, neben *Cataglyphis bicolor* mit 55.1 ± 0.8 °C, zu den hitzetolerantesten Landlebewesen (Gehring und Wehner, 1995). An ihrer silbern glitzernden Erscheinung mitten in den Sanddünen ist diese *Cataglyphis* Art eindeutig zu erkennen. Ein dichtes, silberfarbenes Haarkleid stellt dabei eine Anpassung an die Hitze dar, denn so können die Tiere infrarote Strahlung abhalten und das Aufheizen des Körpers minimieren (Willot et al., 2016; Shi et al., 2015). *Cataglyphis bombycina* bewohnt große Nester mit einer sehr großen Anzahl an Individuen und mehreren Eingängen, welche mehrere Meter voneinander verteilt sind (Molet et al., 2014). Sie stellen die einzige *Cataglyphis*-Art mit Soldaten dar, welche bei einer Störung des Nestes mit gespreizten Mandibeln herauskommen und beißen (Délye, 1957; Lenoir et al., 2009). Als eine weitere Strategie für die Effizienz des Heimlaufens und die Verringerung der Aufenthaltsdauer in den heißen und lebensfeindlichen Sanddünen stehen meist fünf bis zehn Arbeiterinnen regungslos (landmarkengleich) oder grabend um die Nestöffnung herum (siehe Abb. 2), um die Wahrnehmung des Nestbereiches für die heimkehrenden Sammlerinnen zu vergrößern (Wehner 2009). Obwohl *Cataglyphis bombycina* bei einer vergleichbaren Körpergröße mit *Cataglyphis fortis* durchschnittlich 15% kürzere Beinlängen als diese zeigt (berechnet nach Sommer und Wehner, 2012 und Kapitel 6), hält sie trotzdem den Laufgeschwindigkeitsrekord mit 1 ms^{-1} (geschätzt von Wehner, 1983), welchen wir mit dieser Arbeit mit einem exakten Wert von 0.86 ms^{-1} (*Cataglyphis fortis* 0.62 ms^{-1}) erstmals bestätigen konnten.

Abb. 2: *Cataglyphis bombycina* am Nesteingang in der Sahara bei Douz, Tunesien; Foto: Verena L. Wahl

1.2 Navigation und Wegintegration

Navigation und Orientierung sind wesentliche Fähigkeiten für sich fortbewegende Insekten, wie auch für die *Catagyphis* Ameisen. Ihr Überleben hängt davon ab, wie effizient eine Futterstelle lokalisiert und wie sicher das Ziel danach erreicht werden kann. Solch eine Reise kann abhängig von der Motivation (z.B. das Finden von Futter, von Schutz oder einem Paarungspartner) klassifiziert werden und unterscheidet sich in Strategien abhängig von der Entfernung (von sehr kleinen bis zu über 1000 km) (Alexander, 2006). Insekten haben sich trotz ihres, verglichen mit dem des Menschen, winzig kleinen Hirns als herausragende Navigatoren bewährt. Manche Insekten, wie Libellen, Heuschrecken und Schmetterlinge, überqueren hunderte bis tausende Kilometer um zwischen Brut-, Überwinterungs- oder Übersommerungsgebieten zu wechseln (Williams, 1958; Johnson, 1969). Beispielsweise ziehen Monarch-Falter (*Danaus plexippus*) saisonal über 3000 km von Nordamerika nach Mexico, um einen Überwinterungsplatz zu finden (Urquhart 1978, Brower 1996).

Wüstenameisen müssen aber vor allem über kurze Distanzen in der Lage sein akkurat zu navigieren. Ihr Überleben außerhalb des Nestes hängt davon ab, den Aufenthalt so kurz als möglich zu gestalten, da sie sonst Räubern oder dem Hitzetod zum Opfer fallen könnten. Daher hat sich evolutiv betrachtet ein leistungsfähiges und effektives Navigationssystem entwickelt, das die Ausläufe optimiert und das Tier am Ende jeder Exkursion sicher an einen genau definierten Geländepunkt steuert.

Die Wegintegration

Erstmals beschrieb Darwin (1873) die Wegintegration, welche von vielen verschiedenen Arten mit einem festen Heimatstandort genutzt wird. Diese Art von Navigation wird von vielen Tieren verwendet, wie von Spinnen (Görner und Claas, 1985; Mittelstaedt, 1985; Moller und Görner, 1993), verschiedenen Insekten (Frisch, 1965, 1967; Müller und Wehner, 1982; Wehner und Srinivasan, 2003), Krebstieren (Hoffmann, 1984), Vögeln (Mittelstaedt und Mittelstaedt, 1982; Saint Paul, V. v., 1982) und Säugetieren (Mittelstaedt und Mittelstaedt, 1980; Etienne et al., 1985; Séguinot et al., 1993; Etienne und Jeffery, 2004). Auch die alten Seefahrer nutzten ein ziemlich ähnliches System vor der Erfindung des GPS (Gladwin, 1970).

Die Entdeckung, dass Ameisen nach der Sonne navigieren können, machte Santschi Anfang des 20. Jahrhunderts (Santschi, 1911 in Wehner, 1981). Obwohl Vertreter der *Cataglyphis* Wüstenameisen verschiedene Lebensräume bewohnen, überwiegend bestimmt vom Anteil der Vegetation, werden grundsätzlich die gleichen Strategien für die Navigation angewendet. Die Tiere kombinieren dazu

angeborene Navigationsmechanismen mit gelernten Parametern, die sie während früherer Futtersuchläufe gelernt haben. Vom ersten Moment an, wenn eine Ameise ihr Nest verlässt, um nach Futter auszuschwärmen, ist sie über ihr Wegintegrationssystem sicher mit dem Nest verbunden (Müller und Wehner, 1988; Wehner und Srinivasan, 2003). Auf diese Weise ist sie während ihrem gewundenen Suchlauf durchgängig über ihre aktuelle Position relativ zum Nest informiert. Entscheidendes Kriterium dabei ist, dass „das Ziel […] nicht in einem erdfesten Koordinatensystem, sondern nur in seiner relativen Lage zum Tier definiert" ist (Wehner, 1981). Die Kursbestimmung kann bei *Cataglyphis* Ameisen ohne jegliche Ortkenntnis allein aufgrund von Weginformationen erfolgen (Vektornavigation) (Wehner und Wehner, 1986). Ein sogenannter Heimvektor liefert die notwendige Information über die Laufrichtung und die Laufdistanz zum Nest und ermöglicht dem Tier, zu jeder Zeit direkt zurück zum Nest zu gelangen (siehe Abb. 3). Diese zwei Parameter – Richtung und Distanz - laden dann zeitgleich den (Weg-) Integrator auf.

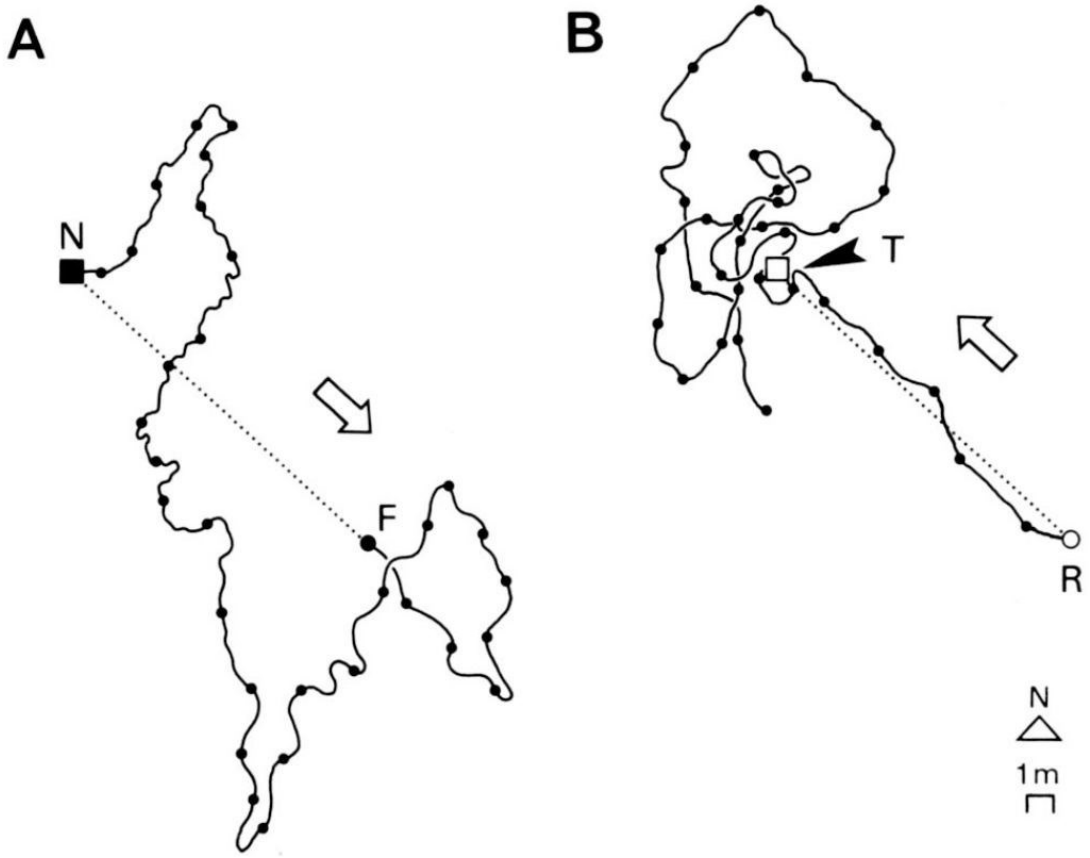

Abb. 3: (**A**) Futtersuchlauf (durchgezogene Linie) einer *Cataglyphis fortis* Wüstenameise vom Nest (N) bis zu einem Futterstück (F). (**B**) Nach Versetzten des Tieres auf ein östlich entferntes Testfeld und dem Geben von Futter läuft das Tier vom Auflasspunkt (R) mit Hilfe des zuvor aufgeladenen Heimvektors an die Stelle, wo es das Nest (T) vermutet und beginnt dann mit dem systematischen Suchprogramm. Beide Läufe wurden 320 sec aufgezeichnet; jeder ausgefüllte Punkt markiert ein Zeitinterval von 10 sec (mit freundlicher Genehmigung von Wehner und Wehner, 1986, Fig.3).

Das Tier kann die Wegintegration aber genauso dazu nutzen, eine zuvor besuchten Futterstelle erneut anzusteuern (Wolf et al., 2012). Dies tritt dabei nur in den seltenen Fällen ein, wenn das Futterstück zu groß oder schwer sein sollte (im Fall von toten Echsen oder Krebstieren), um es tragend, schiebend oder ziehend Richtung Nest zu transportieren. Dann zerlegt die Ameise das Futter in Stücke und transportiert diese nacheinander ab. Stellen Wissenschaftler eine Futterstelle auf, so tritt ebenso genau dieser Fall ein und das Tier lernt die Position und wird darauf trainiert.

Dass die Tiere in der Lage sind, eine Vektorintegration auszuführen, zeigen Versuche, bei denen Kanäle verwendet wurden, um den Tieren eine definierte Richtung vorzugeben. Erfolgt der Hinlauf zum Futter über Katheten eines rechtwinkligen Dreieckes, der Rücklauf dagegen über die Hypotenuse, so liegen die Suchpunkte an den über Pythagoras berechneten Stellen (Wehner, 1981).

Um die **Laufrichtung** während des Auslaufes zu messen, werden bei *Cataglyphis* Ameisen verschiedene Kompasssysteme verwendet. Neben der Position der Sonne im Azimut oder den Spektralgradienten des Himmels und seiner Intensität (Wehner, 1994; 1997; 2003; Wehner und Srinivasan, 2003) hat sich der Polarisationskompass als das dominierende System herausgestellt (Müller und Wehner, 2006, Lebhardt et al. 2012). Dieser Polarisationskompass basiert auf der Anordnung der elektrischen Feldvektoren (e-Elektronen), welche kreisförmig um die Sonne angeordnet sind (Wehner und Lafranconi, 1981; Wehner 1989; Pomozi et al., 2001). Tiere wie die Wüstenameisen können diese Polarisationsmuster über spezielle Felder in ihren Augen (dorsal rim area oder POL area) erkennen und als Referenzsystem nutzen (Marshall und Cronin, 2011). Diese e-Vektoren-Verteilung ändert sich, von der Erde aus gesehen, je nach Tageszeit mit der Position der Sonne (Wehner und Labhart, 2006) und bietet die genauste Methode der Richtungsinformation (Lebhardt, 2015). Eine, wenn vorhanden, relativ konstante Windrichtung kann mit Hilfe der Antennen wahrgenommen und als zusätzlicher Richtungsgeber eingesetzt werden (Wehner und Duelli, 1971; Duelli 1972).

Die Messung der **Laufdistanz** wirft aktuell noch Fragen auf. Verschiedenste Wissenschaftler stellten aber vielversprechende Hypothesen auf und dies führte zu den verschiedensten Diskussionen (Wehner 1992; Ronacher und Wehner 1995; Wittlinger et al., 2006, 2007). In den letzten Jahren wurden dann zwei Hauptmechanismen beschrieben, die *Cataglyphis* Wüstenameisen für die Wegmessung (Odometrie) nutzen: die Integration des ventralen optischen Flusses und die Schrittintegration. Obwohl beide Parameter mit Versuchen nachgewiesen werden konnten, gibt es jedoch noch große Verständnislücken des physiologischen Hintergrundes und der genauen Integration.

Der ventrale optische Fluss ist das Ergebnis der Bildverschiebung des Untergrundes während des Fortbewegens, die optisch messbar ist. Bei fliegenden Hymenoptera, wie Fliegen oder Wespen, konnte bereits gezeigt werden, dass die Distanzmessung über eine Integration einer beim Flug erfassten relativen Bildbewegung (optischer Fluss) stattfindet (Esch und Burns, 1995; Srinivasan et al., 2006). Bei laufenden Insekten scheint dies allerdings eine kleinere Rolle zu spielen (Laufende Honigbiene: Schöne, 1996; laufende Hummel: Chittka et al., 1999). Da Ameisen phylogenetisch eine nahe Gruppe zu den Bienen darstellen, lag die Vermutung nahe, dass auch Ameisen den ventralen optischen Fluss zur Distanzmessung nutzen können. Versuche von Ronacher und Wehner (1995) zeigten allerdings, dass der

optische Fluss wohl nur einen kleinen Einfluss auf die Wegmessung haben kann. Die Distanzmessung kann aber auch ganz ohne visuellen Input funktionieren. Ameisen, die in kompletter Dunkelheit (Thiélin-Bescond, 2005) oder mit überlackierten Augen liefen, waren trotzdem in der Lage, ihre Heimlaufdistanz richtig einzuschätzen (Ronach und Wehner, 1995; Wittlinger und Wolf 2013)).

Aktuelle Experimente von Pfeffer und Wittlinger (2016) zeigen aber auch, dass der Einfluss des optischen Flusses allein genügt, um Distanzen zu messen. Denn werden Ameisen von Nestgenossinnen getragen, so nutzen sie selbst keine Lokomotion sondern erfahren passiv den optischen Fluss. Wird das Paar nach einer gewissen Distanz getrennt, so ist das getragene Tier trotzdem in der Lage die Heimlaufdistanz korrekt einzuschätzen, obwohl es diese zuvor noch nie selbst gelaufen ist. Eine aktive Lokomotion ist zur Distanzmessung nicht unbedingt notwendig (Seidl et al., 2006). Außerdem konnte so gezeigt werden, dass die zwei Systeme der Distanzmessung separat und unabhängig existieren und redundant operieren (Pfeffer und Wittlinger, 2016).

Die Strategie der Schrittintegration oder des Schritte Zählens wurde von M. Wittlinger und Kollegen (2006, 2007) durch das Manipulieren der Schrittlängen enthüllt. Nach einer Dressur auf eine Futterstelle wurden die Tiere dort entnommen und ihnen wurden dann entweder Stelzen angeklebt oder die Beine zu Stummeln abgeschnitten. Ameisen mit gekürzten Beinen unterschätzten die Strecke beim Heimweg, und liefen deutlich zu kurz, bevor sie mit der Nestsuche begannen. Dagegen überschätzten Tiere mit Stelzen diese Strecke und liefen deutlich über ihr Ziel hinaus (Wittlinger et al., 2006; 2007).

Laufen die Tiere aber über hügeligen Boden, so messen die Ameisen dabei die Basisdistanz vom Nest zum Futter anstatt den eigentlichen erwarteten Laufweg von auf und ab (Wohlgemuth et al., 2001, 2002). Dies deutet darauf hin, dass die Tiere die Hügel auf ihrem Weg wahrnehmen.

Alle Ergebnisse zeigen, dass die Tiere das Pedometer nutzen um Distanzen zu messen. Der passende sensorische Input bleibt aber noch immer rätselhaft (Wittlinger et al., 2007b; Heß et al., 2009; Wintergerst und Ronacher, 2012). Um Distanzen richtig abzuschätzen sind Parameter wie die konstante Schrittlänge je Laufgeschwindigkeit, die Schrittfrequenz oder auch Phasenbeziehungen und Gangarten des Tieres weiterhin von besonderer Bedeutung. Informationen des optischen Fluss Integrators können jedenfalls nicht in den Schrittintegrator transferiert werden (Pfeffer und Wittlinger, 2016). Sowohl die funktionelle als auch die physiologischen Mechanismen sind somit derzeit noch nicht genau verstanden und bieten genügend Platz, um nach Antworten zu suchen.

Zusätzliche Faktoren und Strategien

Abhängig vom Lebensraum oder der aktuellen Umgebung sind jedoch unter natürlichen Bedingungen eine Großzahl zusätzlicher Faktoren vorhanden, die die Wegintegration unterstützen. Dies beinhaltet optische Faktoren wie Panorama oder Landmarken, die verwendet werden können, um die Wegintegration zu ergänzen. Die Tiere können eine Art Momentaufnahme des Panoramas während dem Suchlauf machen, speichern und diese dann später mit ihrer aktuellen Umgebung verbinden. Dieser visuelle Input erlaubt das genaue Anpeilen eines gewissen Zieles (Wehner und Räber, 1979; Wehner und Müller, 1985).

Jedoch können nicht nur optische Faktoren sogenannte Landmarken darstellen. Wüstenameisen sind auch dazu in der Lage, Faktoren wie Gerüche (Steck et al., 2009), spürbare Bodenstrukturen (Seidl und Wehner, 2006), oder Magnet- oder Vibrationseigenschaften (Buehlmann et al., 2012) mit der Lage des Nestes zu verbinden. Diese multimodale Herangehensweise des Nutzens aller möglichen Einflussfaktoren macht das Navigationssystem der Wüstenameise besonders effizient.

Eine zusätzliche Strategie ist das sogenannte systematische Suchprogramm (vergleiche hierzu auch Abb. 3). Sind die Tiere ihren Heimvektor abgelaufen und finden am Zielpunkt aber ihr angesteuertes Ziel nicht, beispielsweise weil das Tier auf ein Testfeld versetzt wurde, oder im natürlichen Kontext beispielsweise vom Wind verweht wurde, so startet das Tier ein systematisches Suchprogramm (Wehner und Srinivasan, 1981; Müller und Wehner, 1994). Beginnt das Tier, kreisförmig um das vermeintliche Ziel zu laufen, sprechen wir von einer Suchphase – dagegen wird das Ablaufen des Heimvektors die Anlaufphase genannt. Diese Suchzirkel nehmen zentriert um das erwartetet Ziel und spiralförmig mit zunehmender Suchzeit in der Größe zu. In regelmäßigen Intervallen läuft das Tier zurück zum Startpunkt der systematischen Suche und ändert die eingeschlagene Suchrichtung (Wehner und Wehner, 1986).

1.3 Lokomotion und Laufanalyse

Die Lokomotion, welche die aktive Fortbewegung eines Individuums aus eigener Kraft beschreibt, ist essentieller Bestandteil des Lebens und des Überlebens jeder Ameise. Wenn die *Cataglyphis* Wüstenameisen mit ihren extrem langen Beinen und einem steil aufgestelltem Gaster über die weiten Sandflächen um ihre Nester nach Futter suchen, können sie Geschwindigkeiten von bis zu 1.0 ms^{-1} (*Cataglyphis bombycina*) erreichen und Drehungen vollführen, die in ihrer Schnelligkeit denen der fluggewandtesten Insekten (Collett und Land, 1975) kaum nachstehen (*Cataglyphis fortis*, Wehner, 1981). Cornetz beschrieb dies bereits im Jahre 1910 sehr treffend: « Cet insecte ne marche pas, il court » (Cornetz, 1910, S.93). Denn durch das zusätzliche Aufrichten ihres Gasters können sich die Tiere (*Cataglyphis bicolor* und *Cataglyphis fortis*) mit weniger Kraft und Energie auf gewundenen Pfaden schneller bewegen und evolutionär somit die Lokomotion verbessern (McMeeking et al, 2012).

Neben dem offensichtlichen und wohl wichtigsten Gebrauch der Lokomotion während der Futtersuche wird sie aber auch im Nest selbst genutzt. Untersuchungen zeigen, dass sich die Tiere oft in den Tunneln des Nestes bewegen, um andere Orte zu erreichen, an denen eine spezielle Aufgabe erledigt werden muss (Retana und Cerda, 1991; Cerda et al., 1996). Auch der Transport von Nahrung, welche im Nest auf Arbeiterinnen, Nachwuchs bis hin zur Königin verteilt werden muss, spielt eine wichtige Rolle. Aufgrund des altersabhängigen Polyethismus werden diese Aufgaben von jüngeren Ameisen erfüllt (Schmid-Hempel und Schmid-Hempel 1984; Lenoir et al., 2009). Diese Innenarbeiterinnen werden später zu den Sammlerinnen, bei denen die Lokomotion an Wichtigkeit zunimmt. Insgesamt sind die *Cataglyphis* Wüstenameisen mit einem sehr hochentwickelten Lokomotionsapparat ausgestattet, welcher für sehr hohe Laufgeschwindigkeiten prädestiniert ist. Umso erstaunlicher mag es klingen, dass die Tiere trotz ihrer oft beträchtlichen Größe (bis zu 1.8 cm) selbst wegen ihrer sehr entlegenen Habitaten bei namhaften Myrmekologen des ausgehenden 19. und 20. Jahrhunderts – G. Mayr, *C.* Emery, A. Forel und W.M. Wheeler - erst so spät an entomologischem Interesse gewonnen haben (Wehner, 1981).

Hexapode Lokomotion

Jede Bewegung eines Beines kann als eine Zykluswiederholung von Abheben und Absetzten betrachtet werden - das Bein befindet sich also abwechselnd in der Luft (Schwingphase) und auf dem Boden (Standphase). *Cataglyphis* Wüstenameisen sind für ihre alternierende und robuste Tripod-Koordination bekannt (Zollikofer, 1988). Dabei befinden sich drei Beine zeitgleich in Schwingphase während die anderen drei auf dem Boden stehen. Vorder- und Hinterbein der einen Körperseite bilden mit dem

Mittelbein der anderen Körperseite einen Tripod. Die Tiere sind somit in der Lage, ihre Beine als geometrisch exaktes Muster zu positionieren, welche als alternierend aufsetzende „funktionelle Füße“ mit bipedalen Tieren verglichen werden kann (Full et. Al, 1991). Die Tripod-Koordination ist in sich schnell bewegenden Insekten gut untersucht und stellt ein bemerkenswert robustes Lokomotionsmuster in hexapoden Läufern dar, wie in Schaben und Käfern (Hughes 1952; Delcomyn, 1971), in Stabheuschrecken (Graham 1981; Wendler 1968)), in Fruchtfliegen (Wosnitza et al., 2013) und eben in Ameisen (*Cataglyphis*, *Formica*, *Lasius* und *Myrmica*, Zollikofer, 1994a; Reinhardt und Blickhan, 2014).

Cataglyphis Ameisen nutzen diese Gangart nahezu während der kompletten Geschwindigkeitsspanne. Bei langsamen hexapoden Läufen können aber auch andere Gangarten wie Tripod, Tetrapod oder Wavegaait benutzt werden. Tetrapod (zwei Beine befinden sich zeitgleich in der Schwingphase während die anderen vier Beine Bodenkontakt haben; die schwingenden Beine sind diagonal lokalisiert) und Wavegait (ein Bein ist in der Schwingphase, während die anderen fünf sich am Boden befinden - eine wellenförmige Bewegung vom Hinter- und Vorderbein hat dieser Gangart ihren Namen gegeben) sind dabei nicht die einzigen Gangarten, die auftreten, denn um abrupte und stockende Bewegungen zu vermeiden gibt es auch sogenannte Übergangsformen von einer idealen Beinkoordination zur nächsten, um eine gleichmäßige Fortbewegung zu garantieren (Grabowska et al., 2012). Die beschriebenen Gangarten gehen dabei über in ein Kontinuum (Schilling et al., 2013) mit einem Übergang bei abnehmender Laufgeschwindigkeit von Tripod zu Tetrapod zu Wavegait bis hin zum zeitgleichen Bodenkontaktes aller sechs Beine. Auch in die Gegenrichtung ist dieses Phänomen des gleitenden Überganges zu beobachten, und zwar bei hohen Laufgeschwindigkeiten von Tripod über unvollständige Tripods (zwei Beine oder sogar nur noch ein Bein auf dem Boden) bis hin zum völligen Verlust des Bodenkontaktes, den Flugphasen.

Eine Charakteristik des hexapoden Laufens ist die agile Ausführung unter sich verändernden Umgebungsbedingungen (Watson et al. 2002). In einer komplexen Umwelt werden Insekten von vielerlei Hindernissen herausgefordert, was ein hoch flexibles Laufsystem erfordert. Insekten können auf nahezu jedem Untergrund in jeder Richtungsorientierung relativ zur Schwerkraft agieren (Cruse 1976b; Bässler 1977; Cruse 1979). Auch *Cataglyphis* Ameisen laufen problemlos über schräge Flächen (Seidl und Wehner 2008; Weihmann und Blickhan 2009) und navigieren sogar trotz amputierter Beine akkurat heim (Wittlinger und Wolf, 2013). Die Beinbewegungen und die komplette Lokomotion können somit an vorhandene Situationen angepasst werden.

Laufanalyse

Aber auch Laufparameter können herangezogen werden, um die Lokomotion zu beschreiben. Wird dabei Bezug auf die jeweilige Laufgeschwindigkeit genommen, können beeindruckende Korrelationen mit zunehmender Laufgeschwindigkeit beobachtet werden wie eine lineare Zunahme der Schrittlänge, einer Zunahme der Frequenz bis zum Erreichen eines Frequenzplateaus oder auch die Abnahme der Dauer von Schwing- und Standphase bis hin auf ein Minimum. Die detaillierte Analyse von Schrittparametern und Phasenverhältnissen der Beine soll das Grundverständnis der Lokomotion verstärken.

Kapitel 2

2.1 Umfang der Thesis und Zielsetzung dieser Doktorarbeit

Meine Dissertation besteht aus vier Publikationen, wovon jede eine separate Publikation darstellt. Zwei Manuskripte wurden bereits in angesehenen Fachzeitschriften publiziert (*Journal of Comparative Physiology A* (**Kapitel 4**); *Journal of Experimental Biology* (**Kapitel 5**)). **Kapitel 3** befindet sich aktuell in der Revisionsphase („in revision") im *Journal of Experimental Biology*, und **Kapitel 6** wurde für die Publikation in *Myrmecological News* vorbereitet. Die Publikationen sind somit unabhängig und jede kann einzeln für sich gelesen und verstanden werden. Jedoch bauen alle aufeinander auf und behandeln das vielfältige Phänomen der Navigation, welches bereits in der Einleitung aufgezeigt und im folgenden Abschnitt diskutiert werden soll.

Schon seit langer Zeit wird das faszinierende Orientierungs- und Navigationsverhalten von Insekten untersucht – speziell auch das des Modelorganismus *Cataglyphis.* Es ist uns in **Kapitel 3** nun erstmals gelungen - in Kooperation mit Dr. Hansjürgen Dahmen aus Tübingen, der das Kugelapparatursystem entwickelt hat– ein komplexes Verhalten wie die Wegintegration, als Form der Vektornavigation (Wehner und Wehner, 1986; Wehner und Srinivasan 2003), auf einer Laufkugelapparatur zu realisieren. In der Publikation können wir zeigen, dass der Modelorganismus *Cataglyphis fortis*, ebenso wie *Cataglyphis bicolor*, in solch einer unnatürlichen und abstrakten Situation in der Lage ist, ein überaus komplexes Verhalten wie die Wegintegration zu betreiben. Damit bietet uns das System die Möglichkeit, den zurückgelegten Pfad während des Heimlaufes zu jedem Zeitpunkt und entlang des gesamten aufgenommenen Pfades von über 30 m zu speichern und somit das Tierverhalten zu analysieren.

Das Kugelapparatursystem (Abb. 4) misst die Bewegung der auf einem Luftpolster gelagerten Styroporkugel mit Hilfe von zwei im rechten Winkel ausgerichteten optischen Maussensoren, die zur Erhöhung der Messgenauigkeit (Minimierung der Fehler) mit Weitwinkellinsen ausgestattet sind. Über einen Standardcomputer kann das System dann ohne großen Aufwand die zurückgelegte Strecke des Tieres, welches befestigt auf der Kugel läuft, als exakte Werte (mit 209 XY-Werten pro Sekunde) auslesen, diese in Echtzeit auf dem Computerbildschirm als Livebild anzeigen und abspeichern. Wichtig

für das Gelingen ist neben dem Design der Apparatur und einer ausgehöhlten extrem leichten Styroporkugel auch die richtige Halterung, welche dem Tier eine nahezu natürliche Art von Bewegung auf der Laufkugel ermöglicht. Das Tier kann sowohl seine Körperhöhe als auch seine Laufrichtung nahezu widerstandslos und mit eigenem Trägheitsmoment ändern, was somit schnelle Richtungsänderungen zulässt. Die Kugelapparatur ist so konzipiert, dass die Vertikalachse (auch Gierachse oder engl.: yaw axis genannt) gesperrt ist, denn so kann die Kugel als natürliches „closed-loop" System fungieren.

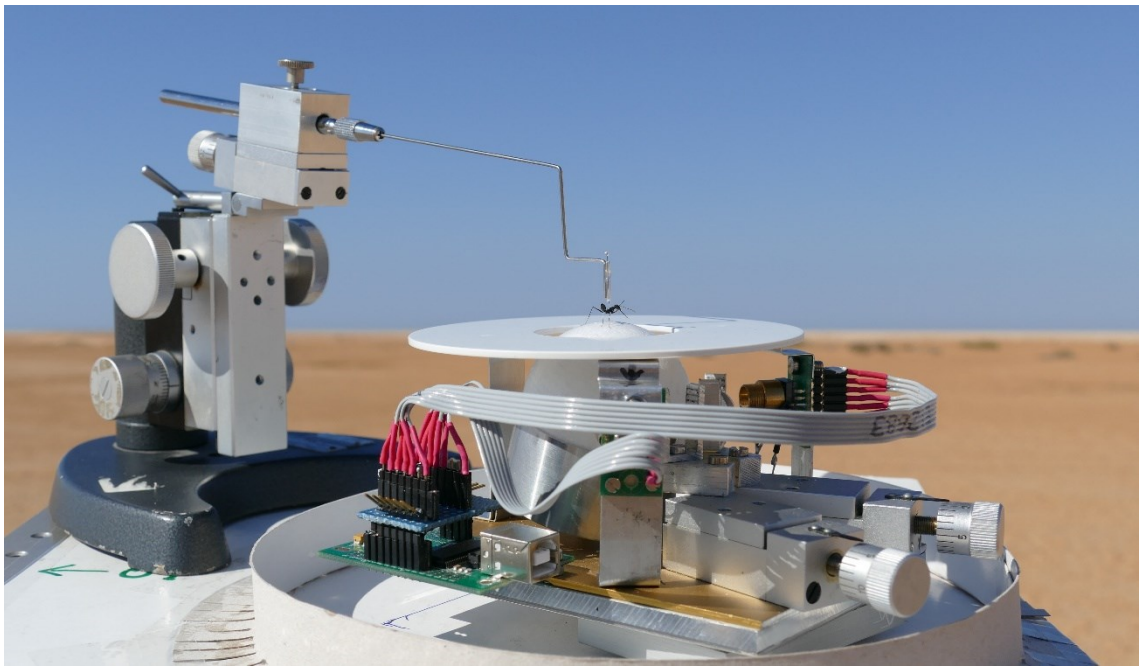

Abb. 4: *Cataglyphis fortis* auf der Laufkugelapparatur, Foto: Matthias Wittlinger

Für dieses Experiment wurden die Tiere auf eine Futterstelle, die eine bestimmte Distanz von ihrem Nest entfernt aufgestellt wurde, auf einem freien Feld trainiert. Erfahrene Tiere, die bereits mehrmals zur Futterstelle zurückkehrten, wurden dann dort abgefangen und auf die Kugelapparatur mit Hilfe der speziellen Halterung befestigt. Bei erneuter Aufnahme eines Futters (wodurch das Tier zeigt, dass es sich in einem motivierten Status befindet) starteten die Tiere direkt mit dem Heimlaufverhalten auf der Kugel in die entsprechend richtige Richtung, nämlich der des Nestes. Dabei benutzte das Tier ausschließlich den visuellen und den Odometer Input. Die mit dem System aufgenommenen Spuren der Heimläufe, bei denen die Tiere gefundenes Futter auf direktem Weg zurück ins Nest transportieren, konnten wir dann auswerten und mit Heimläufen vergleichen, die wir im freien Feld unter natürlichen Bedingungen in ihrem Habitat aufgenommen hatten. Bei diesen Kontrollversuchen, die schon lange etabliert sind, wurden die Tiere nach dem Training auf ein Versuchsfeld einige Meter entfernt vom Nest versetzt. Der Heimlauf konnte dann von Hand protokolliert und später am PC eingelesen und ausgewertet werden. Bei den Ergebnissen von Kugelapparatur- und Kontrollversuchen konnte kein signifikanter Unterschied in Länge und Richtung des Heimlaufes gefunden werden, was bedeutet, dass die Tiere sowohl im Freiland (wie

schon bekannt) als auch befestigt auf einer Laufkugel exakt die Richtung und die Distanz vom Auflasspunkt (hier: Fundort des Futters) zu ihrem Nest kennen, somit exakt heim finden und in beiden Fällen die Wegintegration betreiben.

Als weiteres Ergebnis können wir durch diese Studie zeigen, dass *Cataglyphis* Wüstenameisen verschiedene Heimlaufstrategien benutzen. Denn zwischen der strikt zielgerichteten Heimlaufphase und der Suchphase, in der das Tier mit Suchzirkeln um das fiktive Nest beginnt, gibt es einen signifikanten Geschwindigkeitsabfall zu verzeichnen. Außerdem konnte die Winkelverteilung gemessen werden, welche sich von der geraden Heimlaufphase zur gewundenen Suchphase ändert. In einem weiteren Versuch konnten wir zusätzlich die Winkelkonstanz der Tiere zeigen, denn wurde die Apparatur um 90° gedreht, während sich das Tier auf dem Heimlauf (also in definierte Richtung) befand, so glich das Tier, mit Hilfe des Himmelskompasses, genau diese 90° aus, lies sich davon nicht beeindrucken und lief strikt in die Nestrichtung weiter. Die zeitliche Auflösung, zusätzlich zur bisher benutzten räumlichen, stellt somit eine neue Auswertungsmöglichkeit dar.

Aufgrund der hohen zeitlichen Auflösung des Systems bietet dies uns nun eine detaillierte Einsicht in das natürliche Lauf- und Navigationsverhalten von Tieren. Es bietet dazu eine lokale Unabhängigkeit, denn es kann nicht nur in Laboren, sondern dank seiner robusten und mobilen Bauart, auch im Freiland benutzt werden. Dieses simple und doch sehr komplexe Kugelsystem ermöglicht nun, die Navigation und alle Arten an komplexen Interaktionen wie Panoramablickfeld, Landmarkennavigation, dem Gebrauch von lokalen und globalen Vektoren oder dem oft diskutierten Gebrauch von kognitiven Karten zu testen. Durch unseren Beweis, dass Wegintegration auf einer Laufkugelapparatur als robustes Verhalten möglich ist, haben wir eine Tür für kommende Navigationsexperimente in ganz neuer Art und Weise geöffnet.

Im zweiten Teil meiner Doktorarbeit habe wir uns mit dem Schrittintegrator auseinander gesetzt. Dieser stellt einen der zwei wesentlichen Parameter der Wegintegration dar, denn er ist für die Distanzmessung der Tiere zuständig (Ronacher und Wehner, 1995; Wittlinger et al., 2006, 2007). Der Schrittintegrator könnte eine der Hauptquellen von Fehlern während der Navigation darstellen. Für ein besseres Verständnis des Schrittintegrators benötigen wir eine detaillierte Analyse des Laufverhaltens und der Phasenbeziehungen der Beine über das gesamte Laufgeschwindigkeitsspektrum. Als Grundlage zu dieser Arbeit diente die Thesis von Christopf Zollikofer, der in seiner Zeit in Rüdiger Wehners Labor den Grundstein für Laufanalysen bei den sich schnell bewegenden *Cataglyphis* Wüstenameisen, und somit auch für andere Arten, legte (Zollikofer 1988, 1994a, 1994b, 1994c). Mit der neuen Highspeed-Kamera-Technik waren wir nun in der Lage, einen noch besseren Einblick in die Beinkoordination der Tiere zu erlangen und konnten zusätzlich das Laufgeschwindigkeitsspektrum bis auf von uns erwartete Spitzenlaufgeschwindigkeiten (*Cataglyphis fortis* 0.62 ms^{-1}, *Cataglyphis bombycina* 0.86 ms^{-1}) erweitern. Dabei ging es uns um die flexible Anpassung von Lokomotion und Navigation an äußere Umstände, aber eben auch an Laufgeschwindigkeiten und an die Laufrichtung (vorwärts und rückwärts laufend).

Um den Schrittintegrator als Teil der Wegintegration der *Cataglyphis* Wüstenameisen noch besser verstehen zu können, haben wir in **Kapitel 4 und 5** das Laufverhalten und dazu vor allem verschiedene Laufparameter und Phasenbeziehungen der Beine als Grundlage für die Distanzmessung der Wegintegration von vorwärts- und rückwärtslaufenden *Cataglyphis fortis* und in **Kapitel 6** das von *Cataglyphis bombycina* genauer betrachtet.

Die Wüstenameise *Cataglyphis fortis* stellt eine der am besten untersuchten *Cataglyphis* Ameisenarten dar und sollte uns deshalb zum weiteren Verständnis der Distanzkomponente der Wegintegration dienen. In **Kapitel 4** untersuchen wir dafür die Lokomotion und die Interaktion der Beine bei verschiedenen Laufgeschwindigkeiten von *Cataglyphis fortis*. Dabei konnten wir ein großes und erstmals vollständiges Geschwindigkeitsspektrum von 5 bis 620 mms^{-1} erreichen.

Wir können zeigen, dass *Cataglyphis fortis* zum Erhöhen der Laufgeschwindigkeit hauptsächlich die Schrittlänge benutzt und weniger die Schrittfrequenz. Denn die Schrittfrequenz stagniert ab einer Laufgeschwindigkeit von ungefähr 370 mms^{-1} in ein Plateau, welches trotz weiter steigender Laufgeschwindigkeiten nicht mehr überschritten werden kann. Die Schrittlängen hingegen erhöhen sich nahezu perfekt linear mit ansteigender Laufgeschwindigkeit. Grund dafür ist, dass die Tiere über ihre morphologischen Grenzen hinaus mit Hilfe von Flugphasen (alle sechs Beine verlieren den Bodenkontakt) die Schrittlängen erhöhen können. Deshalb werden die *Cataglyphis* Ameisen auch Schrittlängen-Maximierer (Zollikofer 1988) genannt. Diese Flugphasen setzen genau dann ein, wenn das Tier das Frequenzplateau erreicht und der Duty-Faktor den Wert 0.5 unterschreitet. Man spricht dann von einem Gangartwechsel von Gehen zu Laufen, der aber nicht abrupt sondern in einer Art kontinuierlichem Übergang stattfindet. So überschreiten die Beinpaare zu unterschiedlichen Geschwindigkeiten die 0.5 Marke des Duty-Faktors.Vorder-und Hinterbeinpaar, welche den Wert zuerst unterschreiten, sind für den gleitenden Übergang der Gangarten zuständig, das Mittelbeinpaar bestimmt als letztes Beinpaar den Übergang in die Flugphasen.

Cataglyphis fortis zeigt über nahezu das komplette Geschwindigkeitsspektrum eine stereotypen alternierenden Tripod, welcher für viele schnell laufende Insekten bereits gut untersucht wurde (u.a. Hughes, 1952; Delcomyn, 1971; Graham, 1981). Ein Tripod kann dabei als funktioneller Fuß gesehen werden, den die Tiere Fuß für Fuß, also Tripod für Tripod, aufsetzen. Dabei findet bei *Cataglyphis fortis* immer, wie bei bipoden Tieren, eine Art Abrollen des funktionellen Fußes statt, resultierend daraus, dass das Mittelbeinpaar bei jedem Schrittzyklus die längste Standphase aufzeigt, also am längsten der drei Beine eines Tripods auf dem Boden steht. Daraus folgt die Hypothese, dass das Mittelbeinpaar eine Art Sonderrolle bei den *Cataglyphis fortis* Wüstenameisen spielt. Auch ist das Mittelbeinpaar das Einzige, welches die Schrittamplitude, also die körperbezogenen Auslenkung des Beines, erhöht. Grund dafür könnte sein, dass das Mittelbeinpaar morphologisch den größten Aktionsradius besitzt und damit die anderen Beinpaare übergreifen kann.

Wir können zudem einen Einfluss der Laufgeschwindigkeit auf Qualität und Synchronität des Tripods zeigen, denn der TCS-Wert (Tripodkoordinationsstärke) sinkt von einem Höchstwert von 0.8 mit abnehmender Geschwindigkeit bis auf einen Wert von 0. Je schneller das Tier läuft, umso exakter ist der Tripod. Bei langsamen Läufen, die in der Natur ausschließlich in Nestnähe oder unterirdisch stattfinden,

zeigt sich zudem eine größere Variabilität in der Gangarten abweichend vom Tripod. Denn es findet ein Übergang in andere Gangarten wie Wavegait oder Tetrapod statt, welches ein Kontinuum darstellt.

Zusammenfassend kann also gesagt werden, dass *Cataglyphis fortis* Wüstenameisen ihre hohen Laufgeschwindigkeiten durch eine Kombination aus Langbeinigkeit und hoher mittlerer Schrittfrequenz erreichen. Zusätzlich erhöhen Flugphasen die Schrittlänge. Tripods und damit die Schrittlänge konnten als sehr konstante räumliche Einheiten belegt werden. Folglich könnten die räumlich-zeitliche Beständigkeit eine allgemeine Besonderheit der Distanzmessung für schnell laufende Wüstenameisen darstellen. Ein während nahezu dem kompletten Laufgeschwindigkeitsspektrum ausgeführter Tripod könnte dabei helfen, den Navigationsfehler des iterativen Prozesses der Wegintegration zu reduzieren und unterstützt dabei zweifellos die Stabilität des Tieres.

In **Kapitel 5** untersuchen wir ein weiteres natürliches Lokomotionsverhalten der Ameisen, das Rückwärtslaufen. Findet ein Tier ein Futterstück – z.B. eine dem Hitzetod erlegene Arthropode – welches es auf Grund der Größe oder dem Gewicht oder beidem nicht anheben und heimtragen kann, so zieht und schleppt das Tier dieses Futterstück rückwärtslaufend hinter sich her (siehe Abb. 5). Dieses zuvor noch nicht untersuchte natürliche Verhalten wurde von uns in dieser Publikation für *Cataglyphis fortis* in ihrem natürlichen Habitat in Tunesien untersucht.

Erstaunlicherweise zeigen die Tiere, im Vergleich zum Vorwärtslauf, eine wackelige Bewegung und unstabile Beinanordnungen treten auf. Aufgrund des großen Futterstückes zeigen die Tiere ausschließlich langsame Laufgeschwindigkeiten, welche zudem die Stabilität des Laufens mindern, wie bereits aus Kapitel 4 bekannt ist. Diese für die Lokomotion unvorteilhafte Situation kompensieren die Tiere nahezu perfekt. Zum einen streuen die Tarsalpositionen weiter weg vom Körper als bei vorwärtslaufenden Ameisen. Außerdem erhöhen die Tiere den Bodenkontakt, indem oft mehr als drei Beine auf dem Boden stehen und vergrößern zusätzlich auf indirektem Weg ihn weiter durch ihre Mandibeln, die sie in das Futterstück festklemmen. Die Beine, die sich in der Schwingphase befinden, zeigen zudem eine deutlich schnellere Schwing-geschwindigkeit als *Cataglyphis fortis*, was bedeutet, dass die Zeit der Beine in der Luft zusätzlich reduziert wird.

Abb. 5: Rückwärtsziehende *Cataglyphis fortis*, Foto: Sarah E. Pfeffer

Ein weiterer wichtiger Unterschied zum Vorwärtslaufen ist, dass die Tiere keinen Tripod zeigen. Sie zeigen dagegen irreguläre Gangarten, die sehr variabel sind und keinem festen Muster unterliegen. Es zeigt sich beim Betrachten der Laufparameter auch eine Spezialisierung der Beinpaare in dem betrachteten Geschwindigkeitsintervall von 25.8 bis 65.6 mms^{-1}. Die Vorderbeine machen kleine Schritte und dafür aber viele, die Frequenz ist also hoch, wobei die Mittel- und Hinterbeine große Schritte mit

einer niedrigeren Frequenz zeigen. Die Tiere erhöhen also insgesamt im Rückwärtslaufen ihre Geschwindigkeit über die Schrittlängen und die Schrittfrequenz, wohingegen die Tiere beim Vorwärtslaufen in diesem Geschwindigkeitsspektrum ihre Laufgeschwindigkeit einzig über die Frequenz erhöhen. Insgesamt kann somit geschlussfolgert werden, dass die Beine als eine Art separate Einheit agieren, was eine Anpassung an effizientes Rückwärtsziehen ist.

Erstaunlich ist hierbei noch zu erwähnen, dass in einem weiteren bereits publizierten Paper gezeigt werden konnte (siehe Pfeffer und Wittlinger, 2016), dass die Tiere trotz ihrer irregulären Gangart auch rückwärts sicher nach Hause finden, denn in der Länge des Heimlaufes gab es zwischen vorwärts- und rückwärtslaufenden Tieren keinen signifikanten Unterschied. Folglich steuert jedes Bein einzeln zum gesamten Distanzwert der Wegintegration bei. Der Pedometer scheint somit von der irregulären Beinkoordination und vom kompletten Umdrehen der Umwelt bei den langsamen Läufen nicht beeinflusst zu werden und ist demnach nicht abhängig von einem ordentlich konstanten Schrittmuster.

In **Kapitel 6** untersuchen wir das Laufverhalten bei der schnellsten uns bekannten Ameisenart, *Cataglyphis bombycina*, um Vergleiche und Schlüsse ziehen zu können, wie solch kleine Tiere aus dem Extrembiotop Sanddüne, zu so enormen Geschwindigkeiten von 100 Körperlängen pro Sekunde in der Lage sein können. Obwohl *Cataglyphis bombycina* nahe mit *Cataglyphis fortis* verwandt ist, konnten wir erstaunliche Unterschiede aufdecken.

In dieser Publikation ist es uns gelungen, erstmals Läufe nah an der Maximalgeschwindigkeit mit 0.86 mms^{-1} in Tunesien filmen und analysieren zu können, die von Rüdiger Wehner bereits im Jahr 1983 mit 1 ms^{-1} vermutet wurde. Wir können zudem in dieser Publikation zeigen, dass *Cataglyphis bombycina*, anders als *Cataglyphis fortis*, ausschließlich die Tripod Gangart benutzt. Weiterhin ist es erstaunlich, dass die Tiere bereits ab einer Laufgeschwindigkeit von 120 mms^{-1} ihre ersten Flugphasen zeigen, da der Duty-Faktor die 0.5 Marke unterschreitet.

Als wir jedoch die Laufparameter dazu genauer betrachtet haben, fiel auf, dass sich bei höheren Laufgeschwindigkeiten als 120 mms^{-1} die Schrittlänge, aber eben auch die Schrittfrequenz weiter vergrößert. Bei *Cataglyphis fortis* war der Beginn der Flugphasen verbunden mit dem Eintreten des Frequenzplateaus. Dieses Plateau tritt bei *Cataglyphis bombycina* auch ein, aber erst viel später bei einer Laufgeschwindigkeit von ungefähr 250-300 mms^{-1}. Die Gangart ‚Laufen' untergliedert sich also in zwei verschiedene Teile, wobei beide Flugphasen enthalten. Das Tier fliegt bereits, auch wenn es morphologisch gesehen noch laufen könnte. Der Flugphasenanteil liegt ab dieser Laufgeschwindigkeit von 250-300 mms^{-1} konstant bei knapp über 30% pro Schrittzyklus, was bedeutet, dass sich das Tier über ein Drittel der Zeit eines Schrittes in der Luft befindet. Der Anteil vom Tripod beträgt etwa 40 %, unvollständige Tripods mit zwei oder nur einem Bein auf dem Boden bestimmen den Rest, welche den Tieren einen gleitenden Übergang von Tripod zu Flugphase zu Tripod ermöglicht. Die Verteilung der Gangarten ändert sich bei steigender Laufgeschwindigkeit nicht mehr signifikant. Wird die Tripodkoordinationsstärke (TCS) gemessen, welche die Exaktheit des Tripods beschreibt, so kann auch hier gezeigt werden, dass der Wert über das gesamte Laufgeschwindigkeitsspektrum über einem Wert

von 0.8 liegt, was einen nahezu perfekten Tripod Werte von fast 1.0 auftreten könnten beschreibt aber auf eine Abrollbewegung des funktionellen Fußes hindeutet.

Betrachtet man hierzu nun die Phasenbeziehungen der Beine, so heben alle Beine eines Tripod zeitgleich vom Boden ab, was ein großer Unterschied zu *Cataglyphis fortis* darstellt, welche ihr Habitat auf festem Untergrund haben. Dieses zeitgleiche Abdrücken entspricht einem zeitgleichen Kraftimpuls der Beine für die Beschleunigung des Körpers. Es liegt auch nahe, dass die Ameise dadurch weniger in den feinkörnigen Untergrund einsinken könnte. Indiz hierfür ist auch, dass die Standphase auf 7 ms reduziert wird. Im Vergleich dazu liegt die minimale Standphase bei *Cataglyphis fortis* bei 15 ms, dem etwa doppelten Wert. Ein langer Bodenkontakt und somit ein tiefes Einsinken in den Boden wird verhindert. Werden dazu noch die Fußpositionen bei Absetzen und Abheben jedes Beines betrachtet, so fällt auf, dass *Cataglyphis bombycina* ihre Beine näher am Körper und verglichen zu *Cataglyphis fortis* weiter anterior positioniert. Lediglich das Hinterbein, welches morphologisch am ähnlichsten zu *Cataglyphis fortis* ist, zeigt kaum einen Unterschied in der Position.

Dieses Verhalten haben wir als Anpassung an ihr Habitat beschrieben. Denn diese Art von *Cataglyphis* Ameisen kommt ausschließlich in Gebieten vor, in denen es Sanddünen gibt. *Cataglyphis bombycina* gehört zu den hitzetolerantesten Tieren der Welt (Gehring und Wehner, 1995). Außer ihrem silbernen Haarkleid, welches sie vor langwelliger Strahlung schützt und den langen Beinen zeigt diese Ameisenart noch eine weitere Anpassung. Mit einer Höchstlaufgeschwindigkeit von uns gemessen und dokumentiert bei 860 mms^{-1} gehört diese Ameisenart zu den schnellsten der Welt. Dies ist erstaunlich und bedarf noch weiteren Untersuchungen, denn morphologisch betrachtet sind die Beine von *Cataglyphis bombycia* bei einer vergleichbarer Körpergröße zu *Cataglyphis fortis* signifikant (Hinterbeine 10 %, Mittelbeine 15 % und Vorderbeine sogar 20 % a) kürzer.

2.2 Übersicht Publikationen

Diese Doktorarbeit besteht, neben der Einleitung und einem allgemeinen Teil, aus vier Publikationen, wovon drei bereits publiziert sind (Kapitel 3, 4 und 5). Das Manuskript in Kapitel 6 wurde zum Einreichen vorbereitet. Als Überblick sind die Manuskripte hier vollständig mit den jeweiligen Mitautoren, der Fachzeitschrift und dem Link zum Originalartikel aufgezählt.

Kapitel 3: Naturalistic path integration of *Cataglyphis* desert ants on an air cushioned light-weight spherical treadmill (2017)

Hansjürgen Dahmen, Verena Luisa Wahl, Sarah Elisabeth Pfeffer, Hanspeter A.Mallot, Matthias Wittlinger

H.D. and V.L.W. shared first authorship

Journal of Experimental Biology, 220(4), 634-644.

doi: 10.1242/jeb.148213

http://jeb.biologists.org/content/220/4/634

Kapitel 4: Walking and running in the desert ant *Cataglyphis fortis* (2015)

Verena Wahl, Sarah Elisabeth Pfeffer, Matthias Wittlinger

V.W. and S.E.P. shared first authorship.

Journal of Comparative PhysiologyA, 201(6), 645-656,

doi: 10.1007/s00359-015-0999-2

http://link.springer.com/article/10.1007/s00359-015-0999-2

Kapitel 5: How to find home backwards? Locomotion and inter-leg coordination during rearward walking of *Cataglyphis fortis* desert ants (2016)

Sarah Elisabeth Pfeffer, Verena Luisa Wahl, Matthias Wittlinger

Journal of Experimental Biology 219(14), 2110-2118.

doi: 10.1242/jeb.137778

http://jeb.biologists.org/lookup/doi/10.1242/jeb.137778

Kapitel 6: High frequency locomotion in the Saharan silver ant *Cataglyphis bombycina*

Verena Luisa Wahl, Sarah Elisabeth Pfeffer, Matthias Wittlinger

Prepared for publication in the ***Myrmecological News***

2.3 Referenzen

Alexander, R. McNeill (2006). Principles of Animal Locomotion. University Press Group Ltd; Auflage: New Ed

Bässler, U. (1977). Sensory control of leg movement in the stick insect *Carausius morosus*. *Biological cybernetics*, **25**(2), 61-72.

Brower, L. (1996). Monarch butterfly orientation: missing pieces of a magnificent puzzle. *J. Exp. Biol*. **199**, 93 – 103.

Buehlmann, *C.*, Hansson, B. S., and Knaden, M. (2012). Desert ants learn vibration and magnetic landmarks. *PLoS One*, **7**(3), e33117.

Cerdá, X., Retana, J., Carpintero, S., and Cros, S. (1996). An unusual ant diet: *Cataglyphis floricola* feeding on petals. *Insectes Sociaux*, **43**(1), 101-104.

Cerdá, X., and Retana, J. (2000). Alternative strategies by thermophilic ants to cope with extreme heat: individual versus colony level traits. *Oikos*, **89**(1), 155-163.

Chittka, L., Williams, N. M., Rasmussen, H., and Thomson, J. D. (1999). Navigation without vision: bumblebee orientation in complete darkness. *Pro. R. SoC. Lond. Ser*. B **266**, 45-50.

Collett, T. S., and Land, M. F. (1975). Visual control of flight behaviour in the hoverfly Syritta pipiens L. *J. Comp. Physiol.*, **99**(1), 1-66.Cornetz, 1910, S.93

Cruse, H. (1976). The control of body position in the stick insect (*Carausius morosus*), when walking over uneven surfaces. *Biological Cybernetics*, **24**(1), 25-33.

Cruse, H. (1979). The control of the anterior extreme position of the hindleg of a walking insect, *Carausius morosus*. *Physiological Entomology*, **4**(2), 121-124.

Darwin, *C.* (1873). Origin of certain instincts. *Nature* **7**, 417-418.

Delcomyn, F. (1971). The locomotion of the cockroach *Periplaneta americana*. *J. Exp. Biol*., **54**(2), 443-452.

Délye, G. (1957). Observations sur la fourmi saharienne *Cataglyphis Bombycina* Rog. *Insectes Sociaux*, **4**(2), 77-82.

Dietrich, B., and Wehner, R. (2003). Sympatry and allopatry in two desert ant sister species: how do *Cataglyphis bicolor* and *C. savignyi* coexist?. *Oecologia*, **136**(1), 63-72.

Dillier, F. X., and Wehner, R. (2004). Spatio-temporal patterns of colony distribution in monodomous and polydomous species of North African desert ants, genus *Cataglyphis*. *Insectes Sociaux*, **51**(2), 186-196.

Draper, *C.* S., Wrigley, W. and Hovorka, J. (1960). Inertial guidance. Pergamon Press, New York.

Duelli, P. (1972). The relation of astromenotactic and anemomenotactic orientation mechanisms in desert ants, *Cataglyphis bicolor* (Formicidae, Hymenoptera). In Information Processing in the Visual Systems of Anthropods (pp. 281-286). Springer Berlin Heidelberg.

Esch, H. E., and Burns, J. E. (1995). Honeybees use optic flow to measure the distance of a food source. *Naturwissenschaften*, **82**(1), 38-40.

Etienne, A. S. Teroni, E. Maurer, R. Portenier, V. and Saucy, F. (1985). Short distance homing in a small mammal: the role of exteroceptive cues and path integration. *Experentia* **41**, 122-125.

Etienne, A. S. and Jeffery, J. (2004). Path integration in mammals. *Hippocampus* **14**, 180-192.

Förster, A. (1850). Eine Centurie neuer Hymenopteren. Zweite Dekade. Verhandlungen des Naturhistorischen Vereins des Preussischen Rheinlande, Westfalens u. des Regierungsbezirks Osnabruck **7**, 485-500.

Frisch, K. v. (1950). Die Sonne als Kompaß im Leben der Bienen. *Experientia* **6** , 210–221.

Frisch, K. v. (1965). Tanzsprache und Orientierung der Bienen. Berlin: Springer.

Frisch, K. v. (1967). The dance language and Orientation of Bees. Cambridge: Haravard University Press.

Full, R. J., and Tu, M. S. (1991). Mechanics of a rapid running insect: two-, four-and six-legged locomotion. *J. Exp. Biol*., **156**(1), 215-231.

Gehring, W. J., and Wehner, R. (1995). Heat shock protein synthesis and thermotolerance in *Cataglyphis*, an ant from the Sahara desert. *Proceedings of the National Academy of Sciences*, **92**(7), 2994-2998.

Gladwin, T. (1970). East is a big bird; navigation and logic on Puluwat atoll. Cam-bridge: Haravard University Press.

Görner, P. and Class, B. (1985). in Neurobiology of Arachnids (ed.. Barth, F. G), pp. 275-297. Berlin: Springer.

Grabowska, M., Godlewska, E., Schmidt, J., and Daun-Gruhn, S. (2012). Quadrupedal gaits in hexapod animals–inter-leg coordination in free-walking adult stick insects. *J. Exp. Biol*., **215**(24), 4255-4266.

Graham, D. (1972). A behavioural analysis of the temporal organisation of walking movements in the 1st instar and adult stick insect (*Carausius morosus*). *J. Comp. Physiol.*, **81**(1), 23-52.

Graham, D., and Bässler, U. (1981). Effects of afference sign reversal on motor activity in walking stick insects (*Carausius morosus*). *J. Exp. Biol*., **91**(1), 179-193.

Harkness, R. D., and Wehner, R. (1977). *Cataglyphis*. *Endeavour*, **1**(3), 115-121.

Heß, D., Koch, J. and Ronacher, B. (2009). Desert ants do not rely on sky compass information for the perception of inclined path segments. *J. Exp. Biol*. **212**, 1528–1534.

Hoffmann, G. (1984). Orientation behaviour of the desert woodlouse *Hemilepistus reaumuri*: adaptions to ecological and physiological problems. in The biology of terrestrial isopods (eds. Sutton, S. L., Holdich, D. M..), pp. 405-422. Symp. Zool. So*C.* London.

Hughes, G. M. (1952). The co-ordination of insect movements. *J. Exp. Biol*., **29**(2), 267-285.

Johnson, *C.* G. (1969). Migration and dispersal of insects by flight. Migration and dispersal of insects by flight.

Knaden, M., and Wehner, R. (2003). Nest defense and conspecific enemy recognition in the desert ant *Cataglyphis fortis*. *Journal of Insect Behavior*, **16**(5), 717-730.

Lebhardt, F., Koch, J., and Ronacher, B. (2012). The polarization compass dominates over idiothetic cues in path integration of desert ants. *J. Exp. Biol*., **215**(3), 526-535.

Lebhardt, F. (2015). The desert ant's celestial compass system: evaluating the role of the polarization compass of *Cataglyphis fortis* (Doctoral dissertation, Berlin, Humboldt Universität zu Berlin, Diss., 2015).

Lenoir, A., Aron, S., Cerda, X., and Hefetz, A. (2009). *Cataglyphis* desert ants: a good model for evolutionary biology in Darwin's anniversary year - A review. *Israel J. of Entomology*, **39**, 1–32.

Marshall, J., and Cronin, T. W. (2011). Polarisation vision. *Current Biology*, **21**(3), R101-R105.

McMeeking, R. M., Arzt, E., and Wehner, R. (2012). *Cataglyphis* desert ants improve their mobility by raising the gaster. *Journal of theoretical biology*, **297**, 17-25.

Mittelstaedt, M. L. and Mittelstaedt, H. (1980). Homing by path integration in a mammal. *Naturwissenschaften* **67**, 566-567.

Mittelstaedt, H. and Mittelstaedt, M. L. (1982). Homing by path integration. in: Avian Navigation (eds. Papi, F., Wallra, H. G.). pp. 290-297. Berlin: Springer.

Mittelstaedt, H. (1983). The role of multimodal convergence in homing by path inte-gration. *Fortschr. Zool.* **28**, 197-212.

Mittelstaedt, H. (1985). in Neurobiology of Arachnids (ed. Barth, F. G.), pp. 298-316. Berlin: Springer.

Molet, M., Maicher, V., and Peeters, *C.* (2014). Bigger helpers in the ant *Cataglyphis bombycina*: increased worker polymorphism or novel soldier caste?. *PloS one*, **9**(1), e84929.

Moller, P. and Görner, P. (1993). Homing by path integration in the spider *Agelena labyrinthica* Clerck. *J. Comp. Physiol*. *A* **174**, 221–229.

Müller, M. and Wehner, R. (1988). Path integration in desert ants, *Cataglyphis fortis*. Pro*C.* Natl. Acad. Sci. USA **85**, 5287-5290.

Müller, M., and Wehner, R. (1994). The hidden spiral: systematic search and path integration in desert ants, *Cataglyphis fortis*. *J. Comp. Physiol*. *A*, **175**(5), 525-530.

Pfeffer, S. E., and Wittlinger, M. (2016). Optic flow odometry operates independently of stride integration in carried ants. *Science*, **353**(6304), 1155-1157.

Pomozi, I., Horvath, G., and Wehner, R. (2001). How the clear-sky angle of polarization pattern continues underneath clouds: full-sky measurements and implications for animal orientation. *J. Exp. Biol*., **204**, 2933-2942.

Reinhardt, L., Weihmann, T., and Blickhan, R. (2009). Dynamics and kinematics of ant locomotion: do wood ants climb on level surfaces? *J. Exp. Biol*., **212**(15), 2426-2435.

Reinhardt, L., and Blickhan, R. (2014). Level locomotion in wood ants: evidence for grounded running. *J. Exp. Biol*., **217**(13), 2358-2370.

Retana, J., Cerdá, X., and Espadaler, X. (1991). Arthropod corpses in a temperate grassland: a limited supply?. *Ecography*, **14**(1), 63-67.

Ritzmann, R., and Zill, S. N. (2013). Neuroethology of insect walking. *Scholarpedia*, **8**(9), 30879.

Ronacher, B., and Wehner, R. (1995). Desert ants *Cataglyphis fortis* use self-induced optic flow to measure distances travelled. *J. Comp. Physiol*. *A*, **177**(1), 21-27.

Ruano, F., Tinaut, A., and Soler, J. J. (2000). High surface temperatures select for individual foraging in ants. *Behavioral Ecology*, **11**(4), 396-404.

Saint Paul, V. v. (1982). Homing by path integration. in: Avian Navigation (eds. Papi, F., Wallra, H. G.). pp. 298-307. Berlin: Springer.

Santschi, F. (1911). Observations et remarques critiques sur le mécanisme de l'orientation chez les fourmis. Albert Kündig.

Schilling, M., Hoinville, T., Schmitz, J., and Cruse, H. (2013). Walknet, a bio-inspired controller for hexapod walking. *Biological Cybernetics*, **107**(4), 397-419.

Schmid-Hempel, P., and Schmid-Hempel, R. (1984). Life duration and turnover of foragers in the ant *Cataglyphis Bicolor* (Hymenoptera, Formicidae). *Insectes Sociaux*, **31**(4), 345-360.

Schöne, H. (1996). Optokinetic speed control and estimation of travel distance in walking honeybees. *J. Comp. Physiol. A*, **179**(4), 587-592.

Séguinot, V., Maurer, R., and Etienne, A. S. (1993). Dead reckoning in a small mammal: the evaluation of distance. *J. Comp. Physiol. A* **173**, 103-113.

Seidl, T., and Wehner, R. (2006). Visual and tactile learning of ground structures in desert ants. *J. Exp. Biol.*, **209**(17), 3336-3344.

Seidl, T., and Wehner, R. (2008). Walking on inclines: how do desert ants monitor slope and step length. *Frontiers in zoology*, **5**(1), 1.

Shi, N. N., Tsai, *C. C.*, Camino, F., Bernard, G. D., Yu, N., and Wehner, R. (2015). Keeping cool: Enhanced optical reflection and radiative heat dissipation in Saharan silver ants. *Science*, **349**(6245), 298-301.

Sommer, S. and Wehner, R. (2012). Leg allometry in ants: Extreme long-leggedness in thermophilic species. *Arthropod structure & development* **41**, 71–77.

Srinivasan, M. V., Zhang, S. W., and Reinhard, J. (2006). Small brains, smart minds: vision, perception, navigation and 'cognition' in insects. *Invertebrate Vision*.

Steck, K., Hansson, B. S. and Knaden, M. (2009). Smells like home: Desert ants, *Cataglyphis fortis*, use olfactory landmarks to pinpoint the nest. *Front. Zool*. 6.

Thiélin-Bescond, M. and Beugnon, G. (2005). Vision-independent odometry in the ant *C. cursor*. *Naturwissenschaften*, 92, 193-197.

Urquhart, F. A., and Urquhart, N. R. (1978). Autumnal migration routes of the eastern population of the monarch butterfly (*Danaus p. plexippus L.; Danaidae; Lepidoptera*) in North America to the overwintering site in the Neovolcanic Plateau of Mexico. *Canadian J. of Zoology*, **56**(8), 1759-1764.

Watson, J. T., Ritzmann, R. E., Zill, S. N., and Pollack, A. J. (2002). Control of obstacle climbing in the cockroach, *Blaberus discoidalis*. I. Kinematics. *J. Comp. Physiol. A*, **188**(1), 39-53.

Wehner, R. (1981). Spatial vision in arthropods. Handbook of sensory physiology.

Wehner, R. (1983). Taxonomie, Funktionsmorphologie und Zoogeographie der saharischen Wüstenameise *Cataglyphis fortis* (Forel 1902) stat. nov. Senckenbergiana biol, **64**, 89-132.

Wehner, R. (1987). Spatial organization of foraging behavior in individually searching desert ants, *Cataglyphis* (Sahara desert) and *Ocymyrmex* (Namib desert). *Experientia. Supplementum*, (**54**), 15-42.

Wehner, R. (1989). Neurobiology of polarization vision. *Trends Neurosci*. **12**, 353-359.

Wehner, R. (1992). Arthropods. In Animal homing (pp. 45-144). *Springer Netherlands*.

Wehner, R. (1994). Himmelsbild und Kompaßauge: Neurobiologie eines Navigations-systems. Verh. *Dtsch. Zool. Ges*. 87, 9-37.

Wehner, R. (1997). The ant's celestial compass system: spectral and polarisation chan-nels. In Orientation and Communication in Arthropods (ed. M. Lehrer), pp. 145-185. Basel: Birkhäuser Verlag.

Wehner, R. (2003). Desert ant navigation: how miniature brains solve complex tasks. *J. Comp. Physiol. A* **189**, 579-588.

Wehner, R. (2009). The architecture of the desert ant's navigational toolkit (Hymenoptera: Formicidae). *Myrmecological News*, **12**, 85-96.

Wehner, R. and Duelli, P. (1971). The spatial orientation of desert ants, *Cataglyphis bicolor*, before sunrise and after sunset. *Experientia* **27**, 1364–1366.

Wehner, R., and Labhart, T. (2006). Polarization vision. In Invertebrate vision (pp. 291-348). Cambridge University Press.

Wehner, R. and Lafranconi, B. (1981). What do the ants know about the rotation of the sky? *Nature* **293** , 731–733.

Wehner, R., and Menzel, R. (1969). Homing in the ant *Cataglyphis bicolor*. *Science*, **164**(3876), 192-194.

Wehner, R. and Müller, M. (1985). Does interocular transfer occur in visual navigation by ants? *Nature* **315**, 228–229.

Wehner, R., and Müller, M. (2006). The significance of direct sunlight and polarized skylight in the ant's celestial system of navigation. Proceedings of the National Academy of Sciences, **103**(33), 12575-12579.

Wehner, R. and Räber, F. (1979). Visual spatial memory in desert ants, *Cataglyphis bicolor* (Hymenoptera: Formicidae). *Experientia* **35**, 1569–1571.

Wehner, R., and Srinivasan, M. V. (1981). Searching behaviour of desert ants, genus *Cataglyphis* (Formicidae, Hymenoptera). *J. Comp. Physiol*, **142**(3), 315-338.

Wehner, R., and Srinivasan, M. V. (2003). Path integration in insects. In The Neurobiology of Spatial Behaviour (pp. 9-30). Oxford University Press.

Wehner, R., and Wehner, S. (1986). Path integration in desert ants. Approaching a long-standing puzzle in insect navigation. Monitore Zoologico *Italiano-Italian Journal of Zoology*, **20**(3), 309-331.

Wehner, R. and Wehner, S. (1990). Insect navigation: use of maps or Ariadne's thread? *Ethology Ecology & Evolution* **2**, 27–48.

Wehner, R., and Wehner, S. (2011). Parallel evolution of thermophilia: daily and seasonal foraging patterns of heat-adapted desert ants: *Cataglyphis* and *Ocymyrmex* species*. *Physiological Entomology,* **36**(3), 271-281.

Wendler, G. (1968). Ein Analogmodell der Beinbewegungen eines laufenden Insekts. Kybernetik, **18**, 68-74.

Williams, *C.* B. (1958). Insect migration. Collons, London.

Willot, Q., Simonis, P., Vigneron, J. P., and Aron, S. (2016). Total Internal Reflection Accounts for the Bright Color of the Saharan Silver Ant. *PloS one*, **11**(4), e0152325.

Wintergerst, S. and Ronacher, B. (2012). Discrimination of inclined path segments by the desert ant *Cataglyphis fortis. J. Comp. Physiol. A* **198**, 363–373.

Wittlinger, M., Wehner, R., and Wolf, H. (2006). The ant odometer: stepping on stilts and stumps. *Science*, **312**(5782), 1965-1967.

Wittlinger, M., Wehner, R., and Wolf, H. (2007). The desert ant odometer: a stride integrator that accounts for stride length and walking speed. *J.Exp. Biol.*, **210**(2), 198-207.

Wittlinger, M., and Wolf, H. (2013). Homing distance in desert ants, *Cataglyphis fortis*, remains unaffected by disturbance of walking behaviour and visual input. *Journal of Physiology-Paris*, **107**(1), 130-136.

Wolf, H. and Wehner, R. (2000). Pinpointing food sources: olfactory and anemotactic orientation in desert ants, *Cataglyphis fortis. J. Exp. Biol.* **203**, 857–868.

Wolf, H., Wittlinger, M., and Bolek, S. (2012). Re-visiting of plentiful food sources and food search strategies in desert ants. *Frontiers in Neuroscience*, **6**(102), 1-9.

Wohlgemuth, S., Wehner, R., and Ronacher, B. (2001). Ant odometry in the third dimen-sion. *Nature* **9**, 1043-1050.

Wohlgemuth, S., Wehner, R., and Ronacher, B. (2002). Distance estimation in the third dimension in desert ants. *J. Comp. Physiol. A* **180**, 273-281.

Wosnitza, A., Bockemühl, T., Dübbert, M., Scholz, H., and Büschges, A. (2013). Inter-leg coordination in the control of walking speed in *Drosophila. J. Exp. Biol.*, **216**(3), 480-491.

Zollikofer, *C.* P. E. (1988). PhD thesis, Vergleichende Untersuchungen zum Laufverhalten von Ameisen, University of Zürich.

Zollikofer, *C.* P. E. (1994a). Stepping patterns in ants I. Influence of speed and curvature. *J. Exp. Biol.* **192**, 95-106.

Zollikofer, *C.* P. E. (1994b). Stepping patterns in ants II. Influence of body morphology. *J. Exp. Biol*. **192**, 107-118.

Zollikofer, *C.* P. E. (1994c). Stepping patterns in ants III. Influence of load. *J. Exp. Biol*. **192**, 119-127.

Kapitel 3

3. Manuscript 1

Naturalistic path integration of *Cataglyphis* desert ants on an air cushioned light-weight spherical treadmill

Hansjürgen Dahmen[1], Verena L. Wahl[2], Sarah E. Pfeffer[2], Hanspeter A. Mallot[1], Matthias Wittlinger[2]

HD and VLW share first authorship

[1] Cognitive Sciences, University of Tübingen, Auf der Morgenstelle 28, 72076 Tübingen, Germany
[2] Institute of Neurobiology, Ulm University, Helmholtzstr. 10/1, 89081 Ulm, Germany

The final article is published 2017 in the **Journal of Experimental Biology,** 220(4), 634-644.
and is available under
http://jeb.biologists.org/content/220/4/634
doi: 10.1242/jeb.148213

This article is licensed under the Creative Commons Attribution CC-BY-3.0 License (https://creativecommons.org/licenses/by/3.0/) and the inclusion in the theses is authorized under http://www.biologists.com/user-licence-1-1/

Journal of experimental biology by Company of Biologists Reproduced with permission of COMPANY OF BIOLOGISTS LTD. in the format Republish in a thesis/dissertation via Copyright Clearance Center (Order Detail ID: 70635456, Confirmation Number: 11661718).

© 2017. Published by The Company of Biologists Ltd | Journal of Experimental Biology (2017) 220, 634-644 doi:10.1242/jeb.148213

RESEARCH ARTICLE

Naturalistic path integration of *Cataglyphis* desert ants on an air-cushioned lightweight spherical treadmill

Hansjürgen Dahmen[1,*,‡], Verena L. Wahl[2,‡], Sarah E. Pfeffer[2], Hanspeter A. Mallot[1] and Matthias Wittlinger[2,3,*]

ABSTRACT

Air-cushioned spheres are widely used as treadmills to study behavioural and neurophysiological questions in numerous species. We describe an improved spherical treadmill design that reliably registers the path and walking behaviour of an animal walking on top of the sphere. The simple and robust set-up consists of a very light hollowed styrofoam ball supported by an air stream in a hollow half sphere and can be used indoors and outdoors. Two optical mouse sensors provided with lenses of 4.6 mm focal length detect the motion of the sphere with a temporal resolution of more than 200 frames s^{-1} and a spatial resolution of less than 0.2 mm. The treadmill can be used in an open- or closed-loop configuration with respect to yaw of the animal. The tethering allows animals to freely adjust their body posture and in the closed-loop configuration to quickly rotate around their yaw axis with their own moment of inertia. In this account, we present the first evidence of naturalistic homing navigation on a spherical treadmill for two species of *Cataglyphis* desert ants. We were able to evaluate with good precision the walking speed and angular orientation at any time. During homing the ants showed a significant difference in walking speed between the approach and search phases; moreover, they slowed down significantly as soon as they reached zero vector state, the fictive nest position.

KEY WORDS: Fast response treadmill, Optical mouse motion sensors, Ant navigation, Homing, Orientation behaviour

INTRODUCTION

For several decades spherical treadmills have been important tools in the study of neurophysiological and behavioural questions in many animals. To control the behaviour of walking animals on spherical treadmills two types of treadmills have been invented; a sphere actively rotated by two (Kramer–Kugel; Kramer, 1976) or four (Götz and Gambke, 1968; Varjú, 1975) servo-motors and an air-cushioned passive low-mass sphere that is rotated by the animal itself. In the first case the position of the animal on top of the sphere is recorded by some device and any deviation from the zenith position is fed back to the servo motors that rotate the ball to bring the animal back to the zenith position. In these devices the animal is completely free to move. The difficulty, however, is to make the electronic servo-path from the animal position detector to the motor position correction response fast and precise enough to keep the animal on top of the sphere. It has been concluded that for fast-starting, -stopping and -turning animals (e.g. cockroaches), it is impossible to keep the animals on the zenith of the servo-rotated sphere. In the second type of treadmill the animal is kept fixed on top of the sphere and rotates the sphere itself. Here, the sphere the animal is walking on must be supported with as low friction as possible. To our knowledge the first air-cushioned Styrofoam sphere used as a treadmill in experiments with *Drosophila* was invented by Erich Buchner (Buchner, 1976), with the motion of this small sphere registered optically. In other earlier treadmills the rotation of the ball was registered by two light wheels touching the sphere along its equator at right angles with respect to each other (Dahmen, 1980; Doherty and Pires, 1987; Ye et al., 1995), like in the classic PC mouse with a rubber sphere touching two easily rotatable axes with spoke wheels interrupting light barriers. Later, optical computer mouse sensors were used to register the sphere's rotation (Mason et al., 2001; Hölscher et al., 2005; Hedwig and Poulet, 2004; Lott et al., 2007; Seelig et al., 2010).

Most recently, the so-called FicTrac method has been introduced (Moore et al., 2014). The motion of an air-cushioned sphere is registered by a camera monitoring the movement of a locally unique contrast pattern applied to the sphere. The advantage of this method is that the position of the patterned sphere can be extracted by image-comparing techniques in absolute coordinates where errors do not accumulate in time. However, the sampling rate is limited by the frame rate of the camera, and good imaging of the sphere pattern has to be guaranteed, including proper illumination.

In this account we describe an improved air-suspended spherical treadmill design (see Materials and Methods) with an extremely lightweight white spherical Styrofoam shell. The air cushion is generated by an air stream let in through a single hole in the bottom of a hollow half sphere, the air cup, made of aluminium to prevent electrostatic loading of the Styrofoam sphere. The air stream can be provided by an inexpensive membrane pump in conjunction with a simple air vessel.

The treadmill can be configured as a closed- or open-loop device with respect to yaw of the animal. In the open-loop configuration the body orientation of the animal is kept fixed in space and the sphere is allowed to rotate about all three axes. In the closed-loop configuration the animal is allowed to turn with practically no friction about the yaw axis with its own moment of inertia. Thus very fast turns are allowed and can be monitored. In the closed-loop configuration yaw of the sphere must be inhibited. In both configurations the design of the tether allows the animal to adjust its posture comfortably on top of the sphere. Motion of the sphere is reliably registered by two optical mouse sensors provided with a distance-adjustable external lens. The sampling rate of theoretical 6 kHz is artificially reduced to ~200 Hz to guarantee a stable rate, the spatial resolution of the motion recording is 0.16 mm. The speed of the sphere's surface is limited to 5.6 m s^{-1}. Last but not least,

[1]Department of Biology, University of Tübingen, Auf der Morgenstelle 28, Tübingen 72076, Germany. [2]Institute of Neurobiology, Ulm University, Helmholtzstrasse 10/1, Ulm 89081, Germany. [3]Institute of Biology I, Albert-Ludwigs University of Freiburg, Hauptstrasse 1, Freiburg 70104, Germany.
‡These authors are joint first authors

*Authors for correspondence (Hansjuergen.dahmen@uni-tuebingen.de; matthias.wittlinger@biologie.uni-freiburg.de)

M.W., 0000-0002-9484-0179

Received 15 August 2016; Accepted 28 November 2016

Journal of Experimental Biology

RESEARCH ARTICLE Journal of Experimental Biology (2017) 220, 634-644 doi:10.1242/jeb.148213

owing to the simple and robust hardware, the treadmill is easy to use indoors in the laboratory as well as outdoors in the field.

The most important question is whether animals on the treadmill show naturalistic behaviour. We chose the *Cataglyphis* desert ant that is well known for its robust homing behaviour. *Cataglyphis* desert ants are the true navigators of hot and dry North African deserts. When searching for food they cover large distances in the vast and open landscape to find dead insects or small arthropods that have succumbed to the torridity of the desert. The ants employ path integration, a form of vector navigation, to bring back the food item to the nest as quickly as possible. Like sailors before the advent of GPS navigation, the ants have to integrate angles steered and distances travelled during the entire foraging run and continuously compute their current position relative to their starting position (Müller and Wehner, 1988; Wehner and Wehner, 1990; Collett and Collett, 2000; Ronacher, 2008). Once they have found a food item they are extremely motivated to bring it to the colony and immediately start their homing run. Homing *Cataglyphis* ants swiftly run back to the nest on the beeline, the so-called home vector, which was acquired during the outbound run. Is it possible for the ants to navigate, or rather, path integrate, on the air-suspended spherical treadmill? And if so, how does their behaviour on the treadmill apparatus compare with their behaviour in the natural habitat?

MATERIALS AND METHODS

General considerations on treadmills

Forces and torques

When considering spherical treadmills we have to consider the forces and torques the animal applies on its path, applying discrimination between straight forwards motion and turns.

For forward motion on a sphere with the moment of inertia θ around an axis through its centre we compare the force the animal has to exert to accelerate its mass (M_{animal}) on flat ground with the force the animal has to exert to accelerate the sphere with radius R when tethered on top of the sphere. It can easily be shown that both forces are the same if:

$$\theta/R^2 = M_{animal}. \quad (1)$$

We call θ/R^2 the effective mass (M_{eff}) of the sphere. Ideally M_{eff}=M_{animal}. Because for a homogeneous sphere:

$$\theta_{sphere} = 0.4 M_{sphere} R^2, \quad (2)$$

a thin walled spherical shell:

$$\theta_{shell} = 2/3 M_{shell} R^2, \quad (3)$$

the ideal mass of the sphere the animal runs on should be:

$$M_{sphere} = 2.5 M_{animal}, \quad (4)$$

$$M_{shell} = 1.5 M_{animal}. \quad (5)$$

For most small animals like insects available Styrofoam balls are too heavy and therefore must be hollowed. We manufactured hollowed Styrofoam spheres of 3, 5, 10, 15, 20 and 50 cm diameter with masses of 0.07, 0.3, 1.7, 3, 8 and 85 g, respectively (see Fig. S1).

It might be expected that for small animals, like *Cataglyphis* ants with a body mass of 10 to 60 mg, a 5 cm sphere (300 mg) would be too inert by a factor between 30 and 5. Nonetheless, it turned out that they run quite well on such a ball. Moreover, flies (*Musca domestica*) run on a 5 cm ball, and even *Drosophila* on a 3 cm ball. For larger animals like mice a 20 cm ball of 8 g is actually too light, as is a 50 cm ball of 80 g for rats. In those cases the wall thickness needs to be increased.

For turns, the moment of inertia of the animal can be estimated by a horizontal rod of length L and mass M rotating about the vertical axis through its centre:

$$\theta_{rod} = ML^2/12. \quad (6)$$

The ratio $\theta_{shell}/\theta_{rod}$ for a 5 cm shell of 300 mg and a rod representing a *Cataglyphis* ranges from ∼3000 for a small ant (10 mg mass, 0.7 cm body length) to ∼100 for a large ant (60 mg, 1.5 cm). For studies of the yaw response of animals it is therefore desirable to give the animals the freedom to yaw by themselves with their own moment of inertia about the vertical axis (see 'Tethering', below).

Treadmill configurations

There are two possible configurations of the treadmill, an open and a closed loop with respect to yaw of the animal (a schematic drawing of the two configurations is given in Fig. S3).

In the open-loop configuration the animal is fixed in its azimuth and rotates the sphere around the yaw axis when it turns, whereas the visual surrounding does not change its azimuth with respect to the animal. The sphere must be free to rotate about all three axes. The disadvantage of this treadmill configuration is that especially small animals have to overcome the much larger moment of inertia of the sphere around the yaw axis compared with their own moment of inertia, as discussed above.

In the closed-loop configuration the animal is allowed to freely rotate about its vertical axis and to adjust its azimuth on top of the sphere. The advantage of this set-up is that the animal can rotate around the yaw axis with its own moment of inertia, which allows for natural quick azimuthal changes. In this configuration the sphere must be prevented from rotations about the yaw axis.

Spherical shell production

Precise Styrofoam spheres were produced by boiling standard Styrofoam spheres in an aluminium precision spherical mould for 3 to 15 min, depending on the size of the sphere. The mould consisted of two half-spheres of a slightly smaller diameter (−1 mm) than the raw balls. At ∼100°C the Styrofoam melts and the rest of the gas dissolved in the plastic material makes it expand so that the mould is filled to its spherical edges. After cooling the mould in cold water the two halves are taken apart and the precise sphere taken out and cut into two halves using a tensioned thin steel wire of 0.1 mm diameter, heated by an AC current regulated in order to control the temperature of the wire.

To hollow the sphere, most of the material of its two halves was cut out by hand using a heated loop of thin steel wire. To get a spherical shell as light as possible and with a wall thickness as equal as possible, one half of the precision mould was placed and precisely centred on a turntable (see Fig. S1). The turntable could be rotated about a vertical axis by a stepper motor, the rotation speed of which could be quickly and easily controlled over a wide range. A small heated steel wire loop was fastened on a small base that could be rotated about a horizontal axis that crossed the axis of the turntable exactly at the centre of the sphere.

The wire loop could be adjusted such that it was rotated along a circle of a slightly smaller radius than that of the mould along a longitudinal line of the latter (i.e. it was moved at a small constant distance from the mould wall at all elevations of the mould half-sphere). By putting the roughly hollowed Styrofoam half sphere into the mould, rotating the turntable, heating the loop, and adjusting it at

Journal of Experimental Biology

RESEARCH ARTICLE Journal of Experimental Biology (2017) 220, 634-644 doi:10.1242/jeb.148213

stepwise increased elevations, the rest of the material was cut out in rings down to a thin and light half sphere. The speed of the turntable and the heat of the steel loop have to be adjusted carefully so that the wire loop cuts out the material but does not melt too much of it. After hollowing, the two half spheres were glued together by as little as possible of a two-component epoxy glue (UHU plus), in precisely the same orientation relative to each other as they were cut into halves. In this way spheres of the following diameters and masses were produced (see Fig. S2): 3 cm, 0.07 g; 5 cm, 0.3 g; 10 cm, 1.7 g; 20 cm, 8 g; 50 cm, 85 g.

The air cushion

Our spherical shells are supported by a hollow half sphere, the air cup, made of aluminium to prevent electrostatic loading of the Styrofoam sphere. The air is let in through a single hole in the bottom, which is sufficient because Bernoulli forces keep the sphere in a stable position in the middle of the cup independent of the strength of the air stream. With a strong air stream the sphere is even sucked into the cup, and it is possible to turn the cup upside down and the sphere is kept in place and does not fall out. It is not necessary to blow in the air through several holes in the cup to provide a uniform air support. It may be difficult to control a more or less equal air stream through all holes, and in most cases the air stream leaving small holes with high velocity would produce noise. In addition, the light shell surface may work as a noise amplifier. With a relatively large hole in the bottom, the supporting air stream can be made very slow and free of noise. For spheres up to 20 cm diameter a sufficient air stream can be provided by an inexpensive membrane pump connected to an air vessel (for example, a plastic bottle with two holes in its cap). For spheres of up to 10 cm diameter the air cup should have a diameter ~1 mm larger than the sphere, for larger spheres it should be ~2 mm larger. The depth of the air cup should be slightly less than the radius of the sphere so that the equator of the sphere remains visible, which is of advantage for monitoring the ball's motion.

In the open-loop setup the air cup is simply set up horizontally. In the closed-loop setup the sphere must be prevented from yaw. For this purpose the air cup is tilted by about 10 deg. The sphere floats on the air cushion against two light disks that touch the sphere along the equator (see Fig. 1B–D). The disks are mounted on horizontally aligned thin steel axes with tipped ends that are supported by tip bearings normally used in alarm clocks. The horizontal position of the disks and thus that of the sphere in the cup can be adjusted by micro-manipulators (see Fig. 1B and Fig. S2B,C). The sphere can now rotate about all axes that lie in the plane of the two touch points of the wheels and the centre of the sphere but any rotatory component orthogonal to this plane is disabled (Fig. S3A,B). The two small wheels that prevent the sphere from yaw add ~2% to the moment of inertia in the case of a 5 cm sphere, and less for larger spheres.

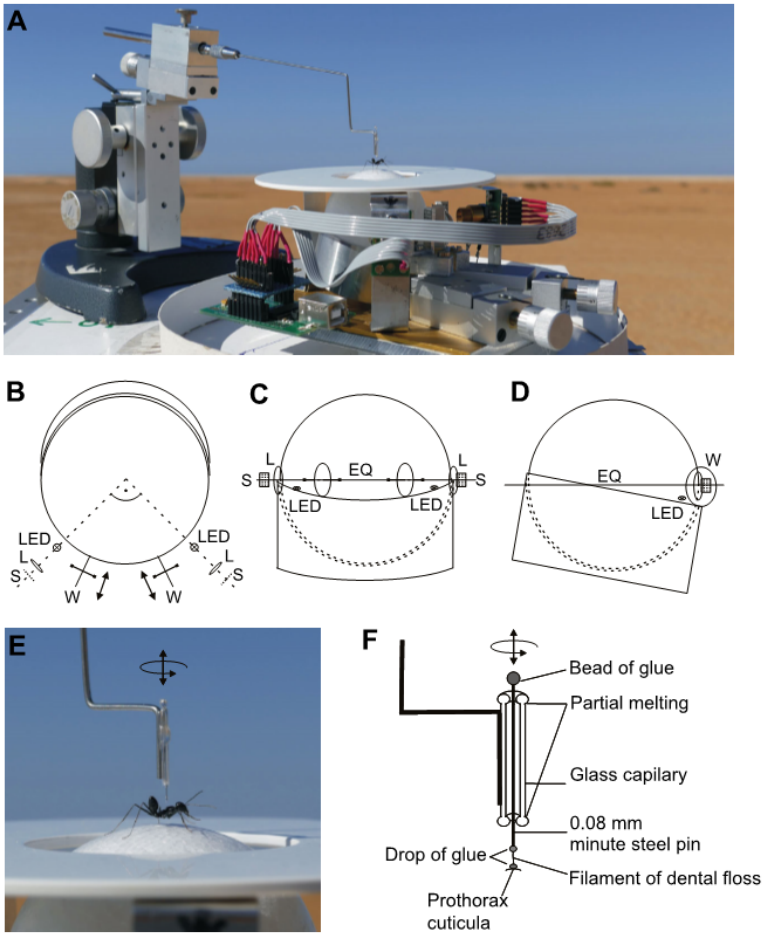

Fig. 1. Closed-loop system: experimental setup and animal tethering. (A) *Cataglyphis fortis* on the closed-loop treadmill with a styrofoam sphere of 5 cm diameter in the desert of Tunisia (complete overview). (B–F) Closed-loop configuration. (B) Top view, (C) front view, (D) side view. The air cup is tilted by 10 deg. Two wheels (W) are mounted on horizontal tip-supported axes and touch the sphere in the plane of its equator (EQ), thus preventing any yaw of the sphere. Motion of the sphere is monitored by two optical mouse sensors (S) that look at 90 deg of azimuth with respect to each other through lenses (L) to the equator of the sphere. Two somewhat tangentially shining LEDs enhance the contrast of the sphere surface sufficiently for safe sensor recordings. The two wheels can be moved horizontally (indicated by arrows in B) by micromanipulators, thus permitting centring of the sphere in the cup. (E) Prepared animal on the holder. (F) Schematic drawing of the holder of the closed-loop configuration.

Journal of Experimental Biology

RESEARCH ARTICLE Journal of Experimental Biology (2017) 220, 634-644 doi:10.1242/jeb.148213

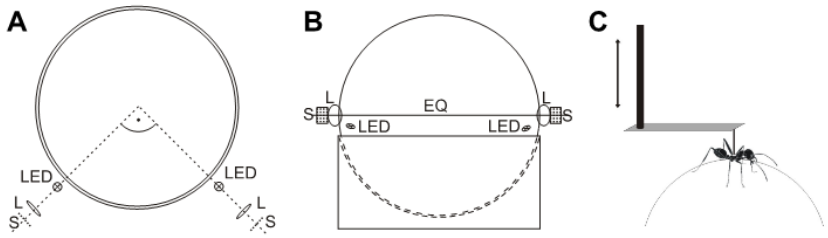

Fig. 2. Open-loop system: experimental setup and animal tethering. (A) Top view, (B) side view. The sphere is allowed to rotate about all three axes. The motion of the sphere is monitored by two optical mouse sensors (S) that look at 90 deg of azimuth with respect to each other through lenses (L) to the equator (EQ) of the sphere. Two somewhat tangentially shining LEDs enhance the contrast of the sphere surface sufficiently for safe sensor recordings. (C) Schematic drawing of tethering an animal by a small rod to a horizontal strip of paper. This way the animal is prevented from yaw and translation but allowed to adjust its height, roll and pitch to some degree on top of the sphere.

Tethering

In the open-loop configuration we successfully tethered small animals (mostly insects) using a horizontal strip of paper, one end glued to a short pin on the prothorax and the other to a vertical rod that could be adjusted in height by a micromanipulator (Fig. 2C). The paper strip allows the animal to move up and down on the zenith of the sphere, to roll and pitch slightly, but prevents any translation or yaw. For larger animals (mice and rats) we used a leather harness connected to a rotatable rod via a thin metal plate and two hinges as shown in Fig. 2D of Hölscher et al. (2005).

In the closed-loop setup the animal is glued to a 1–2 mm long single filament of dental floss (see Fig. 1E,F). The filament is attached to a fine steel rod of 0.08 mm diameter. The rod moves as a rotating axis in a ∼1.5 cm long vertical glass tube, the ends of which are melted slightly to provide a small hole with soft edges. This way the rod can be shifted up and down and rotated but horizontal motion is prohibited. The position of the glass tube is adjusted above the zenith of the sphere by a micromanipulator. The single filament acts as a ball joint. This way the animal is allowed to adapt its posture with respect to height, pitch and roll, and to rotate about the yaw axis with almost no friction. The animal can rotate around the yaw axis on top of the sphere with its own moment of inertia, which allows for extremely quick directional changes. However, when it moves forwards it is kept in place and rotates the sphere. The holes in the glass tube should be as small as possible and the length of the filament as short as possible so that horizontal clearance is kept small. We successfully glued *Cataglyphis* desert ants by hand without any anaesthesia to the 1 mm long single filament of dental floss with a fast UV-bonding glue (Bondic).

Registration of sphere motion

Any motion of the sphere in our treadmills was monitored by two optical mouse sensors (ADNS 3050, www.pixart.com), which look at 90 deg in azimuth with respect to each other through lenses to the equator of the sphere (Fig. 1B–D; Fig. S3). We selected our sensors from the large number of optical mouse sensor types available by the following criteria: a small form factor (eight DIP only), external LED illumination, separate data IN- and OUT-lines, and an operating voltage of 3.2 V, compatible with the operating voltage of many microprocessors. Our sensors contain a light-sensitive area of 0.75×0.75 mm in size with 19×19 quadratic pixels. In contrast to CMOS cameras the pixels in mouse sensors are comparatively large. The small number of pixels and the large light-gathering power allow for a much higher frame rate than with a CMOS camera. Automatic control of the shutter time adapts to variations of image brightness. In addition, a dedicated on-chip digital signal processor allows extraction of the dX- and dY-displacement between two reads and a Q-byte at a theoretical sampling rate of 6 kHz. The maximum allowed displacement speed (S_{max}) of the intensity pattern on the pixel array is 60 inch s^{-1}=1.524 m s^{-1}. The Q-byte allows evaluation of the 'quality' of the contrast in the image on the sensors' pixel array; the better the contrast the larger the Q-byte. A threshold on the quality Q-byte can be used to reject corresponding displacement result because of, for example, poor contrast of the image on the sensor surface. In the so-called 'pixel grab' mode, the image, i.e. the light intensity of each pixel on the sensor surface, can be extracted (see Fig. S6). This mode is very slow because for each pixel intensity a whole image must be sampled. To grab all pixel intensities of a whole image needs 19×19=361 samples. But this mode is essential to achieve the proper adjustment of the lens position.

Because of the short focal length of the factory-provided lenses, distance variations between the sphere surface and the mouse sensors might cause large fluctuations in recordings of the sphere rotation or even disable recording. Attaching a distance-adjustable lens of longer focal length in front of the sensor allows positioning of the sensor at a larger distance from the sphere surface and thus reduces to a large extent the sensitivity of the sensor response to these distance fluctuations. We used well-manufactured small aspheric plastic lenses of 4.6 mm focal length (F) with a relatively large numerical aperture of 0.4, designed by Phillips (CAY046) as collimator lenses for laser diodes. These small lenses have a good imaging quality, are light, inexpensive and easy to find.

The distance (G) of the lens to the sphere surface was ∼25 mm. This meant that fluctuations of the sensor response caused by fluctuations of the sphere distance of ∼1 mm are reduced to 1/25=4%. The image is demagnified by a factor V=(G−F)/F=4.44. Thus, the maximum detectable speed of the sphere surface is ∼6.76 m s^{-1} (=S_{max}×V). The spatial resolution is the smallest displacement of the sphere surface that leads to a change in the answer of the sensor by 1 count. In our case the minimal displacement of the sphere surface is (0.7/19)×V=0.16 mm, which corresponds to 6.12 counts mm^{-1}.

Attachment of a lens allows enlargement of the aperture in front of the sensor surface so that all the light through the lens can hit the sensor surface. The original aperture of 0.8 mm is situated somewhat oblique with respect to the sensor surface, reflecting the intended light path in the original illumination scheme of the PC mouse. We took off the cover of the sensor and drilled a slightly larger and properly side-shifted hole into it, so that the sensor area was open to all the light from the lens.

The sphere was illuminated somewhat tangentially from below or the side by an LED to enhance the contrast of surface irregularities of the sphere, as is normal for PC mouse chip setup. This permits the use of Styrofoam spheres without any pattern on the surface. We

Journal of Experimental Biology

RESEARCH ARTICLE Journal of Experimental Biology (2017) 220, 634-644 doi:10.1242/jeb.148213

normally use red LEDs for this purpose, but an infrared LED also works well, thus allowing the treadmill to be run in total darkness.

The responses of the PC mouse chips were read by a Cypress CY7C68013A-56P microprocessor with an onboard USB2.1 engine via seven general-purpose I/O pins (circuit diagram in Fig. S4). Because the five sensor-IN lines determine the timing and are common to the two sensors, reading the d*X*-, d*Y*- and Q-bytes is done strictly synchronously and in parallel. The transfer of the six bytes via USB bulk transfer to a PC was performed by a small hex file on the microprocessor. The hex file was compiled from a 136-line C-program using a small device C-compiler (SDCC; https://sourceforge.net/projects/sdcc) and was loaded to the microprocessor via USB using FXLOAD (https://sourceforge.net/projects/libusb/libusb-1.0.21/examples). The sampling rate was artificially reduced to ∼200 Hz so that the Windows OS on the PC could accept the USB transfers and store the data at a stable rate. The program that controlled the type, storing and display of the USB data on the PC was also a simple 350-line C-code.

Details of the calibration of the sensors are described in Fig S4, the quality of the sensor response and the control procedure are reported in Figs S5, S6 and S7.

Behavioural experiments

Experimental situation and training

The experiments were performed with two different species of Cataglyphis desert ants, *Cataglyphis fortis* (Forel 1902) and *Cataglyphis bicolor* Fabricus 1793, and took place between June and July 2015 and in January and February 2016.

In the outdoor experiments (salt plains near Maharès, Tunisia, 34.53°N, 10.54°E) the ants were trained to walk a 10 m distance in their natural habitat from their nest entrance to a feeder located east of the nest. After successful training the ants were transferred to a flat and almost featureless remote test field to exclude all familiar olfactory, tactile or visual cues of the nest surrounding. The indoor experiments took place in the laboratory of Ulm University, Germany. Here, the foraging ants were trained to walk through an aluminium channel (7×7 cm) with a length of 4 m, which was illuminated by fluorescent tubes (daylight spectrum with UV, Solar Nature, JBL, Neuhofen, Germany) and covered with a linear polarizer filter (HN38 linear polarization film, 0.3 mm; ITOS GmbH, Mainz, Germany) that provided only the orthogonal polarization direction as compass cue. Because of space constraints in the laboratory the channel was set up with a 90 deg bend. As the orthogonal orientation of the polarizer filter with respect to the channel direction did not change over the entire length of the setup, the ants ignored the actual 90 deg bend and behaved exactly like animals trained in a straight channel (Lebhardt et al., 2012).

Experimental procedures and testing

Ants that reached the feeder and grasped a food crumb were then in the motivational state of homing and we thus refer to them as full-vector ants. For the homebound runs the full-vector ants in our experiments were grasped at the feeder and then the small filament of the tether was glued to their prothorax with the aid of the Bondic glue, which cures under UV light within a few seconds. A big advantage of this procedure is that the ants do not have to be anesthetized. The ants were then tested on the air-suspended spherical treadmill.

As soon as the tethered ants on the top of the treadmill grasp a food item and receive celestial or polarized light compass information (outdoor condition: open sky; indoor condition: polarizer filter and artificial light source) they start to perform a homing run, running off their full-vector to zero-vector state (Wehner et al., 1996). The outdoor experiments in Tunisia were performed with *C. fortis* (*N*=18, OUT-1). The experiments in the laboratory of Ulm were conducted with *C. fortis* (*N*=9, LAB-1) and *C. bicolor* (*N*=8, LAB-2). For comparison we tested homing runs of *C. fortis* recorded in an open test field (20 m by 20 m) in their natural habitat (*N*=20).

For all studies we used the closed-loop treadmill design shown in Fig. 1 (scheme in Fig. S3B) with a hollowed Styrofoam sphere of 5 cm diameter and a mass of 288 mg. The ants were able to freely rotate about their vertical axis very quickly on the top of the sphere (see also Movie 1). A white 5 cm high circular screen around the top of the treadmill prevented the ants from perceiving landmark and panoramic information but allowed for seeing large parts of the sky. This way we ensured that they could only rely on their path integrator to guide them home. The closed-loop treadmill was attached to a tripod stand, which enabled the apparatus to be turned in every direction. The 2D projection of the sensor's *X* and *Y* data were recorded in real time with 209 frames s^{-1}.

In the training site the feeder was located east of the nest. Hence, the apparatus was oriented westbound for testing the global home vector of foraging ants for the entire tracking time of 5 min in Tunisia, and 7 min in the laboratory.

Data analysis

Data were analysed in Matlab (MathWorks, Inc., Natick, MA, USA). To analyse the recorded trajectory we defined the first turning point as marking the position of the run, where the ant starts to differ from its current path direction for at least 30 deg and does not revert to its previous path direction for at least 3 m. We applied this criterion at a minimum distance of 5 m after the releasing point. With the aid of this turning point we separated the straight approach phase from the looping search phase of the ant's walk for the analysis (Merkle et al., 2006; Pfeffer et al., 2015).

With the information of the 209 data points per second, which contain the *XY* coordinates for every point, the corresponding in-time walking speed and angular orientation was calculated.

The angular orientation [alp(*i*)] was analysed for every data point (*i*) by means of the Matlab function atan2(*Y*,*X*) and π:

$$\mathrm{alp}(i) = (180\pi) \times \mathrm{atan2}((\mathrm{Y(i+k)} - \mathrm{Y(i)}), (X(i+k) - X(i)). \quad (7)$$

The walking speed [speed(*i*)] was calculated using the 209 data points per second:

$$\mathrm{speed}(i) = (\mathrm{sqrt}((Y(i+k) - Y(i))^2 + (X(i+k) - X(i))^2))/209. \quad (8)$$

Both were smoothed with *k*=100 (factor of 0.49). The angular speed was calculated as a rate of the change of angular displacement per second.

The search centre is the median position of all *XY* coordinates of the respective search loop or search phase. The index of straightness can estimate the tortuosity of trajectories and is calculated as the division of the straight line distance by the actual length of the trajectory. The accuracy of the nest search indicates how exactly the animals centre their search on the previous nest position. The width of search reflects how focused a particular search performance was and thus provides a measure of the ants' certainty regarding nest position (Pfeffer et al., 2015).

Journal of Experimental Biology

RESEARCH ARTICLE Journal of Experimental Biology (2017) 220, 634-644 doi:10.1242/jeb.148213

To analyse the response of straight-walking ants on the spherical treadmill to imposed changes of compass direction, and therefore a manipulated celestial compass, we tested ants trained to walk to a feeder east of the nest in the open field. We turned the entire apparatus back and forth under the open (and afterwards covered) sky. The starting orientation was westbound, corresponding to the ants' home vector. Before each turning of the apparatus [alternately right-hand (90 deg northbound) and left-hand (90 deg westbound)], we pushed a button to mark the start of turning the treadmill on the trace. We analysed the trajectories after this point to detect the turning points where the ant started to deviate at least 45 deg (the centre of the turn) from its current path direction (with respect to the apparatus) and did not revert to the previous path direction for at least 10 cm. To block celestial cues we used a paper board. The angular orientation with respect to the ant's current walking direction was calculated for N=16 turns with open and N=8 turns with covered sky for N=2 homing ants.

Statistical analysis

For statistical analysis and comparison the laboratory runs were normalized to 10 m vector length. We used SigmaPlot (Systat Software Inc., San Jose, CA) to generate box-and-whisker plots.

Owing to a sometimes relatively small sample size, we only used non-parametric tests. For independent data, we applied the Kruskal–Wallis ANOVA on ranks test (denoted as H-test) with the Dunn's method for *post hoc* multiple comparisons. For pairwise comparisons we used the Wilcoxon signed rank test for paired samples (denoted as Wilcoxon paired) and for multiple comparisons the Friedmann test with Bonferroni as *post hoc* correction. Data and program codes are available on request.

RESULTS

To show the practicability of this treadmill design we tested whether a complex but robust behaviour, such as path integration, can be performed and if it is comparable with the animals' natural behaviour in the open field. We tested homing *Cataglyphis* ants under open sky in Tunisia and in the laboratory setup of Ulm University.

The approach and search phases of homing runs are characteristic features that can be used to assess the quality of homing (Pfeffer et al., 2015).

Fig. 3A shows an example of a single homing run of *C. fortis* on the treadmill recorded under open sky in Tunisia. After running off the full-vector to zero-vector state [reaching the fictive nest site

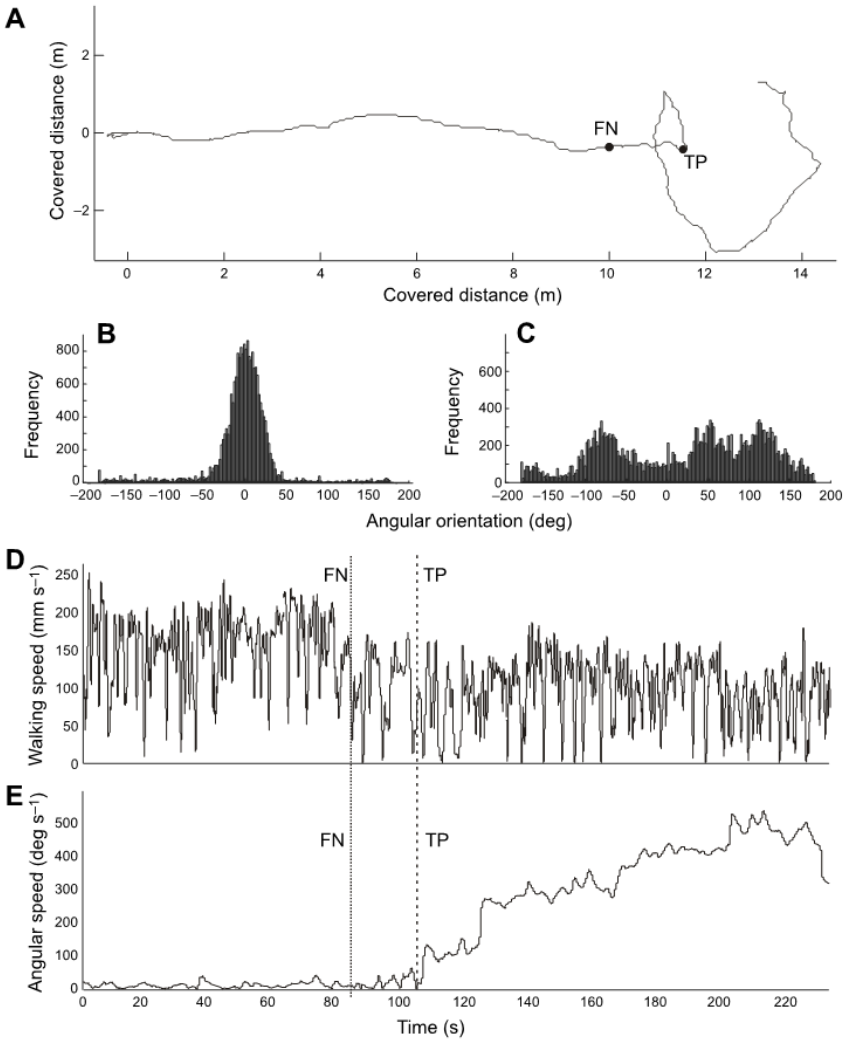

Fig. 3. Homing behaviour of a foraging ant: angular orientation and the walking speed separated into approach and search phases. Example of a tracked homing walk of the *C. fortis* ant after a training distance of 10 m. (A) Frequency histogram of the walking angle for (B) the approach phase before the turning point and (C) the search phase after the turning point (TP). (D) Walking speed plotted against the running time, approach phase (start to TP) with an average speed of 13.9 cm s^{-1} and the search phase (TP to end) with an average speed of 10.4 cm s^{-1}. The walking speed was smoothed with a moving average of a factor of 0.49. (E) Angular speed plotted against the running time, smoothed with a moving average of a factor of 2. The dotted line marks the time when reaching the 10 m point [fictive nest (FN)] whereas the dashed line indicates the turning point (TP).

RESEARCH ARTICLE Journal of Experimental Biology (2017) 220, 634-644 doi:10.1242/jeb.148213

(FN)] the ant's behaviour changes from a straight approach phase (Fig. 3B) to the looping search phase (Fig. 3C), which is indicated by a conspicuous turning point (TP) (Merkle et al., 2006).

Separating the mean walking speed of all runs with respect to the TP, the approach (0–TP) and search phase (TP–end) we can show a significant decrease of speed (Fig. 4A, left panel; Wilcoxon paired $P<0.001$). This reduction of walking speed can also be seen when the ants pass the position of the fictive nest site but when they still seem to be in the straight approach phase (see also Fig. 3D). This indicates that the walking speed was decreased at the FN (Fig. 3D, dotted and dashed line) and before the TP (Fig. 3D, dashed line). Separating the path at FN position shows a significant reduction of the mean walking speed (Fig. 4A, right panel, Wilcoxon-paired: $P<0.001$), irrespective of whether they showed a TP before or after the FN. This can also be observed when we separate the homing trajectories into three parts, depending on whether the ants first passed the fictive nest site while still running straight (Fig. 4B, left panel) or whether they turn (TP) before reaching the FN (Fig. 4B, right panel). During walking around curves the stride length of the inner side of the curve is shortened, whereas that of the outer side of the curve remains independent of the curvature (Zollikofer, 1994). Although there is a biomechanical coupling of linear speed and angular speed that depends on the radius of the curve, the decrease in speed in the data cannot be explained only by an increase in angular speed. When the ants, for example, take a sharp turn of 10 cm radius with a 10 mm distance between outside and inside footfalls at any given walking speed, they would only show a reduction of 5% walking speed resulting from the biomechanical coupling. The drop of walking speed that we show in the data is much larger (Figs 3 and 4, also compare Fig. S8); moreover, in Fig. 3D we can see that walking speed was already decreased at the FN (dotted line) and before the TP (dashed line), although the angular speed was not yet increased (Fig. 3E). In addition, in the search phase the speed is not only reduced during the times when turns occur but also during the times when the ants resume straighter walking in between the turns.

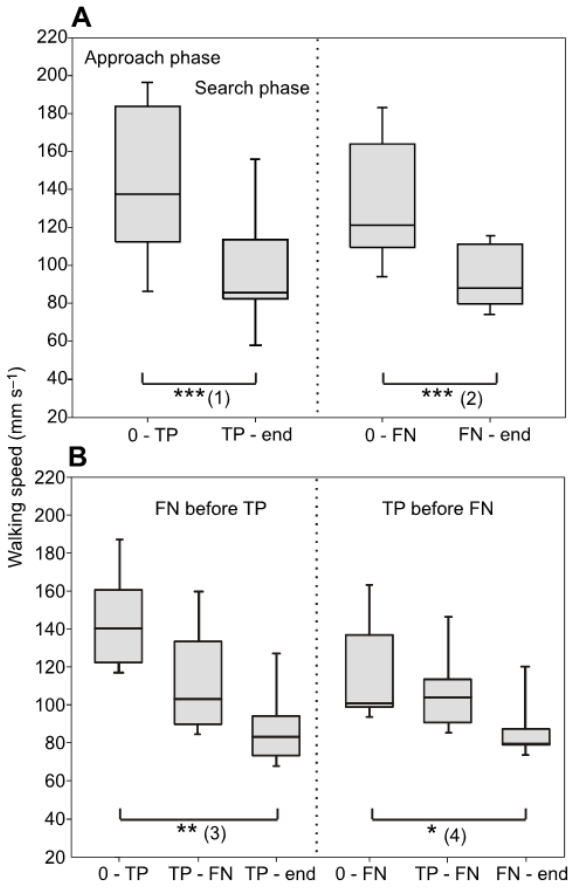

Fig. 4. Statistical analysis of the walking speed of tracked homing ants. (A) Walking speed of the homing runs of *C. fortis* under open sky separated into two phases according to the criterion of the first turning point (TP) (left panel, $N=15$) and separated by the fictive nest site position (FN) (right panel, $N=12$). (B) The homing runs are separated into three parts, depending on whether the ants first pass the fictive nest site before performing the TP (FN=10 m, left panel, $N=6$) or perform the TP before reaching the FN (right panel, $N=5$). Box-and-whisker plots give the 10th, 25th, 50th, 75th and 90th percentile distribution. Asterisks indicate statistical significance by the following analyses: (1) Wilcoxon paired, $P<0.001$; (2) Wilcoxon paired, $P<0.001$; (3) Friedmann test, $P=0.004$; (4) Friedmann test, $P=0.040$.

To compare the treadmill homing runs with open-field homing runs, we separated the approach phase from the search phase by means of the TP in the trajectories (Fig. 5) (Pfeffer et al., 2015). The length of the trajectories of the approach phase corresponds nicely to the nest-to-feeder distance (Fig. 5E) and is not significantly different between the experiments (*H*-test: H=3.016, $P=0.268$). We also found no significant difference between the experiments when we compared the distance of the first turning point with the pinpoint position of the fictive nest site (Fig. 5F; *H*-test: H=3.949, $P=0.389$). The ants tested in the laboratory setup showed a higher variability of the index of straightness (Fig. 5G; *H*-test: H=19.176; multiple comparison $P<0.05$ for Control versus LAB-2, OUT-1 versus LAB-1, OUT-1 versus LAB-2). For the search phase trajectories we determined the search centres that facilitate the comparison of the search behaviour of the tested groups (Pfeffer et al., 2015). It is noteworthy that the ants tested on the treadmill show a search behaviour that is less accurate compared with those tested in the open field. This means that the ants centre their search less on the position of the fictive nest site (Fig. 5H; *H*-test: $H=24.310$; multiple comparison $P<0.05$ for Control versus OUT-1, Control versus LAB-1, Control versus LAB-2). The width of search, which reflects how certain the animals are about the nest position, is not significantly different between the experiments. Nevertheless, the variability of the width of search is larger for the animals tested under artificial laboratory conditions (Fig. 5I; *H*-test: H=0.817, $P=0.845$). The 'loopiness' of the searches, as indicated by the index of straightness, tends to be largest in the open-field tested group, though it is not significantly different for all groups (Fig. 5J; *H*-test: $H=4.133$, $P=0.247$). The fact that all ants were holding on to their food item during the runs on the treadmill (and some ants even during the tethering procedure) proves that they were highly motivated to carry their food back home.

To see whether the ants respond to imposed changes of compass direction we manipulated the celestial compass input by actively turning the entire apparatus back and forth under the open (and afterwards covered) sky (Fig. 6). While turning the apparatus 90 deg back and forth the animals kept walking with a constant heading with respect to the celestial compass input as long as they saw the open sky. This results in a trajectory that shows 90 deg turns because the animals' walking direction changed with respect to the sensors (Fig. 6A,B). As soon as the sky was covered (black asterisk in Fig. 6A) we could not find such a compensation for directional change as the animals no longer had no access to the celestial compass information (Fig. 6A,C).

Journal of Experimental Biology

RESEARCH ARTICLE Journal of Experimental Biology (2017) 220, 634-644 doi:10.1242/jeb.148213

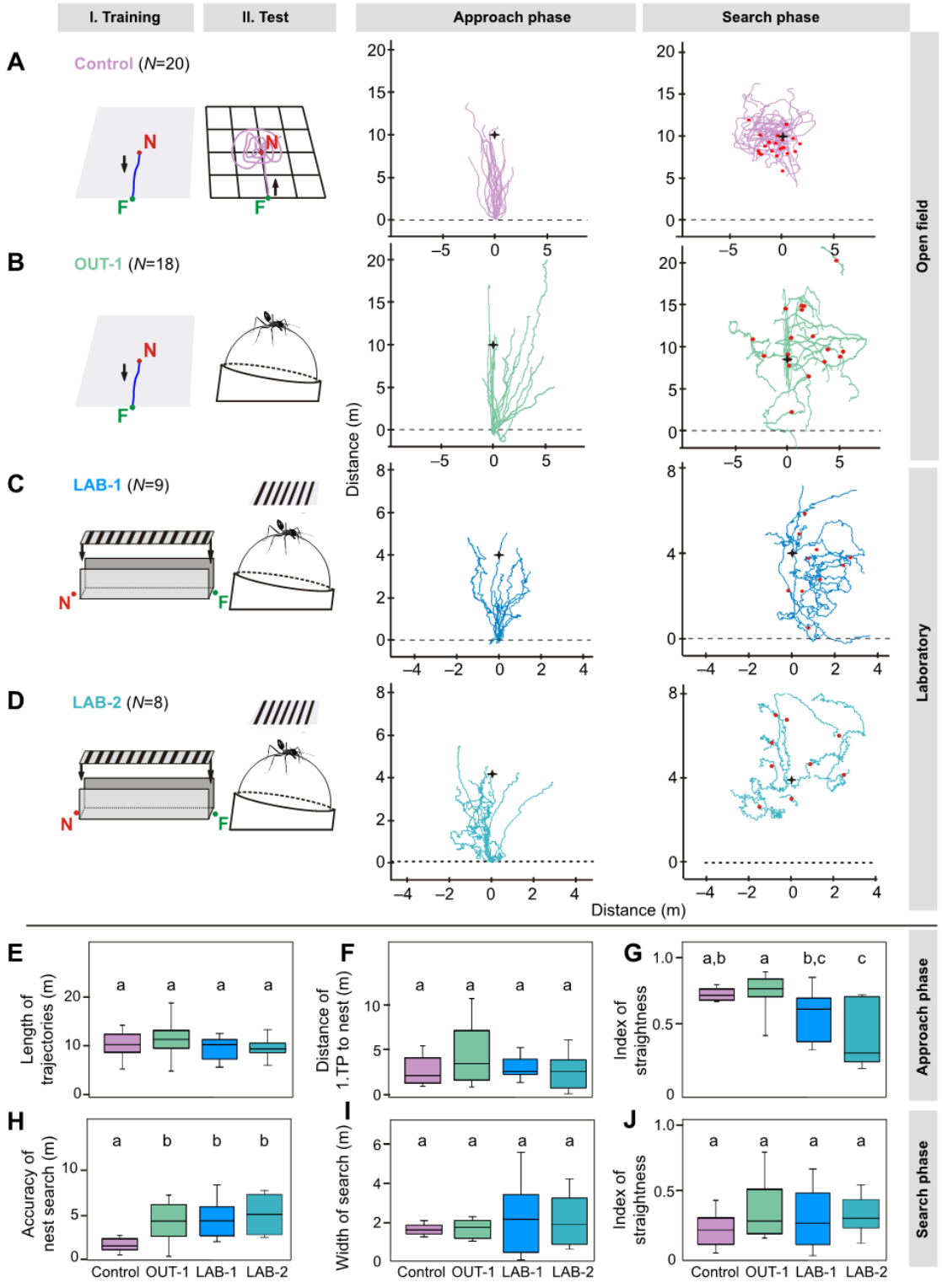

Fig. 5. See next page for legend.

RESEARCH ARTICLE Journal of Experimental Biology (2017) 220, 634-644 doi:10.1242/jeb.148213

Fig. 5. Approach and search phases of tracked homing walks of two different *Cataglyphis* species trained and tested under open-field or laboratory conditions. (A–D) First and second column show training and test setup for *Cataglyphis fortis* (A–C) and *Cataglyphis bicolor* (D). F, feeder position; N, nest position. Third column shows approach phases, fourth column shows search phases. For the third and fourth column, the trajectories of all ants have been superimposed; the first 20 m of the search phases are represented. The experiments in A and B were conducted under open sky in the desert of Tunisia. The animals were trained to visit a feeding site at a distance of 10 m. Homing runs were tested in an open test field (Control, *N*=20; A), and on the spherical treadmill (OUT-1, *N*=18; B). The experiments in C and D were conducted in the laboratory of Ulm. We trained the animal to walk to a feeding site through an aluminium channel of 4 m distance covered with a polarisation filter (represented as a black/white pattern) and tested their homing run on the spherical treadmill. (C) *Cataglyphis fortis* (LAB-1, *N*=9); (D) *C. bicolor* (LAB-2, *N*=8). A black cross marks the fictive nest position. The red dots show the search centres of every search phase. Corresponding analyses are shown for the approach phase: (E) length of the approach trajectories, (F) distance of first turning point to the nest, (G) index of straightness. For the search phase: (H) accuracy of nest search, (I) width of search, (J) index of straightness. For comparison, the laboratory data were normalised to 10 m distance. Box-and-whisker plots show the median as the box centre, plus 10th, 25th, 75th and 90th percentiles. Results of the statistical evaluation are indicated above the plots by letters; data sets with the same letters indicate an absence of significant difference, different letters indicate significant differences (for details, see text).

DISCUSSION

In our setup we wanted to demonstrate improvements to the well-introduced air cushioned sphere as a treadmill in studies on the orientation behaviour of animals that are fixed in space.

Improvements described are: (1) the production of lightweight spheres, (2) the use of air cups with a single and silent air inlet, (3) the reliable simple registration and calibration of the sphere's motion by optical mouse sensors with properly attached lenses, (4) high temporal (over 200 frames s^{-1}) and (5) spatial resolution (6 counts mm^{-1}), (6) the possibility to investigate open- and closed-loop orientation behaviour of animals mounted on top of the sphere, (7) the improved tethering of the closed-loop setup and (8) the easy transport and use of the device in outdoor environments.

The crucial improvement is the attachment of a distance-adjustable lens with a longer focal length than that provided by the manufacturer of the sensor chips. We show that mouse sensors prepared this way provide a fast and reliable registration technique that overcomes the criticisms of the mouse registration in, for example, Moore et al. (2014). However, the errors of mouse registration accumulate over time. Control of imaging and calibration are thus of great importance. When a single LED (or IR LED) illuminates the sphere, the normal irregularities of the Styrofoam surface provide enough contrast for the sensors to respond to any motion. No pattern on the sphere is needed.

Thanks to the mobile and robust design of the spherical treadmill (consisting of the treadmill device, a simple membrane pump driven from a battery, a plastic bottle as air vessel and a laptop computer), not only indoor but also outdoor experiments can easily be accomplished.

Owing to the high resolution of the spherical treadmill setup, we were able to study the homing runs not only spatially but also temporally with high precision.

The improved tethering of the closed-loop treadmill was essential for the comfortable posture of the animals, thus showing a naturalistic behaviour. For fast-turning animals like desert ants it is crucial that they can rotate around the yaw axis with their own moment of inertia (McMeeking et al., 2012).

The reconstructed paths on the spherical treadmill under open sky and in the laboratory are comparable with the homing trajectories

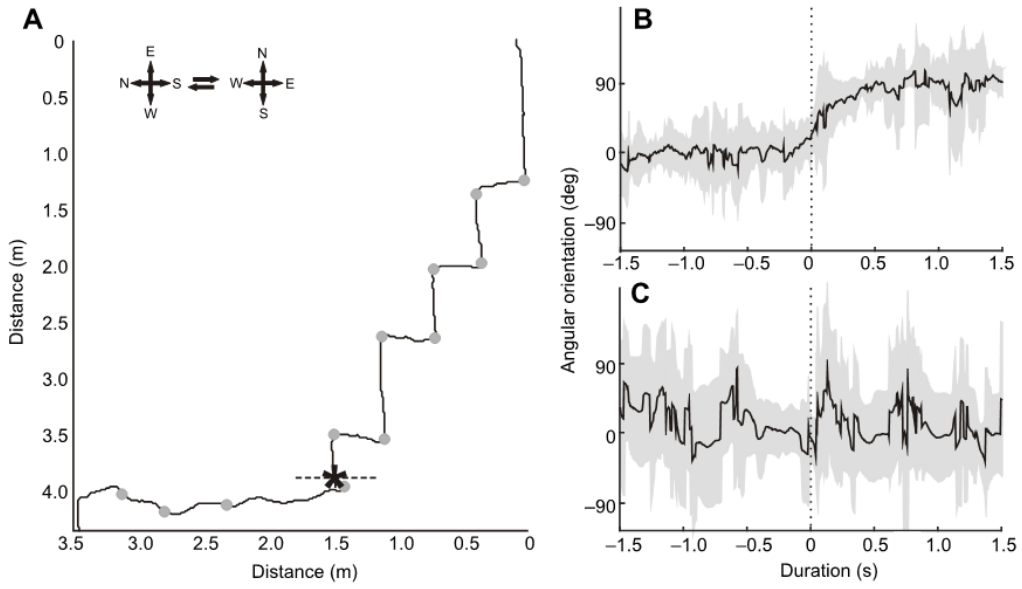

Fig. 6. Course correction response to imposed changes of the compass directions by turning the entire apparatus back and forth under the open sky. (A) Example of a homing run tracked on the spherical treadmill while alternately rotating the apparatus 90 deg to the right (northbound) and 90 deg to the left (westbound). The ant's starting position is at the zero point (0,0) and the ant initially moved westward towards its fictive nest position. The black asterisk marks the time when the sky was covered. The grey dots indicate the times when the apparatus was rotated. (B,C) The angular orientation with respect to the ant's current walking direction of *N*=2 homing runs with (B) open (*N*=16 turns) and (C) covered sky (no celestial information, *N*=8 turns). The dashed line indicates the centre of the turning behaviour of the ants. Turns to the left were mirrored and the angular orientations were smoothed with a moving average of a factor of 5. The bold black line indicates the mean value; the grey area marks the span of the standard deviation.

Journal of Experimental Biology

RESEARCH ARTICLE Journal of Experimental Biology (2017) 220, 634-644 doi:10.1242/jeb.148213

recorded in the open test field (Fig. 5A–D). The navigation and nest search performance is also comparable with results from *Cataglyphis* ants from previous decades (e.g. Wehner, 1982; Müller and Wehner, 1994; Åkesson and Wehner, 2002; Wehner et al., 2002; Merkle et al., 2006; Pfeffer et al., 2015) and also from Australian desert ant *Melophorus bagoti* (only nest search performance; Schultheiss and Cheng, 2011).

An interesting difference in our data is that the ants from captive laboratory colonies seem to show a less straight approach phase when running back to their nest site on the treadmill (Fig. 5G). A possible explanation might be the slower walking speed on the treadmill. In general the treadmill-tested groups performed less accurately in the nest search than the open-field-tested group (Fig. 5H). Although the precision or certainty about the nest position (width of search) is not significantly different between the groups the laboratory tested ants showed a larger variability within the width of search distribution (Fig. 5I). The ants from the laboratory do have plenty of food and no predatory pressure or heat stress (Wehner et al., 1992; Schmid-Hempel and Schmid-Hempel, 1984) so speed, accuracy and precision might not be so crucial. In the field we have highly motivated ants from wild colonies, higher temperatures and the celestial compass input is natural. Nevertheless, *Cataglyphis* ants from colonies kept in the laboratory are motivated enough to show typical path integration homing behaviour under artificial illumination.

Interestingly, homing ants that reached zero-vector state, the FN position, while they were still in the straight approach phase slowed down even before they started the looping search phase. Here, angular speed did not increase, suggesting that this drop in speed cannot be explained by a biomechanical coupling of linear and angular speed when walking around turns. In addition, ants that started the looping search phase before they reached the fictive nest slowed down at zero-vector state. The straight approach path and the looping search path show no difference in speed before reaching the FN. Previously, various measures for the first turn have been applied to determine when and where the ants 'think' they have reached their goal. The reduction of speed once the animals reach the fictive nest site can now be taken as a measure of the target probability function and therefore offers a new window to study path integration in more detail.

The possibility to investigate orientation behaviour of animals mounted on top of a sphere under natural closed-loop conditions allows us to analyse complex behaviour in great detail. We can say that *Cataglyphis* ants show typical homing behaviour, with a straight approach phase and looping search phase, and hence navigate in a naturalistic way under the artificial conditions on the treadmill.

In future applications, one could imagine many ways of manipulating the ants' surrounding visual or olfactory environment to investigate how it interacts with, for instance, path integration. The newly improved spherical treadmill is a valuable tool to better understand the remarkable features of the ants' navigational toolkit.

Acknowledgements
We gratefully thank Harald Wolf, Ulm University, for generous support. Hanspeter Mallot, Tübingen University, kindly supported the manufacturing of various versions of the treadmill by permitting H.D. to use the workshop, rooms and equipment. We thank Ursula Seifert for her help in organising the field excursions and for editing the text, Andrea Wirmer for statistical advice and Dennis Grüninger, Elena Haugg, Mario Hildebrand and Stephanie Offergeld for their help during the experiments.

Competing interests
The authors declare no competing or financial interests.

Author contributions
H.D. designed and developed the apparatus. H.A.M. provided crucial support for manufacturing the devices. M.W. and V.L.W. designed the experiments; M.W., V.L.W. and S.E.P. performed the behavioural experiments. V.L.W. and S.E.P. analysed the data. H.D., V.L.W. und M.W. wrote the manuscript, and H.A.M. revised the manuscript.

Funding
The University of Ulm and Eberhard Karls Universität Tübingen provided basic financial support and infrastructure.

Supplementary information
Supplementary information available online at
http://jeb.biologists.org/lookup/doi/10.1242/jeb.148213.supplemental

References

Åkesson, S. and Wehner, R. (2002). Visual navigation in desert ants Cataglyphis fortis: are snapshots coupled to a celestial system of reference? *J. Exp. Biol.* **205**, 1971-1978.
Buchner, E. (1976). Elementary movement detectors in an insect visual system. *Biol. Cybern.* **24**, 85-101.
Collett, M. and Collett, T. S. (2000). How do insects use path integration for their navigation? *Biol. Cybern.* **83**, 245-259.
Dahmen, H. J. (1980). A simple apparatus to investigate the orientation of walking insects. *Experientia* **36**, 685-687.
Doherty, J. A. and Pires, A. (1987). A new microcomputer-based method for measuring walking phonotaxis in field crickets (Gryllidae). *J. Exp. Biol.* **130**, 425-432.
Götz, K. G. and Gambke, C. (1968). Zum Bewegungssehen des Mehlkäfers tenebrio molitor. *Kybernetik* **4**, 225-228.
Hedwig, B. and Poulet, J. F. A. (2004). Complex auditory behaviour emerges from simple reactive steering. *Nature* **430**, 781-785.
Hölscher, C., Schnee, A., Dahmen, H., Setia, L. and Mallot, H. A. (2005). Rats are able to navigate in virtual environments. *J. Exp. Biol.* **208**, 561-569.
Kramer, E. (1976). The orientation of walking honeybees in odour fields with small concentration gradients. *Physiol. Entomol.* **1**, 27-37.
Lebhardt, F., Koch, J. and Ronacher, B. (2012). The polarization compass dominates over idiothetic cues in path integration of desert ants. *J. Exp. Biol.* **215**, 526-535.
Lott, G. K., Rosen, M. J. and Hoy, R. R. (2007). An inexpensive sub-millisecond system for walking measurements of small animals based on optical computer mouse technology. *J. Neurosci. Methods* **161**, 55-61.
Mason, A. C., Oshinsky, M. L. and Hoy, R. R. (2001). Hyperacute directional hearing in a microscale auditory system. *Nature* **410**, 686-690.
McMeeking, R. M., Arzt, E. and Wehner, R. (2012). Cataglyphis desert ants improve their mobility by raising the gaster. *J. Theor. Biol.* **297**, 17-25.
Merkle, T., Knaden, M. and Wehner, R. (2006). Uncertainty about nest position influences systematic search strategies in desert ants. *J. Exp. Biol.* **209**, 3545-3549.
Moore, R. J. D., Taylor, G. J., Paulk, A. C., Pearson, T., van Swinderen, B. and Srinivasan, M. V. (2014). FicTrac: a visual method for tracking spherical motion and generating fictive animal paths. *J. Neurosci. Methods* **225**, 106-119.
Müller, M. and Wehner, R. (1988). Path integration in desert ants, Cataglyphis fortis. *Proc. Natl. Acad. Sci. USA* **85**, 5287-5290.
Müller, M. and Wehner, R. (1994). The hidden spiral: systematic search and path integration in desert ants, Cataglyphis fortis. *J. Comp. Physiol. A* **175**, 525-530.
Pfeffer, S. E., Bolek, S., Wolf, H. and Wittlinger, M. (2015). Nest and food search behaviour in desert ants, *Cataglyphis*: a critical comparison. *Anim. Cogn.* **18**, 885-894.
Ronacher, B. (2008). Path integration as the basic navigation mechanism of the desert ant Cataglyphis fortis (Forel 1902) (Hymenoptera: Formicidae). *Myrmecol. News* **11**, 53-62.
Schmid-Hempel, P. and Schmid-Hempel, R. (1984). Life duration and turnover of foragers in the ant Cataglyphis bicolor (Hymenoptera, Formicidae). *Insectes sociaux* **31**, 345-360.
Schultheiss, P. and Cheng, K. (2011). Finding the nest: inbound searching behaviour in the Australian desert ant, Melophorus bagoti. *Anim. Behav.* **81**, 1031-1038.
Seelig, J. D., Chiappe, M. E., Lott, G. K., Dutta, A., Osborne, J. E., Reiser, M. B. and Jayaraman, V. (2010). Two-photon calcium imaging from head-fixed drosophila during optomotor walking behaviour. *Nat. Methods* **7**, 535-540.
Varjú, D. (1975). Stationary and dynamic responses during visual edge fixation by walking insects. *Nature* **255**, 330-332.
Wehner, R. (1982). Himmelsnavigation bei Insekten: Neurophysiologie und Verhalten. *Neujahrsblatt. Naturforsch. Ges. Zürich* **184**, 1-132.
Wehner, R. and Wehner, S. (1990). Insect navigation: use of maps or Ariadne's thread? *Ethol. Ecol. Evol.* **2**, 27-48.
Wehner, R., Marsh, A. C. and Wehner, S. (1992). Desert ants on a thermal tightrope. *Nature* **357**, 586-587.

Journal of Experimental Biology

RESEARCH ARTICLE Journal of Experimental Biology (2017) 220, 634-644 doi:10.1242/jeb.148213

Wehner, R., Michel, B. and Antonsen, P. (1996). Visual navigation in insects: coupling of egocentric and geocentric information. *J. Exp. Biol.* **199**, 129-140.
Wehner, R., Gallizzi, K., Frei, C. and Vesely, M. (2002). Calibration processes in desert ant navigation: vector courses and systematic search. *J. Comp. Physiol. A* **188**, 338-683.
Ye, S., Dowd, J. P. and Comer, C. M. (1995). A motion tracking system for simultaneous recording of rapid locomotion and neural activity from an insect. *J. Neurosci. Methods* **60**, 199-210.
Zollikofer, C. P. E. (1994). Stepping patterns in ants I. Influence of speed and curvature. *J. Exp. Biol.* **192**, 95-106.

Journal of Experimental Biology

Journal of Experimental Biology 220: doi:10.1242/jeb.148213: Supplementary information

SUPPLEMENTARY INFORMATION

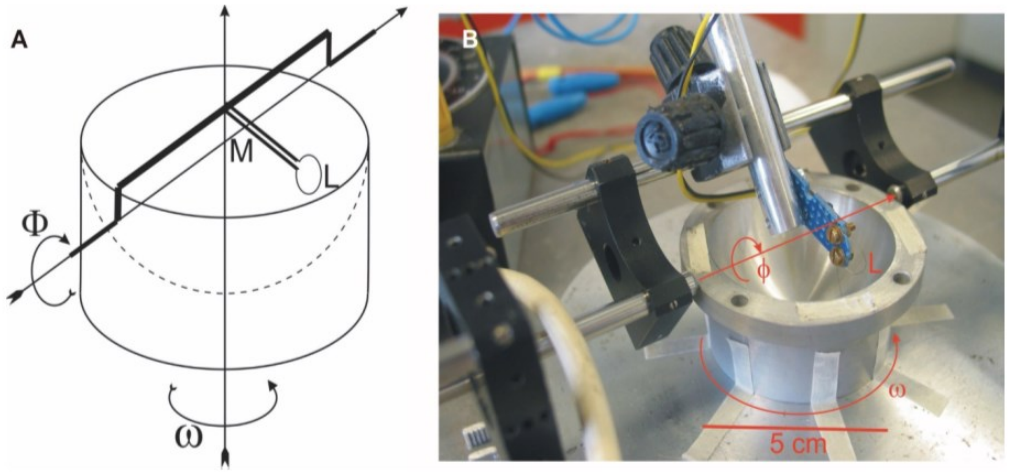

Fig. S1: Hollowing the Styrofoam sphere

To get a light spherical shell with equal wall thickness, a pre-hollowed half sphere was placed into one half of the precision mould precisely centred on a turntable. The turntable could be rotated about a vertical axis by a stepper motor, the rotation speed ω of which was carefully controlled. A small heated steel wire loop L could be rotated about a horizontal axis that crossed the axis of the turntable exactly at the centre M of the sphere.

The wire loop L was rotated along a circle of a slightly smaller radius than that of the mould along a longitudinal line of the latter (i.e. it was moved at a small constant distance to the mould wall at all elevations of the mould-half-sphere). Rotating the turntable, heating the loop, and adjusting it at stepwise increased elevations ϕ the rest of the material was cut out in rings down to a thin and light half sphere. The speed of the turntable and the heat of the steel loop have to be adjusted carefully so that the wire loop only cuts out the material but does not melt too much of it.

Journal of Experimental Biology • Supplementary information

Journal of Experimental Biology 220: doi:10.1242/jeb.148213: Supplementary information

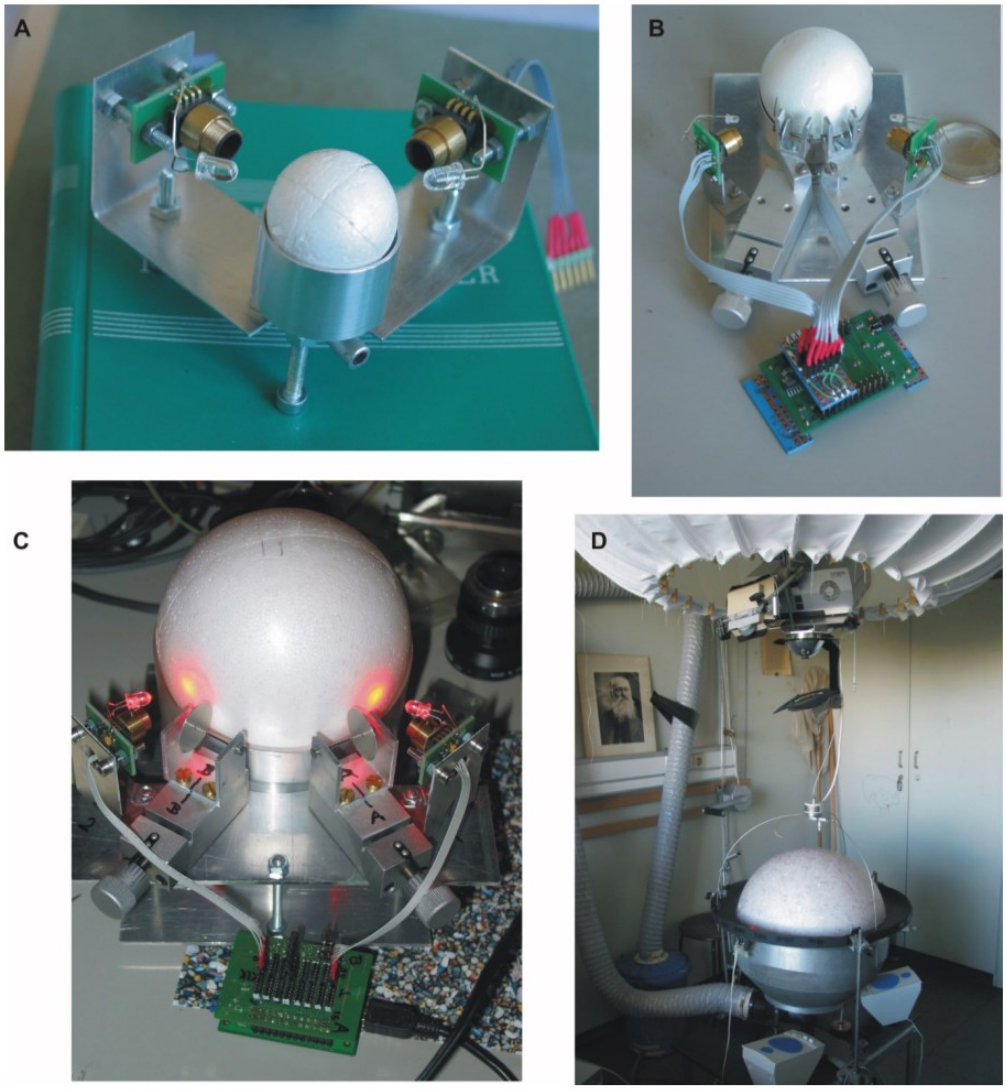

Fig. S2: Four Treadmill Examples

Four examples of treadmills are depicted: (**A**) a 3 cm and (**B**) a 5 cm sphere for smaller insects. (**C**) a 10 cm sphere intended for locusts and crickets (**D**) a 50 cm sphere for rats. In (**B**), (**C**), and (**D**) the sphere is prevented from yaw. (**A**) is an open loop configuration, (**B, C, D**) are closed loop configurations.

Journal of Experimental Biology • Supplementary information

Journal of Experimental Biology 220: doi:10.1242/jeb.148213: Supplementary information

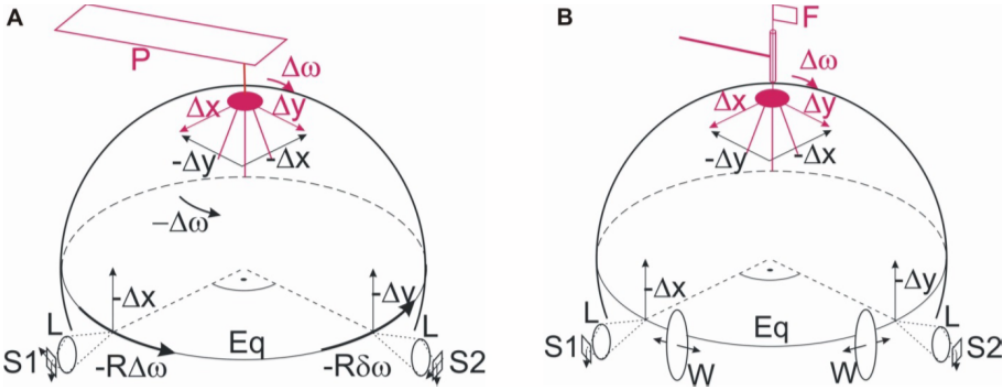

Fig S3: Schematics of the two possible configurations of the treadmill

Fig S3A shows the scheme of the open loop configuration, Fig S3B that of the closed loop configuration (the air cup was omitted). Both configurations are open loop with respect to translation: when the animal moves on the ground (i.e. the apex of the sphere) by a small distance Δx (Δy) it counter-rotates the sphere because of its tethering by -Δx (-Δy) which leads to a displacement of -Δx (-Δy) in the Y direction of sensors S1 (S2), respectively. But there is no visual feed-back to the animal's translation (besides of the small optic flow induced by the moving structure of the white sphere's surface underneath the animal).

The situation is different for yaw: In Fig. S3A the paper stripe P prevents any yaw of the animal and the sphere is free to rotate about all 3 DOFs. When the animal yaws on its ground by a small amount Δω it counter-rotates the sphere by –Δω but its orientation is kept fixed in space. This leads to a displacement of –RΔω in the X-direction of both sensors (R = radius of the sphere). But there is no visual feed-back to the animal induced by its yaw. This is an open loop situation with respect to yaw.

In Fig. 3B the animal is free to yaw with very little friction and its own moment of inertia. Any yaw of the sphere is prevented by the two wheels W. The consequence of the animal's yaw is immediately fed back to its visual system (and other organs), the yaw loop is closed. The apparatus does not respond to any rotation on the spot (besides of the rotation of the flag F). It only records changes in the running direction (and speed) of the animal with time- and space resolution described in the text.

Journal of Experimental Biology • Supplementary information

Journal of Experimental Biology 220: doi:10.1242/jeb.148213: Supplementary information

Reading the sensor response

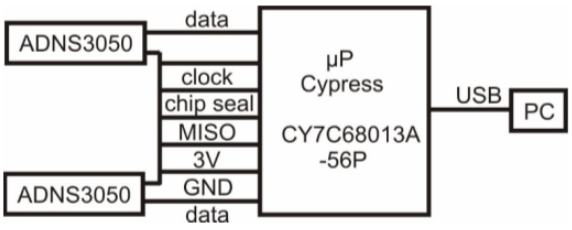

Fig. S4: Sensor-µP connections

Circuit diagram of the connection between the two mouse sensors ADNS3050 and the µP. The five In-lines of the sensors go to common GP Out pins of the µP, the two data out lines from the sensors to separate GP In pins. Thus the data transfer from both sensors to the µP is synchronous.

Sensor calibration

In order to calibrate the sensors' response in cm with the actual sphere, the latter is rotated by a weak extra air beam blown tangentially to the top of the sphere. The tip of a fine needle touches gently the sphere's surface in the centre of the visual field of say sensor one. In this way the sphere is forced to rotate about the axis through the tip of the needle and the centre of the sphere. Because the two sensors look at right angles to each other to the sphere's equator the sphere's motion in the visual field of sensor two is now vertical along a great circle through the zenith of the sphere. Recording the response to say 50 revolutions allows to calculate the response of sensor two to 1 cm of the sphere's motion. Sensor one is calibrated in the same way by touching the sphere by the needle in the visual field of sensor two. With our lens setup we get about 7-10 counts/mm depending on the actual distance of the sensors to the sphere's surface. Because the X- and Y -sensitivity are the same no X-calibration is necessary.

Journal of Experimental Biology • Supplementary information

Journal of Experimental Biology 220: doi:10.1242/jeb.148213: Supplementary information

Establishing the quality of the sensors‘ response

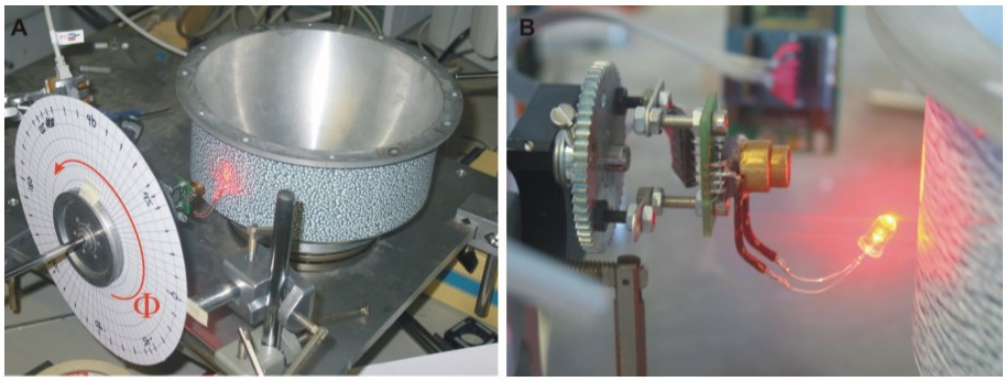

Fig. S5: Sensor response control: setup

(**A**) A vertical cylinder of 20.1 cm diameter was carefully centre on a table which could be rotated about a vertical axis by a stepper motor. A mouse sensor ADNS3050 with a 4.6 mm lens attached (see detail in (**B**)) looked along a horizontal axis to a contrasted pattern on the wall of the cylinder. The sensor could be rotated about its viewing axis by well controlled angles ϕ. The distance of the pattern to the frontal nodal point of the sensor's lens was 30 mm.

The quality of the sensor’s response

To judge about the quality of the sensors' motion recording we used a setup shown in Fig.S3. A motion sensor ADNS3050 with attached 4.6 mm lens and illumination LED looked along a horizontal viewing axis at right angles to the wall of a vertical cylinder of 20.1 cm diameter, carefully centred on a table which could be rotated by a stepper motor about a vertical axis (see Fig.S3A). To control the correct adjustment of the lens distance, the pattern of a 18pt large letter 'e' together with a set of stripes of 1mm distance (Fig. S4A) was attached to the wall of the cylinder and its image recorded in 'pixel grab' mode (Fig. S4B). From the stripes on the right edge of Fig. S4A we extract that the image of five stripes (distance = 4 mm) occupies about 16 pixels i.e. 16 x 0.75 / 19 = 0.63 mm. Thus the demagnification factor is about 4/0.63 = 6.33.

The distance of the wall to the frontal nodal point of the lens was about 30 mm (Fig: S3B). From the lens equation we conclude that the demagnification factor is therefore 30/4.6 = 6.5 which is in reasonable agreement with the estimate from the pixel image. We now attached a contrasted pattern to the cylinder wall shown in Fig. S3B and rotated the cylinder with a constant rotational speed of 13.4 sec per revolution which leads to a pattern speed of 4.72 cm/sec. We accumulated the dX-dY -responses of the sensor for various angular orientations ϕ of the sensor (Fig. S5A). We fit a straight line through the recordings of five cylinder-revolutions (316.25 cm) and plotted the slope against ϕ (Fig. S5C). The slope of the accumulated dX-responses should follow a cos (ϕ) function, that of the dY -responses a sin (ϕ) function. The plot shows the strict quadratic structure of the pixel array of the sensor, the sensitivities in X- and Y- direction are equal (see the equal amplitude of the slope at ϕ = 45° and -135°). The good fit of the Y -response to sin (ϕ) for ϕ around 0° and ±180° and that of the X-

Journal of Experimental Biology • Supplementary information

Journal of Experimental Biology 220: doi:10.1242/jeb.148213: Supplementary information

response to cos (ϕ) for ϕ around ±90° shows the excellent response of the sensor to slow optic flow. This is supported by Fig. S5B where the responses to the slowest flow in our series are depicted.

To test the sensor response for larger speeds we rotated the cylinder at pattern speeds from 4.72 cm/sec to 121.5 cm/sec. The theoretical speed limit for our demagnification factor of 6.33 is about 886 cm/sec. Because of the limited clock-rate of our stepper motor we could not reach that maximum. The time for 5 revolutions has been recorded by a stop watch by hand. Also the accumulated X-response for each cylinder-revolution has been stopped by hand. The result is presented in Fig. S5D. We conclude that within the hand stopping errors the accumulated X-response is the same for each revolution irrespective of the pattern speed.

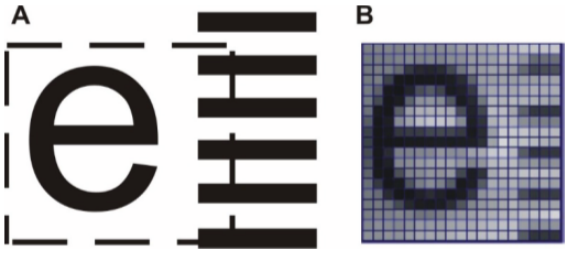

Fig. S6: Control of imaging quality

(**A**) Original and (**B**) 'pixel grab' of a 18pt large 'e'. The dark stripes at the right border are stripes and images of stripes with a line width of 0.25 mm and a distance of 1 mm. From the image of the stripes the demagnification factor of 1/6.33 can be extracted.

Journal of Experimental Biology • Supplementary information

Journal of Experimental Biology 220: doi:10.1242/jeb.148213: Supplementary information

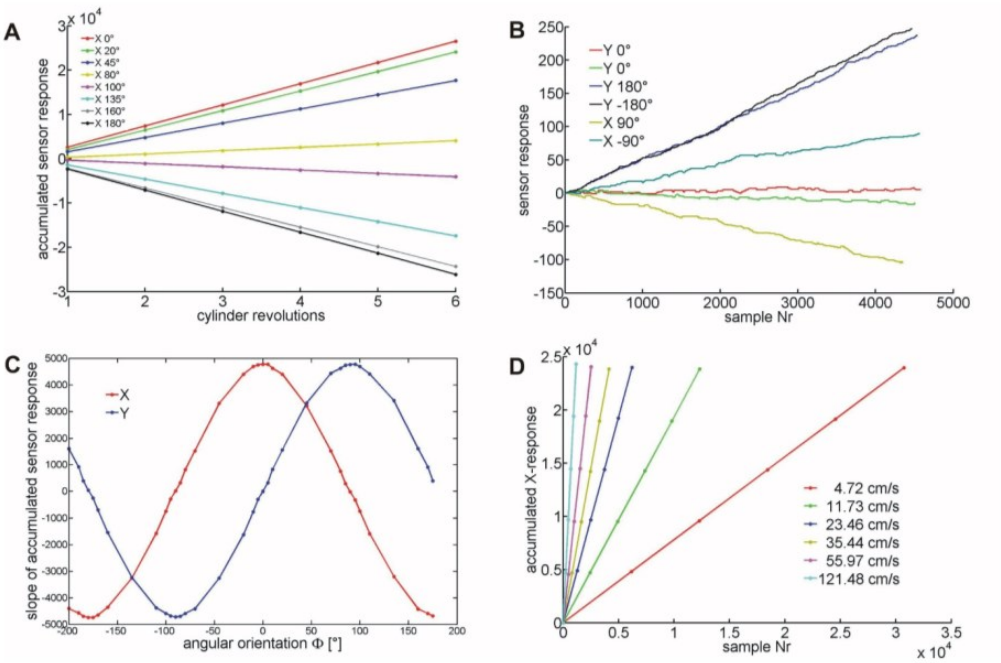

Fig. S7: sensor response control

(**A**) The sensors' accumulated X-response to selected angular orientations ϕ (see Fig. S3) versus the number of revolutions of the pattern cylinder. (**B**) The response to the slowest flow components in our sensor response control runs (please note the scale). (**C**) The slope of the sensor's accumulated dX-dY -responses plotted versus the angular orientation ϕ of the sensor. For ϕ = 0° the X-axis of the sensor is parallel to the pattern velocity. For further discussion see text. (**D**) The accumulated X-response to five cylinder-revolutions at various speeds. The response to each revolution is marked by a point. The X-response is independent of the speed of the pattern.

Journal of Experimental Biology • Supplementary information

Journal of Experimental Biology 220: doi:10.1242/jeb.148213: Supplementary information

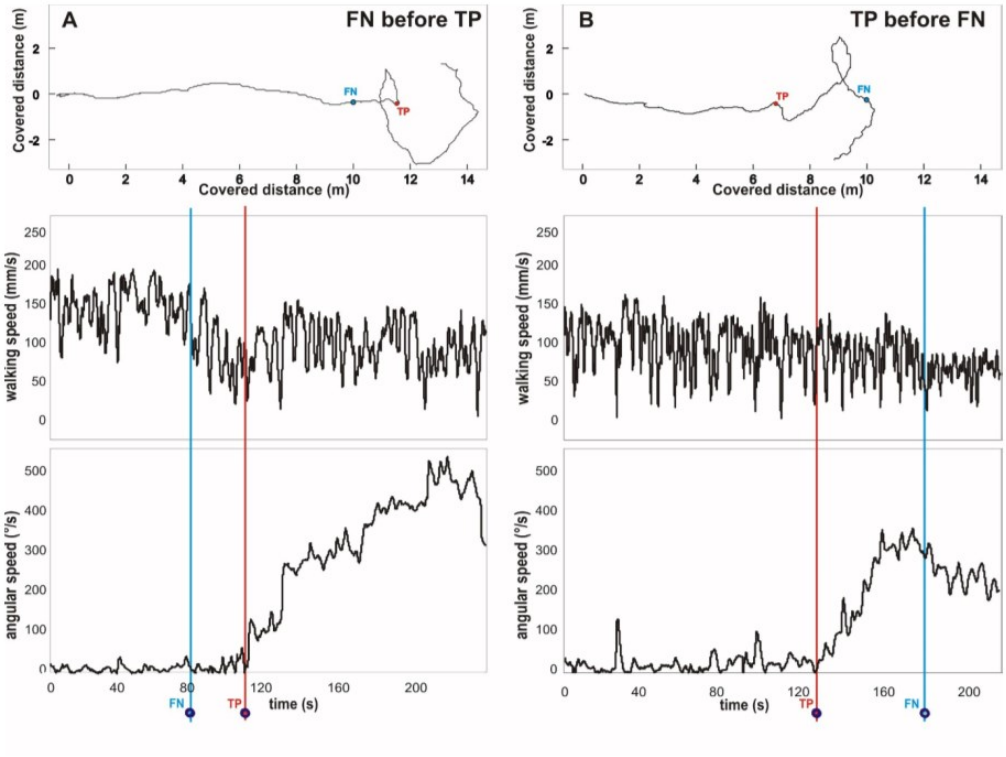

Fig. S8: Homing behaviour of two foraging *Cataglyphis fortis* ants with associated walking speed and angular speed

Example of two homing trajectories with (**A**) an ant first passing by the fictive nest position (FN, indicated as blue line) before showing a turning point (TP, indicated as red line) and (**B**) an ant showing the TP before passing by the FN. The walking speed was smoothed with a moving average of a factor of 1 and the angular speed was smoothed with a moving average of a factor of 2.

Journal of Experimental Biology • Supplementary information

Journal of Experimental Biology 220: doi:10.1242/jeb.148213: Supplementary information

SUPPLEMENTARY MOVIE

Movie S1

Example video of a homing *Cataglyphis fortis* desert ant on the closed loop setup.

Journal of Experimental Biology • Supplementary information

Kapitel 4

4. Manuscript 2

Walking and running in the desert ant *Cataglyphis fortis*

Verena Wahl, Sarah E. Pfeffer, Matthias Wittlinger

Institute of Neurobiology, Ulm University, 89069 Ulm, Germany

The final article is published 2015 in the **Journal of Comporative Physiology A**, 201(6), 645-656 and is availabe under
doi: 10.1007/s00359-015-0999-2
http://link.springer.com/article/10.1007/s00359-015-0999-2

This article is published with open access (© The Author(s) 2015) at Springerlink.com.
This article is distributed under the terms of the Creative Commons Attribution License which permits any use, distribution, and reproduction in any medium, provided the original author(s) and the source are credited.

J Comp Physiol A (2015) 201:645–656
DOI 10.1007/s00359-015-0999-2

ORIGINAL PAPER

Walking and running in the desert ant *Cataglyphis fortis*

Verena Wahl · Sarah E. Pfeffer · Matthias Wittlinger

Received: 25 November 2014 / Revised: 4 March 2015 / Accepted: 5 March 2015 / Published online: 1 April 2015
© The Author(s) 2015. This article is published with open access at Springerlink.com

Abstract Path integration, although inherently error-prone, is a common navigation strategy in animals, particularly where environmental orientation cues are rare. The desert ant *Cataglyphis fortis* is a prominent example, covering large distances on foraging excursions. The stride integrator is probably the major source of path integration errors. A detailed analysis of walking behaviour in *Cataglyphis* is thus of importance for assessing possible sources of errors and potential compensation strategies. Zollikofer (J Exp Biol 192:95–106, 1994a) demonstrated consistent use of the tripod gait in *Cataglyphis*, and suggested an unexpectedly constant stride length as a possible means of reducing navigation errors. Here, we extend these studies by more detailed analyses of walking behaviour across a large range of walking speeds. Stride length increases linearly and stride amplitude of the middle legs increases slightly linearly with walking speed. An initial decrease of swing phase duration is observed at lower velocities with increasing walking speed. Then it stays constant across the behaviourally relevant range of walking speeds. Walking speed is increased by shortening of the stance phase and of the stance phase overlap. At speeds larger than 370 mms^{-1}, the stride frequency levels off, the duty factor falls below 0.5, and *Cataglyphis* transitions to running with aerial phases.

V. Wahl and S. E. Pfeffer equally contributed to the manuscript.

Electronic supplementary material The online version of this article (doi:10.1007/s00359-015-0999-2) contains supplementary material, which is available to authorized users.

V. Wahl · S. E. Pfeffer · M. Wittlinger (✉)
Institute of Neurobiology, University of Ulm, 89069 Ulm, Germany
e-mail: Matthias.wittlinger@uni-ulm.de

Keywords Desert ant · *Cataglyphis* · Stepping pattern · Inter-leg coordination · Gait

Introduction

If you are in a North African salt pan in the middle of the day, you would probably encounter *Cataglyphis fortis* desert ants pacing around with tremendous speeds on their long legs, insects Rüdiger Wehner likes to call "race horses in the insect world" (Wehner 2009). Like race horses with their shiny and delicate bodies, they can doubtlessly exert a fascination on the observer when they attain high walking speeds while swiftly manoeuvring through their harsh environment, always on the look-out for dead insects that succumbed to the heat of the day (Wehner 1983). Individuals with a prey item, one can see running along an imaginary straight line which connects the place where they had encountered the food with the nest entrance. The kind of navigation that *Cataglyphis fortis* ants perform on their foraging excursions is an approximate form of dead reckoning, the so-called path integration where the ants are constantly connected to the nest location via an invisible link (Collett and Collett 2000; Wehner and Srinivasan 2003; Wehner and Wehner 1986, 1990). Combining path integration as a navigation mode and high walking speeds, *Cataglyphis* ants maximize their chances of finding food and returning to the nest even in the hottest times of the day without succumbing to the hostile conditions. To perform path integration *Cataglyphis* ants would need two inputs: (1) information about angles steered, that is, the direction and (2) information about the distance travelled. Directional information is provided by a celestial compass (Wehner 1982; Müller and Wehner 1988), and distance information is gained by means of a stride integrator (Ronacher and

Wehner 1995; Wittlinger et al. 2006, 2007) which might be a major source of navigational errors. To better understand the stride integrator, we need a detailed analysis of walking behaviour and thus the inter-leg coordination across the entire range of walking speeds employed by *Cataglyphis fortis*. Zollikofer (1994a) demonstrated consistent use of the tripod gait in desert ants and suggested an unexpectedly constant stride length as a possible means of reducing navigation errors. During his time in Rüdiger Wehner's lab, Christoph Zollikofer pioneered the work on walking kinematics in these fast running desert ants, and since then many details have been revealed about the locomotor behaviour of *Cataglyphis fortis* compared to other species, namely the influence of speed and curvature, of body morphology and load (Zollikofer 1988, 1994a, 1994b, 1994c) or locomotion on sloped surfaces (Seidl and Wehner 2008; Weihmann and Blickhan 2009). Nevertheless, with advanced high-speed videography at hand, we are now able to get a more thorough insight into *Cataglyphis*' walking behaviour. Moreover, we can extend these studies not only by more detailed analyses of inter-leg coordination but also expand the range of walking speeds to where we assume its limits. The aim of this paper is to investigate the effect of walking speed on the inter-leg coordination or gait, stride length, walking speed and stride amplitude, duty factor, as well as swing and stance phase and phase relationships of all six legs.

Materials and methods

Ant colonies

High-speed video recordings were performed in the field near Maharès, Tunisia and in the laboratory at University of Ulm, Germany. For the laboratory recordings, several colonies of *Cataglyphis fortis* were kept and raised under annual temperature and daily light–dark cycles based on conditions in their natural habitat (20–35 °C, winter–summer; 14 h:10 h, light:dark cycle in summer). The colonies in the laboratory consisted of several hundred ants, with an active forager force of approximately 10 % of the population size. Estimated from the number of active foragers, the field colonies and the colony size were comparable. The laboratory ants received water ad libitum and were fed with honey water and insects, five times a week.

Experimental procedure

Medium to large sized (2.5–3.3 mm alitrunk length) *Cataglyphis fortis* ants were individually marked and were filmed with a camera placed above the channel while they walked in a linear channel with a width of 7 cm and channel wall height of 7 cm. We video filmed the running ants between 0900 and 1600 h. The highest walking speeds were usually recorded around noon, when the highest air temperatures were reached in the field. Channel floors were evenly coated with a very fine layer of firmly attached white sand (0.1–0.4 mm particle size) to provide good traction and thus to facilitate slip-free natural walking and running kinematics. Film recordings were made with a high-speed camera (MotionBlitz Eosens Mini1, Mikrotron Unterschleissheim, Germany) at 500 and 1000·frames per second (Fig. 1) and shutter times of 100–200 µs. The indoor laboratory video shoots were illuminated with two fibre optic cold light sources (Schott KL 1500LCD, 150W, Schott AG, Mainz, Germany) whereas videos filmed under open sky outdoor conditions needed no external light sources since the sun provided plenty light. To get videos of very slowly walking desert ants, the channel setup was cooled down to about 10–15 °C by means of cooling pads.

Data analysis

In the experiments, the ants walked through the channel at different speeds. Both inbound and outbound walking ants were considered for the walking analysis. Especially in the outdoor video sessions, the inbound walking ants sometimes carried a minute food item. Each individual was video recorded up to five times, consequently in the data of $N = 388$ runs up to five runs might origin from one ant. Only those individuals exhibiting regular straight and linear walks without de- or acceleration or abrupt stops were used for the tests. Each analysed walk contained at least three step cycles per leg. A 5 cm long black and white scale bar was filmed after each set of videos with the same settings to calibrate the analysed videos. Tarsal footfall positions as well as times of lift-off (or movement away from the contact point) and touch-town of the tarsal tips were digitized with ImageJ (US National Institutes of Health, Bethesda, Maryland, USA, http://imagej.nih.gov/ij/) on a frame-by-frame basis. The duration of swing phases were calculated as the difference between the time the tarsal tip lifts off the ground and subsequent touchdown of the tarsal tip of the same leg for the swing phase or vice versa for the stance phase. In the hind legs, the tarsal tip often is dragged over the floor without being lifted off the ground. Here, we define the moment when the tarsal tip leaves the contact point on the floor as start of the swing phase (Reinhardt and Blickhan 2014). The onset of stance was used as the reference time for the analysis of temporal coordination of all legs for the phase analyses. The CircStat Toolbox in MATLAB was used for phase analyses and the corresponding plots (Berens 2009; Wosnitza et al. 2013). Stride frequency is defined as the walking speed divided by the stride length. The stride length was calculated for each leg

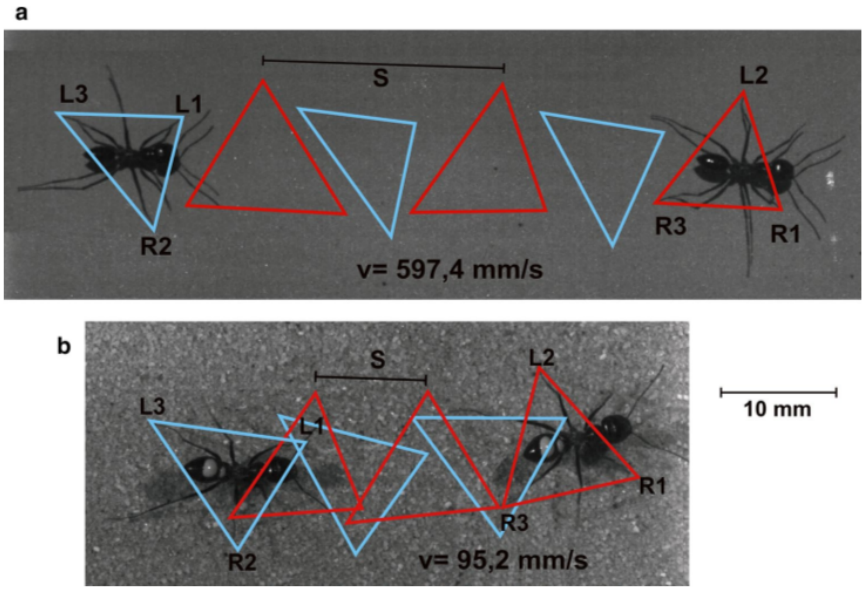

Fig. 1 Tripod gait of a fast running and a slowly walking *Cataglyphis* individual. Six complete strides—three of each body side—captured by high-speed video are shown. Tripods formed by the right front and hind leg (R1, R3) and the left middle leg (L2) are drawn in *red*; tripods formed by the left front and hind legs (L1, L3) and right middle (R2) leg are drawn in *blue*. Stride length (*s*) was determined as the distance between two successive footfalls of the same leg. **a** Very fast running ant showing the typical tripod gait ($s = 19.8$ mm; $v = 597.4$ mm s^{-1}). **b** A rather slowly walking ant also showing the typical tripod gait, however, with reduced stride length ($s = 9.1$ mm; $v = 95.2$ mm s^{-1}). Single video frames of the ant, taken during the first and sixth captured steps, are pasted into the tripod analysis figure

pair (L1, R1; L2, R2; L3, R3) as the mean of each leg pairs' strides in one video sequence. Stride length is specified as the measure from two successive footfalls of the same leg of one body side (Alexander 2003). A stride should not be confused with a step, which is the distance the body covers from the footfall of a leg pairs' left leg to the footfall of the right leg or vice versa. A stride thus basically incorporates two steps, the left and the right. Stride length is therefore actually double the step length (assuming the left step is more or less the same as the right step and walking speed is constant). When we look at the tripod shaped gait in Fig. 1, one stride describes the relationship of two successive triangles of the same colour whereas one step describes the relationship of two differently coloured successive triangles. In this account, we only employ the term stride as mentioned above and as it is defined in Alexander (Alexander 2003). The stride amplitude is a measure for the swing of one leg during a stride without the additional body movement during the swing phase (Wosnitza et al. 2013). We calculated the stride amplitude as the stride length minus swing phase duration multiplied by walking speed. The stride amplitude (Wosnitza et al. 2013) which is misleadingly called "stride length" in Hughes (1951) is technically a body coordinate based measure for the swing movement of a leg. We, however, calculated the mean stride amplitude of a run as an indirect measure from geocoordinate based data, such as the means of stride length, swing phase duration and walking speed. We also assume a constant mean walking speed for all runs evaluated. Therefore, minor errors might occur. Although a certain variability of walking speed within a step cycle might be observed especially for the slow walks, we only evaluated video sequences with a constant mean walking speed over several step cycles. Mean walking speed was measured from the start of the first step cycle to the end of the last step cycle in one video sequence.

We calculated the tripod coordination strength (TCS) which evaluates the quality of the tripod coordination (Wosnitza et al. 2013; compare also Spagna et al. 2011). First, we calculated the time from the earliest swing onset to the latest swing termination. This gave us time t_1, during which at least one of the three legs was in swing phase. Then we determined time t_2, during which all three legs were in swing phase at the same time. The ratio t_2/t_1 then described the TCS. A TCS of 1 indicated perfect tripod coordination; it approached 0 when the temporal relationship of swing phases shifted to other coordination patterns (Wosnitza et al. 2013). The duty factor, a ratio of stance phase

to cycle period can be used as a measure that describes the transition from walking to running (Alexander 2003). We measured the cycle period as the time between successive touchdowns of the same limbs. Thus, one gait cycle begins when the reference foot contacts the ground and ends with subsequent touchdown of the same foot. Since cycle period of very slow walks gets more variable and calculations of TCS or duty factors do not deliver appropriate, comparable values, we carried out a separate evaluation of walking behaviour during slow locomotion (Fig. 5). We did a frame-by-frame analysis of 76 videos within a speed range of 4.5 to 29.9 mms^{-1} (five different speed groups I–V) by classifying each frame according to its gait pattern similar to the work of Mendes et al. (2013). Each frame was assigned a certain colour and a number representing the different leg coordination types. For the different leg combinations used for our gait analysis, see supplementary material. If none of the listed leg combinations was found, the frame was classified as 'undefined'. For each of our five speed groups, we calculated a percentage distribution of different leg combinations, which the ants applied during slow walks. Further, the frames' gait index was averaged for each video and pooled according to the five speed groups to accomplish a more inter-individual comparison. Statistical analyses were performed with SigmaPlot 11.0 (Systat Software Inc., San Jose, California, USA). Pair-wise comparisons (Fig. 5) and comparisons of slope and y-intercept (Figs. 3a, 6b) were performed with a t test, since respective groups were all normally distributed. We fitted data with linear, power and polynomial functions and calculated R^2 in Microsoft Office Excel 2013.

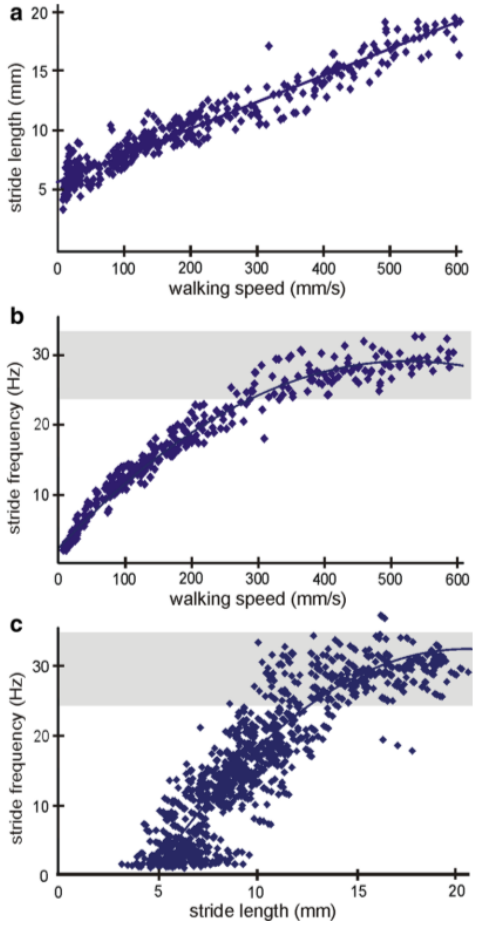

Fig. 2 General walking parameters, stride length, stride frequency and walking speed and their relationships. Only middle leg data are plotted; *each data point* represents one video sequence ($N = 388$). **a** Stride length as a function of walking speed for the entire walking speed range. Linear regression is indicated; $y = 0.023 \times x + 5.93$; $R^2 = 0.93$. **b** Stride frequency as a function of walking speed. Best fit regression is indicated; $y = -0.0001\ x^2 + 0.11x + 1.63$; $R^2 = 0.97$. **c** Stride frequency as a function of stride length. Best fit regression is indicated; $y = -0.115x^2 + 4.78x - 19.77$; $R^2 = 0.81$. The *grey horizontal bar* highlights the frequency plateau (**b**, **c**)

Results

The walking parameters of *Cataglyphis fortis* were evaluated spatially and temporally over the entire walking speed range from 4.5 to 619.2 mms^{-1}.

With increasing walking speed, the stride length increases in an almost perfectly linear fashion (Fig. 2a). The faster the ant runs, the longer the strides get. The stride length increases more than fourfold over the entire speed range from 3.5 mm (at 4.5 mms^{-1}) to 19.8 mm (at 589.5 mms^{-1}). Stride frequency increases as a function of walking speed and levels off at a frequency plateau of around 30 Hz beginning somewhere between 300 and 400 mms^{-1} (Fig. 2b). In the desert ants, the start of the frequency plateau is a first indication that the ants attain aerial phases. Ants that are achieving longer strides, increase stride frequency to a maximum at which the frequency reaches the upper level while the strides are still getting larger. From this point on, walking speed is increased by increasing stride length only. To maximise stride length in spite of a stagnant stride frequency, the ants become "airborne" from footfall to footfall to cover a larger distance (Fig. 2c).

The stride amplitude (Wosnitza et al. 2013), is a body coordinate based measure for the swing of a leg. The stride amplitude of the middle leg shows a good linear correlation with increasing walking speed. The amplitude of the middle legs doubles, whereas the amplitudes of front and hind legs do not increase significantly and show only a weak correlation ($R^2 = 0.28$, front legs; $R^2 = 0.66$, middle legs; $R^2 = 0.20$, hind legs) (compare Fig. 3a). For the middle leg,

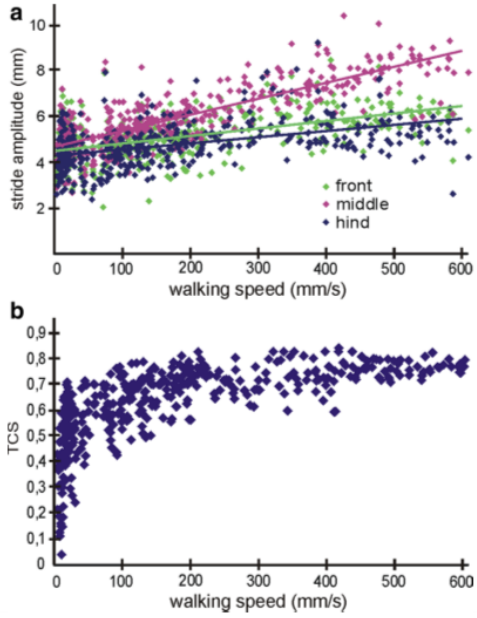

Fig. 3 Walking parameters of $N = 388$ high-speed videos. **a** Stride amplitude as a function of walking speed for all three leg pairs. Leg pairs are represented in *green* (front legs), *magenta* (middle legs) and *blue lines* (hind legs); linear regression lines are indicated, front legs: $y = 0.0032 \times x + 4.54$; $R^2 = 0.28$; middle legs: $y = 0.0067 \times x + 4.72$; $R^2 = 0.66$; hind legs: $y = 0.0026 \times x + 4.33$; $R^2 = 0.20$. The slope of front and middle legs differ significantly (t test, $p < 0.05$) as well as that of the middle and the hind legs (t test, $p < 0.05$) while front and hind legs are not significantly different. For all leg pair combinations, the y-intercept is significantly different (t test, $p < 0.05$). **b** Tripod coordination strength (TCS, for definition see "Materials and methods") as a function of walking speed

this means that 66 % of the variability can be described by the linear regression model.

Since *Cataglyphis* is known to employ tripod coordination over most of the walking speed range (Seidl and Wehner 2008; Wittlinger et al. 2006, 2007; Zollikofer 1988, 1994a), we evaluated the quality and synchrony of the tripods by means of the tripod coordination strength (TCS) (Wosnitza et al. 2013; compare also Spagna et al. 2011). The variability of the TCS decreases with increasing walking speed and at the same time converges towards the maximum levels of around 0.7 to 0.85. From a walking speed of around 300 mms^{-1}, the variability is least whereas at lower speeds, the TCS varies between 0.02 and 0.78. Above walking speeds of around 300 mms^{-1}, t_2 and t_1 of the TCS both remain at constant levels of 12–22 ms (t_2) and 24–34 ms (t_1). To further analyse the inter-leg coordination and the phase relationships of the tripods, we made footfall patterns or podograms that show the swing and stance phases of every leg as black (swing) and white (stance) bars along a timeline (Fig. 4a–d). The podogram in Fig. 4a shows a very slow locomotion. This walk with 6.9 mms^{-1} is at the lower edge of walking speed and exemplifies that calculations used for the walking speed larger than 30 mms^{-1} (e.g. TCS and duty factor) do not provide any useful information in this case. Therefore, slow walks were analysed and quantified separately in Fig. 5. In contrast, the podograms of the higher walking speeds (Fig. 4b–d) beautifully show tripod coordination. The green bar in Fig. 4b highlights the stance phase overlap where all six legs are on the ground at the same time (hexa support phase) for a relatively slow walk. The blue bar in a very fast run (Fig. 4d), however, exemplifies the swing phase overlap (aerial phase) which is the time where the ant is airborne—all legs lost ground contact—except for some cases where the hind legs might be dragged over the substrate. We also calculated phase plots of the stance phase onset of all six legs with respect to the left hind leg (Fig. 4e, f). Each of the three leg pairs shows an antiphasic relation. The legs are more or less coordinated as a tripod of L1, L3, R2 and L2, R1, R3. Figure 4e and f show that the middle leg of one tripod tends to touchdown first, and then the hind leg touches the ground, followed immediately by the front leg, which is nearly in phase with the hind leg. The data points (blue) of slow walks (Fig. 4f) are more spread than in the fast walks (Fig. 4e). This also confirms what we already know from the TCS analysis. The tripods are never perfectly in phase and the TCS improves with increasing walking speed. Nevertheless, we can see how a tripod is temporally formed. The three legs of one tripod never touch down or lift-off the ground simultaneously but the temporal coordination improves with increasing walking speed.

In a separate analysis, we focused on walking behaviour during slow locomotion below walking speeds of 30 mms^{-1}. A continuous gait transition from tripod to tetrapod to wavegait coordination is proposed for hexapods with decreasing walking speeds (Schilling et al. 2013). Throughout its entire walking speed range, *Cataglyphis fortis* ants predominantly walk in tripod-fashion, which is also true for the runs at the lower edge of walking speeds (Fig. 5b). However, it seems evident that with decreasing speed, the tripod coordination is getting more inconsistent and the number as well as the proportion of other stepping patterns increases. We observed that ants use poorly coordinated or non-tripod pattern only for a short period of time. Almost all ants that show tetrapod, wavegait or other undefined stepping patterns during more than one step cycle, subsequently display the transition into tripod coordination within the same video sequence (Fig. 5a).

To illustrate the variability of leg coordination of very slow walks, we not only used the podograms but also colour coding and indexing of stepping patterns (see examples in Fig. 5a, 6.9 mms^{-1} with the transition from tetrapod to tripod

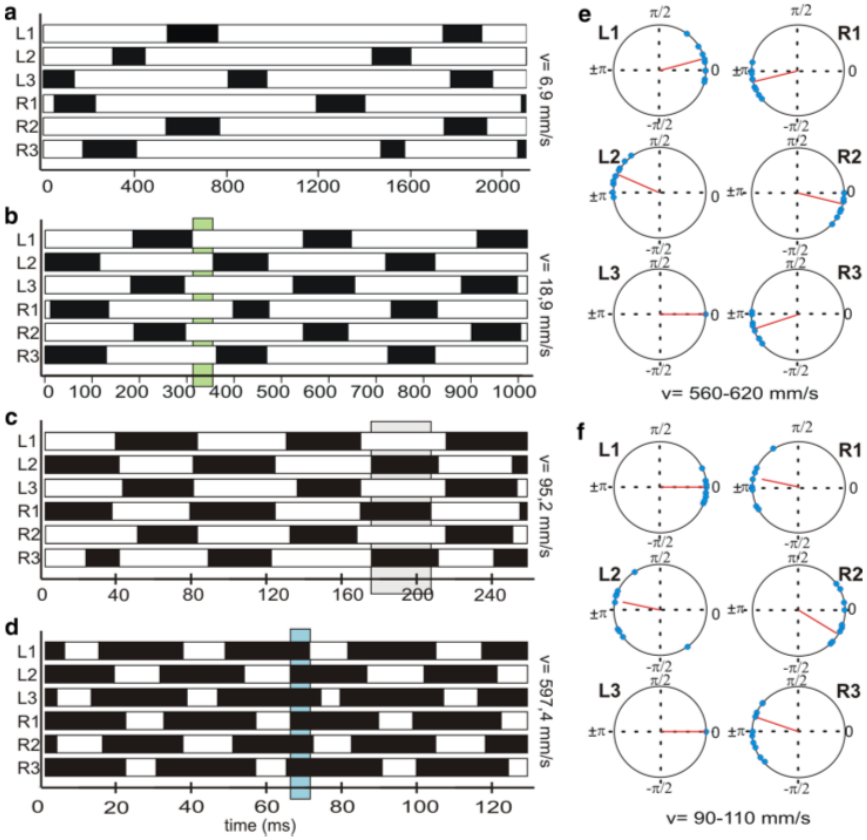

Fig. 4 Analysis of inter-leg coordination. (**a**–**d**) Footfall patterns, podograms, of all six legs from four runs with different walking speeds, from minimum to almost maximum speed. *White bars* represent stance phases, *black bars* represent swing phases; *L* left, *R* right body side; *1*, *2* and *3*, front-, mid- and hind leg. *Shaded areas* highlight exemplary tripod gait patterns with stance phase overlap (*green*, see **b**) and swing phase overlap (*blue*, compare **d**). *Shaded area* (*grey*, compare **c**) highlights an exemplary footfall pattern with a TCS of 0.77. Walking speeds are 6.9 mms^{-1} (**a**), 18.9 mms^{-1} (**b**), 95.2 mms^{-1} (**c**) and 597.4 mms^{-1} (**d**). (**e**, **f**) Phase plots of the stance, phase onset of all legs with respect to the left hind leg; *L1*, *L2*, *L3*, left side front, middle and hind leg; *R1*, *R2*, *R3* right side front, middle and hind leg. Two exemplary walking speed ranges are shown, 560–620 mms^{-1} (**e**) and 90–110 mms^{-1} (**f**). *Blue* data from five runs; *red line* mean vector

coordination; and Fig. 5b, 6.0 mms^{-1} with tripod coordination). The colour coding and indexing was also applied to quantify the leg coordination in all ($N = 76$) videos below walking speeds of 30 mms^{-1}. In Fig. 5c, we give a summary of percentage values of different gait patterns. They show that with increasing speed, the proportion of tripod gait increases, while tetrapod coordination and wave gait decreases as well as the time where all six legs have ground contact simultaneously (hexa support phase). To further compare the individual performance, we averaged the index that was assigned to each frame in one video (Fig. 5d). This shows that with increasing speed the indices also increase, which reflects the increasing consistency of the tripod.

Note that a large fraction of non-tripod combinations forms in the transitional time from one tripod group (e.g. L1, R2, L3) to the subsequent one (L2, R1, L3). When we look at Fig. 5b, we clearly notice tripod coordination in the podogram, though other coordinations are also present to a large extent (compare Fig. 5b, colour coding and indexing graph). Hence, our analysis shows that even slow walking *Cataglyphis* ants preferentially employ tripod coordination, but with decreasing speed, the tripod gets more variable and other leg coordination are used as well.

We will now have a look at the swing and stance phase durations as a function of walking speed (Fig. 6a). Both the swing phases and the stance phase are significantly reduced at the initial part of the walking speed range. While the stance phases are longer than the swing phases at lower walking speeds, this relation reverses at higher walking speeds. Interestingly, the reversal in the hind legs and front legs occur much earlier (hind legs: 95 mms^{-1}) than in the middle legs (middle legs: 349 mms^{-1}). The duration of swing and stance phases in *Cataglyphis* decrease with increasing walking speed in the fashion of a power function (compare Fig. 6a) and remains more or less constant from a walking speed of 300 mms^{-1} in (Fig. 6a). For a large part of the range, the walking speed is increased by reducing the stance phase while the swing phase stays rather constant. At highest walking speeds, the middle legs have the shortest swing phase and longest stance phase of all legs. Hence, the middle legs are the first to touch the ground and the last to lift-off again. We define the swing phase as the time where the leg is in motion, that is, the time from where the tarsal tip of one leg leaves the contact point on the substrate to the subsequent contact point on the ground. The hind legs displayed a peculiarity in that they often moved the

J Comp Physiol A (2015) 201:645–656

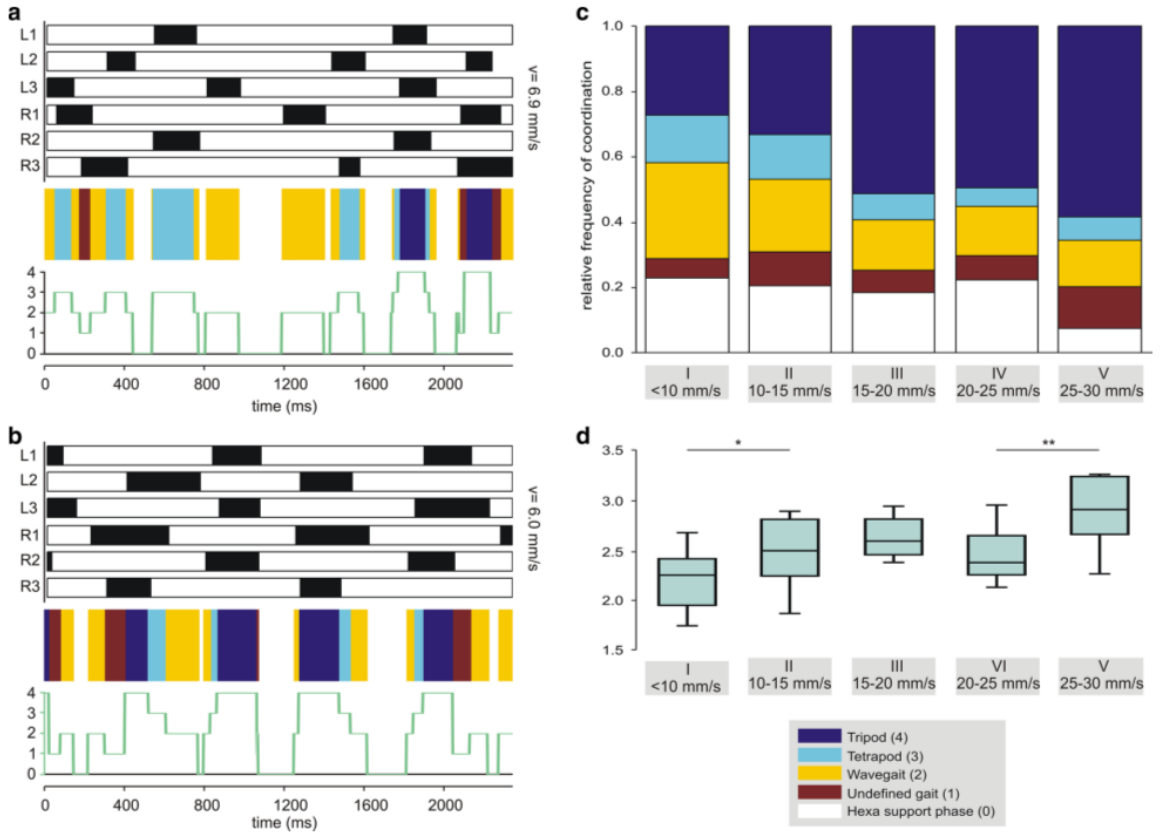

Fig. 5 Quantification of gait pattern during slow walking. Gait Pattern analysis for ants walking at **a** 6898 mms^{-1} and **b** 5959 mms^{-1}. (**a**, **b**) Podogram (*above*), coloured coding (*middle*) and indexing (*below*). Illustration details of the podograms as in Fig. 4. For the colour coding and the indexing we used five different classifications: 'tripod' (*dark-blue*, 4), 'tetrapod' (*light-blue*, 3), 'wavegait' (*yellow*, 2) or 'hexa support phase' (*white*, 0). If none of these possibilities were applicable, the frame was classified as 'undefined' (*red*, 1). For the list of exact leg combinations representing a typical gait see supplementary material. **c** Quantification of the $N = 76$ slow walking speed videos were grouped into five categories: *I* 5–10 mms^{-1} (17 videos, 8950 frames; 27, 14, 29, 6, 23 %), *II* 10–15 mms^{-1} (16 videos, 7376 frames; 33, 14, 22, 10, 21 %), *III* 15–20 mms^{-1} (20 videos, 7116 frames, 51, 8, 15, 6, 18 %), *IV* 20–25 mms^{-1} (14 videos, 4284 frames; *V* 25–30 mms^{-1} (9 videos, 2423 frames; 58, 7, 15, 13, 7 %). The percentage information in *brackets* after the semicolon is rounded and is arranged as follows: tripod, tetrapod, wavegait, undefined gait, hexa support phase. **d** The averaged index for each video provide a more individual analysis of the ants' walk. Group I differs significantly from group II (*t* test; $p = 0{,}014$); the same was true for group IV and group V (*t* test; $p = 0{,}004$). The three intermediate speed groups (II, III, IV) do not show any statistically significant differences to their respective neighbouring groups

tarsi along the floor without being lifted off the floor. This "gliding phase" is part of the swing phase, although the gliding hind legs that are basically dragged behind the ants still touched the ground. This phenomenon has recently been observed in *Formica* ants as well where the tarsi of the hind legs were regularly dragged over the substrate without being significantly raised off the ground (Reinhardt and Blickhan 2014). In some video sequences, we were able to observe that the tarsal claws were retracted before the gliding phase and thus the swing phase started.

Another measure for the phase relationship is the duty factor. Besides, it is one measure that characterises the dynamics of when the transition from walking to running occurs. It is assumed that at values of around 0.5, this transition happens (Alexander 2003). With increasing walking speed, the duty factor decreases linearly for all three leg pairs. The hind legs are the first to fall below the duty factor of 0.5 at 132 mms^{-1}, then the front legs (at 182 mms^{-1}) followed by the middle legs (at 369 mms^{-1}). The middle legs are the last to reach aerial phases and thus determine the walking speed threshold at which the transition from walking to running occurs. From that speed on the ants are "jumping" from step to step to further increase their strides (compare the gaps between the triangles in Fig. 1a).

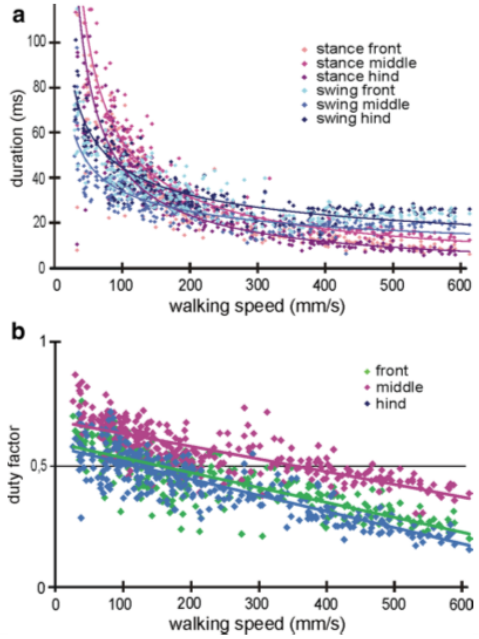

Fig. 6 Stance and swing phase duration and duty factor. **a** Durations of stance (*three shades of purple*) and swing phases (*three shades of blue*) as a function of speed of all three leg pairs. Graphical fits are represented for middle and hind legs in *purple* ($y = 0.22x^{-0.38}$, $R^2 = 0.75$; $y = 0.26x^{-0.41}$, $R^2 = 0.77$) and *blue lines* ($y = 1.76x^{-0.83}$, $R^2 = 0.88$; $y = 1.58x^{-0.79}$, $R^2 = 0.84$), respectively. Runs without tripod coordination with walking speeds below 25 mms^{-1} have not been considered for these graphs. **b** Duty factor, which is the ratio of stance phase duration to duty cycle, versus walking speed for all three leg pairs. Leg pairs are represented in *green* (front legs), *magenta* (middle legs) and *blue lines* (hind legs); linear regression lines are indicated, front legs: $y = -0.0005x + 0.59$; $R^2 = 0.66$; middle legs: $y = -0.0004x + 0.66$; $R^2 = 0.61$; hind legs: $y = -0.0006x + 0.57$; $R^2 = 0.73$. The slopes of front and middle legs differ significantly (t test, $p < 0.05$) as well as that of the middle and the hind legs (t test, $p < 0.05$) while front and hind legs are not significantly different. For all leg pair combinations, the y-intercept is significantly different (t test, $p < 0.05$)

Discussion

In 1850, the long legged desert ant of the genus *Cataglyphis* was described as a "most remarkable appearance within the insect fauna of old world desert areas" (Foerster 1850). With its long legs that characterise all *Cataglyphis* species, *Cataglyphis fortis* reaches the highest running speeds with values of up to 0.7 ms^{-1} in the literature (Wehner 1983). How are these ants able to reach such high running speeds? This question was already tackled by Christop Zollikofer when he was a PhD student in Rüdiger Wehner's lab (Zollikofer 1988, 1994a, 1994b, 1994c). His work was the beginning and basis of our data collections and analyses that we present here. With more advanced techniques, we were able to expand the range of walking speeds to its limits and to extend the analysed parameters.

Contribution and role of the leg pairs to locomotion

The variation in stride amplitude as well as in stance and swing phase duration of the front legs tends to be higher than that of the middle and hind legs. A freer and unhampered positioning of the frontal tarsi is possible here because there are no legs in front of them with which they could interfere and thus limit their range in frontal direction. One could assume that the front legs generate the smallest forces with reference to the body movement. In *Acheta domestica* (Harris and Chiradella 1980), *Carausius morosus* (Cruse 1976) and *Periplaneta americana* (Full and Tu 1991) force measurements confirm the front leg part in keeping the body's stability. The longitudinal forces of the protarsi act against the moving direction.

Interestingly, Zollikofer (1988) observed a higher correlation of the front leg stride length with walking speed than that of the middle and hind legs. Moreover, he describes that when sprinting, the front legs of *Cataglyphis bombycina* specimens would often not leave any tarsal imprints on the smoked-glass plates that he used for the stride analysis. This fact made him conclude that at very high running speeds, the ant's front legs would stop touching the ground, performing a form of quadrupedalism (Zollikofer 1994b). Loss of ground contact is well known in insects (*Periplaneta americana*: Full and Tu 1991), in crabs (*Ocypode quadrata*: Blickhan and Full 1987) and in vertebrates (Heglund et al. 1974).We cannot confirm this observation in *Cataglyphis fortis*, although we analysed a large number of runs from the laboratory and the field over the entire speed range. Sometimes, however, when ants got startled, they showed a short sequence where they accelerated, rising the head and prosoma and lifted the forelegs off the ground. They performed a movement comparable to a "wheelie" known from motorbikes when their front wheel loses ground contact during high accelerations. However, we did not see this behaviour in fast running ants with constant speed.

The middle legs seem to play a distinctive role in the locomotor apparatus of *Cataglyphis fortis* desert ants. They show the longest stance phase and the shortest swing phase of all legs. The middle leg of the tripod is thus the first leg touching down and the last lifting off the ground. Hence, the duty factor of the middle legs is the last to underscore 0.5 with increasing speed and thus determines the start of aerial phases. At high running speeds, the tarsi of the middle legs show the most distal trace of swing and are positioned at a great lateral distance reaching over the neighbouring legs without interfering with them (Zollikofer 1988). Although this overlap happens, the legs are not

hampering each other. Further, the middle legs also perform the largest stride amplitude. Considering all this, we may conclude that the middle legs exert the biggest influence on the speed and thus on locomotion.

The stance phase of the hind legs at high walking speeds is very short compared to that of the other legs. This might be due to the fact that the hind legs display something like an intermediate phase where the tarsi are moved along the floor without being lifted off the ground. This gliding phase is a part of the swing phase, although the gliding hind legs that are basically dragged behind the ants' body probably still provide support and thus stability, while they are already swung. This phenomenon has also been recently observed in spiders and Formica ants (Spagna et al. 2011; Reinhardt and Blickhan 2014). Moll et al. (2013) also present an example of a grass-cutting ant that gains static stability by sliding hind legs during transport of load.

Stepping pattern of slow and fast walking ants

Leg coordination during locomotion is flexible and can be adapted according to environmental circumstances (Alexander 1989). Walking speed can be one of those factors modulating locomotor output. With changes in walking speed quadrupeds, like horses, adapt their leg coordination to achieve an energetically optimal locomotion (Hoyt and Taylor 1981). Thereby, the transition from one to the next gait occurs in a discontinuous way. In hexapods also different gait types are known, but the question of gait transition has not yet been resolved (Graham 1985; Mendes et al. 2013). After examinations in several species, the current understanding is that the different leg patterns are part of a continuum with a continuous transition from tripod to tetrapod to wavegait coordination with decreasing walking speed (Schilling et al. 2013).

Stick insects (*Carausius morosus*) have been observed to use tetrapod coordination during slow locomotion but switch to tripod pattern with higher speeds (Wendler 1964; Graham 1972, 1985). The analysis of kinematics and walking behaviour in cockroaches (*Periplaneta americana* and *Blaberus discoidalis*) revealed two different types of tripods for locomotion, a low-speed amble and a high-speed trot (Delcomyn 1971; Bender et al. 2011). Fruit flies (*Drosophila melanogaster*) prefer tripod gait during the entire range of walking speeds, but leg coordination also gets more variable with the decrease in walking speed (Strauss and Heisenberg 1990; Mendes et al. 2013; Wosnitza et al. 2013). Wood ants (*Formica polyctena*) show stable tripod coordination during the entire range of running speed (Reinhardt and Blickhan 2014).

Our results show that the walking behaviour of desert ants (*Cataglyphis fortis*) is in close agreement with that described in *Drosophila melanogaster* and *Formica polyctena*. Desert ants employ tripod gait as their major coordination pattern over the entire walking speed. This was also the case for very slow walks, where tripod pattern was generally preserved. However, it also becomes apparent that during slow walks, synchrony of tripod coordination could be reduced or other non-tripod combinations, especially tetrapod coordination could occur, as well. This variability shows that *Cataglyphis fortis* does not need to rely strictly on tripod coordination and is *per se* able to use different patterns during walking.

However, the still preferred use of tripod seems to be kind of advantageous, probably it is an option to reduce errors arising from the iterative processes of path integration. The preference of tripod coordination also during slow walks shows that *Cataglyphis* ants mostly remain at the upper end of gait continuum proposed for hexapods (see explanation above). Regarding the higher variability of leg coordination during slow locomotion, ants scale down slightly from this upper end. It is conceivable that ants might also be able to reach the lower part of the continuum, yet in our investigation this was never evident.

The very slow walks rarely occur in the field. We know from observations that the walking speed employed during foraging is reached within the first two strides. To make the ants constantly walk below 30 mms^{-1} speed, we had to chill the environment, which in this case was a walking channel in the laboratory. Very rarely did we observe ants in the field in late spring and on relatively chilly early mornings walking at very low speeds out of the nest and soon back into the nest. They have never been observed to forage under these chilly conditions.

The quality of tripod coordination can be evaluated by means of a simple measure of tripod coordination strength (TCS) (Fig. 3b) (Wosnitza et al. 2013; compare also Spagna et al. 2011). With increasing walking speed, the TCS reaches values above 0.7 but never goes beyond 0.85. The legs of one tripod are at a minimum 15 % out of phase, even at highest walking speeds with maximum stride frequencies. From a walking speed of around 300 mms^{-1} on t_2 and t_1 of the TCS, both remain at a constant level of 12–22 ms (t_2) and 24–34 ms (t_1). This corresponds to the swing and stance durations that remain relatively constant for these higher speeds (see Fig. 6a). A TCS of 1.0 might increase the chance of jerky movements concentrating all impact forces of one tripod into one instant; especially at high speeds, there are less than 18 ms to distribute all ground reaction forces over the contact phase (compare Fig. 6a). As a result, a slight cutback of the TCS still assures a smooth run with maximum stability. The ants reach a TCS larger than 0.5 (an overlap of at least 50 %) from very low walking speeds on, while TCS smaller than 0.5 only occurs at walking speeds below 100 mms^{-1}. If we compare TCS of *Cataglyphis* and *Drosophila* which

can be between 0.1 and 0.8 (Wosnitza et al. 2013), we find that *Drosophila* at top speeds displays TCS comparable to *Cataglyphis*. Due to the wide range of walking speeds, *Cataglyphis* reaches top TCS values already at one-fifth of its speed range. The ants never touch ground with the tarsi associated with one tripod at the same time but kind of unroll the tripod like a 'functional foot' tarsal claw after tarsal claw. Especially at high walking speeds, the legs seem to act in a specific sequence. This tendency was also observed in *Drosophila* (Wosnitza et al. 2013). The alternating tripods are comparable to the alternating footfalls of bipedal walking animals (Full and Tu 1991). The big difference, however, is that tripods engage a larger area and thus provide more static stability especially for slower walking speeds whereas at higher walking speeds static stability is replaced by dynamic stability (Ting et al. 1994; Zollikofer 1994c).

How do *Cataglyphis* ants reach high running speeds?

Stride frequency increases in a nonlinear fashion with increasing walking speeds. The stride frequency levels off at around 30 Hz and shows a frequency plateau. From this point on, walking speed is increased by increasing stride length only. Heglund et al. (1974) described that a constant stride frequency can be an indicator for a change in gait. Small animals reach a certain speed with smaller strides and higher stride frequencies (Heglund et al. 1974; Zollikofer 1988). In the desert ants, the start of the frequency plateau is a first indication that the ants attain aerial phases. Zollikofer already presumed a frequency plateau for *Cataglyphis,* although he did not observe one. With maximum frequencies of 28 Hz, the plateau was not yet evident (Zollikofer 1988).

Aerial phases during running are also known from cockroaches (Full and Tu 1990, 1991) and vertebrates (Heglund et al. 1974). However, this is not necessarily true for all animals. For instance, ghost crabs, wood ants, ostriches, cockroaches and the American wandering spider can reach a frequency plateau without aerial phases by means of compliant legs and the employment of grounded running (compare Blickhan and Full 1987; Reinhardt and Blickhan 2014; Rubenson et al. 2004; Ting et al. 1994; Weihmann 2013). The difference is probably due to the relatively longer legs of *Cataglyphis*, which changes the biomechanics of walking. Longer legs mean larger strides in terms of stride amplitude and stride length. This characterizes the desert ants as stride length maximizers (Zollikofer 1988).

The duty factor, a ratio of stance phase to cycle period, is a measure that describes the transition from walking to running (Alexander 1984, 2003). At values below 0.5, swing phases are longer than stance phases, and thus aerial phases occur. Horses, dogs, ostriches and lizards reach duty factors well below 0.5 (Alexander 1984; Fieler and Jayne 1998). Cockroaches as fast-running specimens in the insect world, however, rarely reach such small duty factors (Ting et al. 1994). The middle legs of *Cataglyphis fortis* are the last of the three leg pairs to fall below the duty factor of 0.5 at a speed of 369 mms^{-1} (compare Fig. 6b). At speeds between 132 and 369 mms^{-1}, the ants are in a kind of transitional phase where the front and middle legs are already showing aerial phases while at least one middle leg has still ground contact. The gait transition is not abrupt at all, which means that the ants probably adopt a kind of grounded running within quite a wide range of running speeds. Thus, the dynamics of *Cataglyphis fortis*' locomotor apparatus seems to be quite similar to those of *Formica* worker ants and even similar to birds, but distinctively different from those of human beings (compare Reinhardt and Blickhan 2014; Rubenson et al. 2004).

In several insect species (Wilson 1966; Graham 1972; Strauss and Heisenberg 1990), stance phase duration becomes shorter with increasing speed, while swing phase duration remains largely constant; at the fastest speeds, the durations of both swing and stance phases equalize (Mendes et al. 2013; Wosnitza et al. 2013). The duration of swing and stance phases in *Cataglyphis* decreases with increasing walking speed and remain more or less constant at the upper end of the range (Fig. 6a). This corresponds approximately with the observations Delcomyn made in *Periplaneta americana* (Delcomyn 1971). In his observations, the swing and stance phases are reduced at low stride frequencies. While in *Cataglyphis* at lower speeds, stance phases are longer than swing phases, at high walking speeds the swing phases are longer than the stance phases. This reversal occurs for the hind legs already at around 95 mms^{-1}, and for the middle legs only at much higher speeds of 349 mms^{-1}. The walking speed (from 200 mms^{-1} on) is increased by reducing stance phase while the swing phase stays rather constant.

Walking speeds of up to 0.7 ms^{-1} have been reported for *Cataglyphis fortis* (Wehner 1983). Although we video filmed in the field several times at optimal conditions, we never measured higher walking speeds than 0.62 ms^{-1}. We believe that this is the upper limit of walking speeds for *Cataglyphis fortis* ants in the field site near Maharès, coastal Tunisia, which admittedly never reaches such temperature extremes like for instance the Chott El Cherid in central Tunisia.

Why is fast running important anyway? Fast running helps the ants to quickly cover large areas and thus to enhance the chance of finding food and then back home. It is probably also advantageous with regard to potential danger coming from predators and enemies like robber flies,

spiders, fringe toe lizards and conspecific ants (Dahbi et al. 2008; Schmid-Hempel and Schmid-Hempel 1984; Wehner et al. 1992). Hence, the ants reduce the time they are exposed to their harsh habitat. Long legs do not only help to reach larger strides and thus high walking speeds. They can also help to minimize heat stress (Zollikofer 1994b). Even slightly above the hot desert floor, temperatures decrease to values that the ants still can tolerate (Zollikofer 1988; Wehner et al. 1992; Gehring and Wehner 1995).

Outlook

It seems that every pair of leg contributes in a distinctive way to the ants' locomotion. The middle legs seem to play a major role in gaining speed and the hind legs contribute in supporting stability. Nevertheless, ground reaction force measurement of the legs would be desirable to further confirm our conclusions. With higher walking speed, the stride frequency levels off and *Cataglyphis fortis* ants show aerial phases to expand the walking speed range. Each tripod group is used as a functional foot literally jumping from footfall to footfall comparable to our human run. Consistent tripod coordination throughout the entire walking speed range may be advantageous for the stride integrator. The occurrence of very slow walking speeds, where the non-tripod stepping patterns are mostly observed is usually restricted to walks inside the nest and the immediate surroundings of the nest entrance. Especially on foraging excursions, where higher walking speeds occur—never below 30 mms^{-1}—robust and steady stepping coordination might induce errors as minimal as possible.

Acknowledgments We express our gratitude to Rüdiger Wehner for sharing his outstanding knowledge of this fascinating ant. We also thank Ursula Seifert for editing the text, Nadja Eberhardt, for recording the very slow walks. Till Bockemühl deserves a special thanks for providing Matlab code for the phase shift analysis plots. Harald Wolf provided the high-speed camera system and supported this study in many ways. We are much indebted to two anonymous referees for their many valuable suggestions on an earlier version of the manuscript. Initial Part of this investigation was supported by grants from the Volkswagen-Stiftung (project I/78580) and the Deutsche Forschungsgemeinschaft (WO466/9-1) to H. W. Financial and infrastructural support was provided by the University of Ulm.

Conflict of interest The authors declare that they have no competing interests.

Ethical standard All experiments comply with the current laws and regulations of the University of Ulm and of the country where they have been performed.

Open Access This article is distributed under the terms of the Creative Commons Attribution License which permits any use, distribution, and reproduction in any medium, provided the original author(s) and the source are credited.

References

Alexander RM (1984) Walking and running: legs and leg movements are subtly adapted to minimize the energy costs of locomotion. Am Sci 72:348–354

Alexander RM (1989) Optimization and gaits in the locomotion of vertebrates. Physiol Rev 69:1199–1227

Alexander RM (2003) Principles of animal locomotion. Princeton University Press

Bender JA, Simspon EM, Tietz BR, Daltorio KA, Quinn RD, Ritzmann RE (2011) Kinematic and behavioral evidence for a distinction between trotting and ambling gaits in the cockroach *Blaberus discoidalis*. J Exp Biol 214:2057–2064

Berens P (2009) CircStat: a MATLAB toolbox for circular statistics. J Stat Softw 31:1–21

Blickhan R, Full RJ (1987) Locomotion energetics of the ghost crab: II. Mechanics of the centre of mass during walking and running. J Exp Biol 130:155–174

Collett M, Collett TS (2000) How do insects use path integration for their navigation? Biol Cybern 83:245–259

Cruse H (1976) The function of the legs in the free walking stick insect, *Carausius morosus*. J Comp Physiol 112:235–262

Dahbi A, Retana J, Lenoir A, Cerdá X (2008) Nest-moving by the polydomous ant *Cataglyphis iberica*. J Ethol 26:119–126

Delcomyn F (1971) Locomotion of cockroach *Periplaneta americana*. J Exp Biol 54:443–452

Fieler C, Jayne BC (1998) Effects of speed on the hindlimb kinematics of the lizard *Dipsosaurus dorsalis*. J Exp Biol 201:609–622

Foerster A (1850) Eine Centurie neuer *Hymenopteren*. Verh Naturh Ver Preuss Rheinlde Westphal, Bonn 7:485–518

Full RJ, Tu MS (1990) Mechanics of six-legged runners. J Exp Biol 148:129–146

Full RJ, Tu MS (1991) Mechanics of a rapid running insect: two-, four- and six-legged locomotion. J Exp Biol 156:215–231

Gehring WJ, Wehner R (1995) Heat shock protein synthesis and thermotolerance in *Cataglyphis*, an ant from the Sahara desert. PNAS 92:2994–2998

Graham D (1972) A behavioural analysis of the temporal organisation of walking movements in the 1st instar and adult stick insect (*Carausius morosus*). J Comp Physiol A 81:23–52

Graham D (1985) Pattern and control of walking in insects. Adv Insect Physiol 18:31–140

Harris J, Chiradella H (1980) The forces exerted on substrate by walking and stationary crickets. J Exp Biol 85:263–279

Heglund NC, Taylor CR, McMahon TA (1974) Scaling stride frequency and gait to animal size: mice to horses. Science 186:1112–1113

Hoyt DF, Taylor CR (1981) Gait and the energetics of locomotion in horses. Nature 292:239–240

Hughes GM (1951) The co-ordination of insect movements. I. The walking movements of insects. J Exp Biol 29:267–285

Mendes CS, Bartos I, Akay T, Márka S, Mann RS (2013) Quantification of gait parameters in freely walking wild type and sensory deprived *Drosophila melanogaster*. Elife. doi:10.7554/eLife.00231

Moll K, Roces F, Federle W (2013) How load-carrying ants avoid falling over: mechanical stability during foraging in *Atta vollenweideri* grass-cutting ants. PLoS One 8(1):e52816

Müller M, Wehner R (1988) Path integration in desert ants, *Cataglyphis fortis*. PNAS 85:5287–5290

Reinhardt L, Blickhan R (2014) Level locomotion in wood ants: evidence for grounded running. J Exp Biol 217:2358–2370

Ronacher B, Wehner R (1995) Desert ants *Cataglyphis fortis* use self-induced optic flow to measure distances travelled. J Comp Physiol A 177:21–27

Rubenson J, Heliams DB, Llooyd DG, Fournier PA (2004) Gait selection in the ostrich: mechanical and metabolic characteristics of walking and running with and without an aerial phase. Proc R Soc Lond B 271:1091–1099

Schilling M, Hoinville T, Schmitz J, Cruse H (2013) Walknet, a bio-inspired controller for hexapod walking. Biol Cybern 107:397–419

Schmid-Hempel P, Schmid-Hempel R (1984) Life duration and turnover of foragers in the ant *Cataglyphis bicolor* (*Hymenoptera*, *Formicidae*). Insectes Soc 31:345–360

Seidl T, Wehner R (2008) Walking on inclines: how do desert ants monitor slope and step length. Front Zool 5:8. doi:10.1186/1742-9994-5-8

Spagna JC, Valdivia EA, Mohan V (2011) Gait characteristics of two fast-running spider species (*Hololena adnexa* and *Hololena curta*), including an aerial phase (*Araneae*: *Agelenidae*). J Arachnol 39:84–91

Strauss R, Heisenberg M (1990) Coordination of legs during straight walking and turning in *Drosophila melanogaster*. J Comp Physiol A 167:403–412

Ting LH, Blickhan R, Full RJ (1994) Dynamic and static stability in hexapedal runners. J Exp Biol 197:251–269

Wehner R (1982) Himmelsnavigation bei Insekten. Neurophysiologie und Verhalten. Neujahrsbl Naturforsch Ges Zür 184:1–132

Wehner R (1983) Taxonomie, Funktionsmorphologie und Zoogeographie der saharischen Wüstenameise *Cataglyphis fortis* (Forel 1902) *stat. nov*. Senckenbergiana Biol 64:89–132

Wehner R (2009) The architecture of the desert ant's navigational toolkit (*Hymenoptera: Formicidae*). Myrmecol News 12:85–96

Wehner R, Srinivasan MV (2003) Path integration in insects. In: Jeffrey KJ (ed) The neurobiology of spatial behaviour. Oxford University Press, Oxford, pp 9–30

Wehner R, Wehner S (1986) Path integration in desert ants. Approaching a long-standing puzzle in insect navigation. Monit Zool Ital 20:309–331

Wehner R, Wehner S (1990) Insect navigation: use of maps or Ariadne's thread. Ethol Ecol Evol 2:27–48

Wehner R, Marsh AC, Wehner S (1992) Desert ants on a thermal tightrope. Nature 357:586–587

Weihmann T (2013) Crawling at high speeds: steady level locomotion in the spider *Cupiennius salei*—global kinematics and for centre of mass dynamics. PLoS One 8(6):e65788

Weihmann T, Blickhan R (2009) Comparing inclined locomotion in a ground-living and a climbing ant species: sagittal plane kinematics. J Comp Physiol A 195:1011–1020

Wendler G (1964) Laufen und Stehen der Stabheuschrecke *Carausius morosus*: Sinnesborstenfelder in den Beingelenken als Glieder von Regelkreisen. Z Vergl Physiol 48:198–250

Wilson DM (1966) Insect walking. Annu Rev Entomol 11:103–122

Wittlinger M, Wehner R, Wolf H (2006) The ant odometer: stepping on stilts and stumps. Science 312:1965–1967

Wittlinger M, Wehner R, Wolf H (2007) The desert ant odometer: a stride integrator that accounts for stride length and walking speed. J Exp Biol 210:198–207

Wosnitza A, Bockemühl T, Dübbert M, Scholz H, Büschges A (2013) Inter-leg coordination in the control of walking speed in *Drosophila*. J Exp Biol 216:480–491

Zollikofer CPE (1988) Vergleichende Untersuchungen zum Laufverhalten von Ameisen. Dissertation, University of Zürich, Switzerland

Zollikofer CPE (1994a) Stepping patterns in ants—influence of speed and curvature. J Exp Biol 192:95–106

Zollikofer CPE (1994b) Stepping patterns in ants—influence of body morphology. J Exp Biol 192:107–118

Zollikofer CPE (1994c) Stepping patterns in ants—influence of load. J Exp Biol 192:119–127

Journal of Comparative Physiology A

Supplementary Material

Walking and running in the desert ant Cataglyphis fortis.

Verena Wahl, Sarah Pfeffer, Matthias Wittlinger

Institute of Neurobiology, University of Ulm, D-89069 Ulm, Germany

Corresponding author: Matthias Wittlinger

Matthias.wittlinger@uni-ulm.de

Institute for Neurobiology

Helmholtzstraße 10/1

University Ulm

89081 Ulm

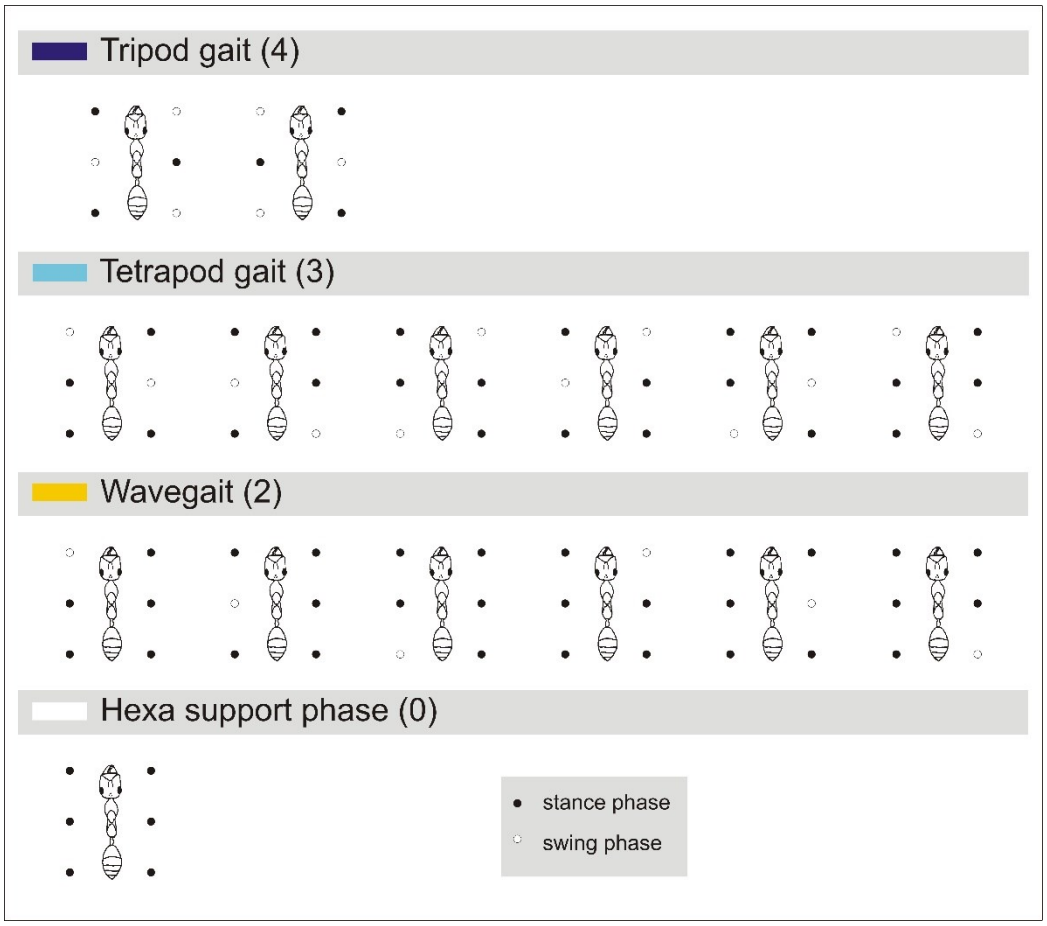

Supplementary Figure.
Leg combinations used for respective gait patterns.

The classification of different leg combinations were used for the colour coding and the indexing to quantify slow walking ants according to their used gait patterns. The analysis was similar to the quantification of gait parameters in *Drosophila melanogaster* of Mendes (Mendes et al. 2013, see their figure 4). But in contrast to this work we used more categories to describe the ants' walks. We added 'wavegait' and 'hexa support phase' to our analysis. This is in our case reasonable since we looked at the lower range of walking speeds. Locomotion within the speed range of 4.5 mm s^{-1} to 29.9 mms^{-1} gets more variable as well as slower and therefore the number of frames showing wavegait and frames where all six legs have ground contact increase considerably.
In 'tripod gait' three legs are in swing phase at once, while the other three are in stance phase. One tripod contains the fore and hind leg of one side and the middle leg of the contralateral side. In 'tetrapod gait' two legs are in swing phase, while the other four are in stance phase. The lifted or moved legs must be on the contralateral side but not from the same leg pair. In 'wavegait' one leg is in swing phase, while the other five are in stance phase. In the category of 'hexa support phase' no leg was in swing phase, but all in stance phase. All legs had ground contact, tarsal claws not moving.

Kapitel 5

5. Manuscript 3

How to find home backwards? Locomotion and inter-leg coordination during rearward walking of *Cataglyphis fortis* desert ants

Sarah E. Pfeffer, Verena L. Wahl and Matthias Wittlinger

Institute of Neurobiology, Ulm University, 89069 Ulm, Germany

This article is published 2016 in the **Journal of Experimental Biology,** 219(14), 2110-2119 and is available under
doi: 10.1242/jeb.137778
http://jeb.biologists.org/lookup/doi/10.1242/jeb.137778

This article is licensed under the Creative Commons Attribution CC-BY-3.0 License (https://creativecommons.org/licenses/by/3.0/).

Journal of experimental biology by Company of Biologists Reproduced with permission of COMPANY OF BIOLOGISTS LTD. in the format Republish in a thesis/dissertation via Copyright Clearance Center (Order Detail ID: 70635460, Confirmation Number: 11661720).

© 2016. Published by The Company of Biologists Ltd | Journal of Experimental Biology (2016) 219, 2110-2118 doi:10.1242/jeb.137778

RESEARCH ARTICLE

How to find home backwards? Locomotion and inter-leg coordination during rearward walking of *Cataglyphis fortis* desert ants

Sarah E. Pfeffer*, Verena L. Wahl and Matthias Wittlinger

ABSTRACT

For insects, flexibility in the performance of terrestrial locomotion is a vital part of facing the challenges of their often unpredictable environment. Arthropods such as scorpions and crustaceans can switch readily from forward to backward locomotion, but in insects this behaviour seems to be less common and, therefore, is only poorly understood. Here we present an example of spontaneous and persistent backward walking in *Cataglyphis* desert ants that allows us to investigate rearward locomotion within a natural context. When ants find a food item that is too large to be lifted up and to be carried in a normal forward-faced orientation, they will drag the load walking backwards to their home nest. A detailed examination of this behaviour reveals a surprising flexibility of the locomotor output. Compared with forward walks with regular tripod coordination, no main coordination pattern can be assigned to rearward walks. However, we often observed leg-pair-specific stepping patterns. The front legs frequently step with small stride lengths, while the middle and the hind legs are characterized by less numerous but larger strides. But still, these specializations show no rigidly fixed leg coupling, nor are they strictly embedded within a temporal context; therefore, they do not result in a repetitive coordination pattern. The individual legs act as separate units, most likely to better maintain stability during backward dragging.

KEY WORDS: Locomotion, Backward walking, *Cataglyphis* desert ant, Flexible motor control, Inter-leg coordination

INTRODUCTION

Insects, which are among the most successful groups in the animal kingdom, are mostly all capable of terrestrial locomotion. The movements of the six legs can be characterized as regularly coordinated during forward walking, which results in rhythmical stepping patterns. However, leg coordination of insects is not inflexibly predetermined; rather, it can be adapted to the behavioural context and to the environmental conditions, such as upcoming obstacles, transport of different loads or to cope with changes in walking direction (Ritzmann and Zill, 2013). Studying inter-leg coordination in different demanding situations is crucial for understanding locomotion behaviour. This might further provide an important insight into neuronal control and could be useful for the implementation of biologically inspired hexapod robots.

We know that different inter-leg coordination patterns (gaits) can be found in hexapods during forward locomotion. In wavegait coordination, one leg is in swing phase, while the other five legs remain on the ground. The swing propagates from back to front, first on one and then on the other body side. This kind of walking behaviour is seen in some insects during very slow walking or load-carrying, observable, for example, in stick insects (*Carausius morosus*, Hughes, 1952; Wilson, 1966) and fruit flies (*Drosophila melanogaster*, Wosnitza et al., 2013). In tetrapod gait, two diagonally located legs are in swing phase at once, while the other four legs are in stance phase. This walking behaviour is seen in insects with an intermediate walking speed. Good model organisms, where the tetrapod gait pattern is well studied, are stick insects (*Carausius morosus*, Graham, 1972; *Aretaon asperrimus*, Jeck and Cruse, 2007). During tripod coordination, three legs are in swing phase, while the other three legs are in stance phase. Thereby, the front and hind legs on one body side step in unison with the middle leg of the other body side. This kind of locomotion is well known from fast walking insects, such as cockroaches (*Periplaneta americana,* Delcomyn, 1971; *Blaberus discoidalis*, Bender et al., 2011; *Blatta orientalis*, Hughes, 1952), fruit flies (*Drosophila melanogaster*, Wosnitza et al., 2013) and ants (*Cataglyphis*, *Formica*, *Lasius* and *Myrmica*, Zollikofer, 1994a).

It should be noted that this kind of classification represents idealized forms of coordination patterns, but walking insects produce also intermediate versions to avoid jerky movements (Grabowska et al., 2012). The different gait patterns described show a transition into each other, forming a continuum (Schilling et al., 2013; Wilson, 1966). Leg patterns within this continuum are interlinked by several coordination rules (Cruse, 1990; Cruse et al., 2007), which assume that legs may be coupled via mechanical and neurobiological signals. The rules were derived from behavioural experiments on different species and have been successfully implemented in hexapod robots. Rules 1–3 affect the timing of the transition between stance and swing phase. Together, they produce a back-to-front sequence of swing movements (a so-called metachronal wave). Rule 4 causes legs to be placed in locations very similar to where the anterior leg neighbour was standing. Rule 5 addresses the force distribution to spread the load efficiently. Rule 6, the treading-on-tarsus (TOT) reflex, enforces a correction step to avoid stumbling because of a leg placement error.

Arthropods with more than six legs, such as scorpions or crustaceans, can also be examined according to their walking pattern. Scorpions are known to move with two alternating tetrapods, which means that the first and third leg pairs move in synchrony as well as the second and fourth leg pairs, which could be regarded as an eight-legged extension of the insects' alternating tripod gait (Bowerman, 1981). Crustaceans show less coupling of the appendages between the contralateral body sides. The leg coupling mechanisms on the ipsilateral side, however, are much more distinctive, leading to a metachronal wave of sequential

Institute of Neurobiology, University of Ulm, Ulm D-89069, Germany.

*Author for correspondence (sarah.pfeffer@alumni.uni-ulm.de)

S.E.P., 0000-0003-1470-5055

Received 21 January 2016; Accepted 29 April 2016

Journal of Experimental Biology

RESEARCH ARTICLE Journal of Experimental Biology (2016) 219, 2110-2118 doi:10.1242/jeb.137778

stepping on one body side (Sleinis and Silvey, 1980; Marshall and Diebel, 1995). Scorpions or crustaceans are known to often walk backwards, demonstrating a simple reversal of the forward stepping pattern, although a slight decrease of inter-leg coupling exists (Clarac and Chasserat, 1983).

In insects, however, backward walking is less understood, simply because there are not many apparent cases. There are only a few examples mentioned in the literature, such as the escape behaviour of stick insects (Jeck and Cruse, 2007; Graham and Epstein, 1985), the manoeuvring out of blind alleys in fruit flies (Bidaye et al., 2014) or the backward rolling of dung balls in several species of dung beetles (Byrne et al., 2003; Hanski and Cambefort, 2014).

The present study provides the first quantitative analysis of backward locomotion in ants. We use the natural behaviour of rearward food dragging in *Cataglyphis fortis* (Forel 1902), where ants walk backwards, voluntarily and persistently over a long period of time. Compared with forward locomotion, we find remarkable differences in backward walking ants.

MATERIALS AND METHODS

Our experiments were conducted with *C. fortis* in its natural habitat of alluvial salt plains near Maharès, Tunisia (34.53°N, 10.54°E). All data were obtained during the summer months of 2013, 2014 and 2015.

How to convince the ants to walk backwards?

To persuade the ants to take their homebound trip backwards, we offered them a large food item, which they were not able to carry. Thus, the ants did not lift it up to carry it in a regular forward-faced body orientation (Fig. 1B,C). Instead, the load was dragged backwards. This behaviour allowed us to investigate rearward locomotion and the ants' walking performance under realistic, natural conditions.

Food load

The large food items were either made of biscuit crumbs or mealworms. To make the load sufficiently heavy we concealed a tin-solder wire in the middle of the food item. The food items weighed 186 50 mg (mean s.d.) and were all elongated in shape. The food loads were carefully chosen to ensure that each ant (14 4 mg) was able to drag its load backwards.

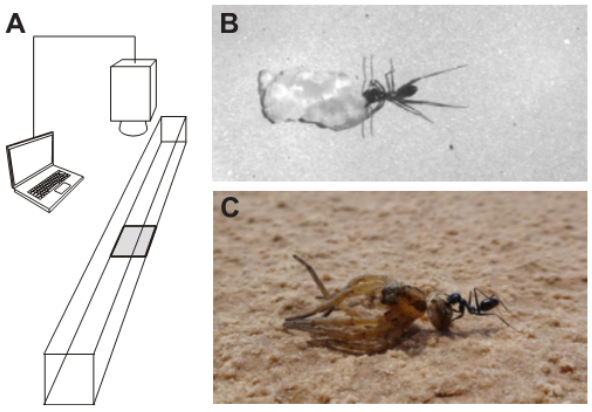

Fig. 1. Experimental setup and backward dragging ants. (A) Experimental setup. Ants were dragging a heavy food item backwards for 5 m before film recordings were performed with a resolution of 1280×1024 pixels (see grey area within the channel). (B,C) Still images showing the food-dragging behaviour (B) from a high-speed video in the channel and (C) under natural conditions.

Data analysis

We made high-speed video recordings within an aluminium channel to characterize the backward walking performance (Fig. 1A). The recordings (MotionBLITZ EoSens mini1, Mikrotron, Unterschleissheim, Germany) had a sampling frequency of 250 and 500 frames s^{-1}. The backwards (n=20) and forwards (n=20) moving ants were filmed in top view. We examined at least 300 frames of backward walking or three step cycles of forward walking.

Walking speed was analyzed with Ethovision software (Noldus Information Technology, Wageningen, The Netherlands). The ants' movements were tracked automatically (sampling rate of 50 Hz). We further analyzed the lift-off and touchdown moments of the tarsal tips for each leg, which were used to determine each ant's stepping pattern. We define a leg to be in swing phase as long as the tarsal tip is lifted off the ground or is in motion, and in stance phase as long as the tarsal tip touches the ground without moving.

To visualize the sequence of swing and stance phases, we plotted podograms. To illustrate and quantify the ants' inter-leg coordination, we assigned each frame of the videos with a number and a colour that classifies each frame according to its leg combination, similar to the work of Mendes et al. (2013) and Wahl et al. (2015). We categorized each frame into one of the following groups: tripod, tetrapod, wavegait, undefined gait and hexa support phase (see Fig. S1). To visualize the variability of the inter-leg relationship according to the swing phase onsets, we used phase plots. We used the MATLAB environment (MathWorks, Natick, MA, USA) for frame-by-frame indexing, calculation of podograms and phase plots. In particular, the phase plot analysis was realized by means of the 'CircStat' toolbox (Berens, 2009), where the phase shifts of legs L1, L2 and R1–3 were calculated with respect to L3. We measured the distance between the position of the lift-off and the position of the touchdown event in every leg throughout the video and averaged the values for each leg pair to obtain a mean stride length. We defined the swing movement without the body movement as stride amplitude, which was calculated as stride length minus swing phase duration multiplied by walking speed (Wahl et al., 2015). To calculate stride frequency, we divided walking speed by stride length. To calculate swing speed, we divided stride length by the corresponding swing phase duration. We measured the x/y coordinates of the tarsal tips with respect to the petiole in the frame before and after a swing phase to quantify the ant's footfall geometry (similar to the work of Mendes et al., 2013 and Seidl and Wehner, 2008). We considered the petiole as the centre of mass (Reinhardt and Blickhan, 2014). The measurements were conducted using ImageJ (US National Institutes of Health, Bethesda, MD, USA).

Statistical analysis

We used SigmaPlot (Systat Software, San Jose, CA, USA) for statistical comparison and to generate box-and-whisker plots. For pairwise comparison of normally distributed data we applied the t-test, and for non-normally distributed data we applied the Mann–Whitney rank sum test (denoted as U-test). For a multiple comparison of normally distributed data we used one-way ANOVA; for non-normally distributed data we used ANOVA on ranks. Box-and-whisker plots show the median as the box centre, 25th and 75th percentiles as box margins, and 10th and 90th percentiles as whiskers.

Journal of Experimental Biology

RESEARCH ARTICLE Journal of Experimental Biology (2016) 219, 2110-2118 doi:10.1242/jeb.137778

RESULTS

We wanted to determine how ants coordinate their leg movements during backward locomotion. We made high-speed video recordings during rearward (20 animals) and forward (20 animals) walking and analyzed the stepping coordination according to several parameters that will be presented in the following sections (example videos have been uploaded to the Dryad Digital Repository; for video overview, see Fig. S4).

Stance-and-swing envelopes

To give an impression of how ants move their legs during backward and forward locomotion, we exemplarily show the spatial tarsal traces (envelopes) for one step cycle during the stance and swing phase in relation to the ant's body position (Fig. 2A). Swing and stance envelopes are a body-coordinate-based measure for the tarsal tip position during swing and stance. It is noticeable that the envelopes (from the stance phase as well as from the swing phase)

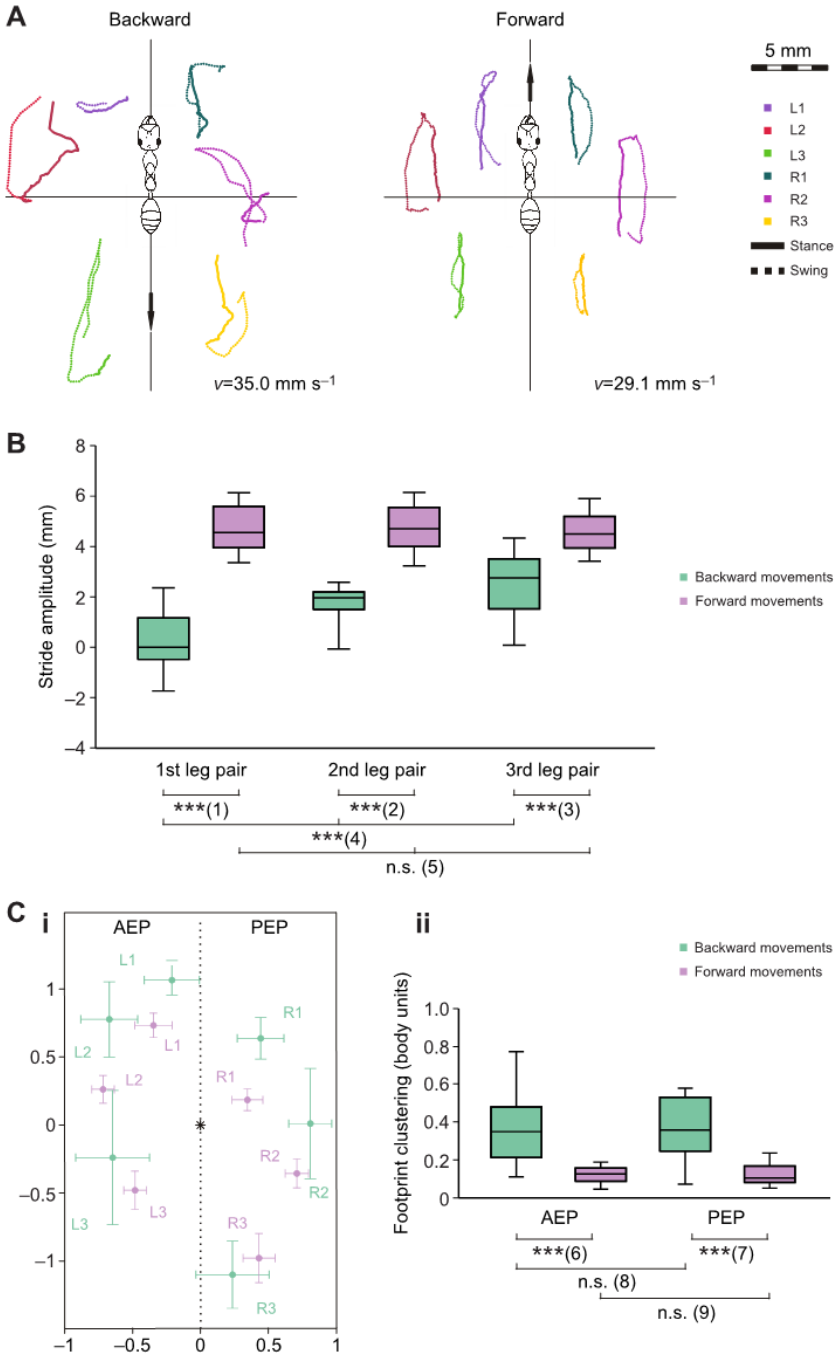

Fig. 2. Examples of stance and swing envelopes and quantitative analysis of stride amplitudes. (A) Stance and swing envelopes of the tarsal tip of each leg during one step cycle tracked relatively to a fixed position of the ant's body (2nd abdominal segment, petiole). The black arrows indicate the direction of movement. L, left, R, right body side; 1, 2 and 3, front, middle and hind leg. *v*, speed. (B) Quantitative comparison of the stride amplitudes. Mean stride amplitudes of each of *n*=20 backward and forward walking animals. Box plots give the 10th, 25th, 50th, 75th and 90th percentile distributions. Statistical analysis: (1) *t*-test, $P \leq 0.001$; (2) *t*-test, $P \leq 0.001$; (3) *U*-test, $P=0.001$; (4) ANOVA on ranks, $P=0.001$ (Tukey *post hoc* test shows difference for all pairwise comparisons, except 2nd and 3rd leg pairs), (5) one-way ANOVA, $P=0.849$. (C) Footfall geometry during backward and forward locomotion (each *n*=5). Selected videos cover the entire walking speed range. Values were normalized to body length. (Ci) Footfall position with respect to the petiole (origin of plot, marked with asterisk, considered as centre of mass). AEP, anterior extreme position; PEP, posterior extreme position. (Cii) Quantification of footprint clustering using the standard deviation. Box plots give the 10th, 25th, 50th, 75th and 90th percentile distributions. Statistical analysis: (6) *U*-test, $P \leq 0.001$; (7) *U*-test, $P \leq 0.001$; (8) *t*-test, $P=0.639$; (9) *t*-test, $P=0.876$.

Journal of Experimental Biology

RESEARCH ARTICLE Journal of Experimental Biology (2016) 219, 2110-2118 doi:10.1242/jeb.137778

show more uneven contours and are more curved during backward locomotion compared with the envelopes from a normal forward walk.

These visually distinguishable differences can further be supported by the modified index of straightness (Batschelet, 1981). This index value sets the actual distance moved by a leg in relation to its straight line distance; values were calculated for the example envelopes shown in Fig. 2. A value of 1 describes a straight line between the stride onset and stride touchdown. The lower the value, the longer and more complex the respective swing or stance traces. The median value (for all legs) of the modified index of straightness decreases from 0.92 in the forward envelopes to 0.82 in the backward envelopes. The same is true for the swing movements, where the median index value decreases from 0.59 in the forward envelopes to 0.49 in the backward envelopes (for exact values, see Table S2).

Although we here show only one example of stance and swing envelope for each leg, one can expect quite similar envelopes for other step cycles (given the fact that we visually confirmed this in all videos). If we consider the petiole as the ant's centre of mass (in compliance with Reinhardt and Blickhan, 2014), our results suggest that rearward movements are more wobbly and it can be assumed that the ant has to balance its centre of mass more frequently.

In order to illustrate the leg swing independent of body movements, we calculated the stride amplitude, which is a body-coordinate-based measure for the leg in swing phase (Fig. 2B). It turns out that the stride amplitudes during backward movements are significantly shorter than those during forward movements of the respective leg pair. Further, it is noteworthy that during backward movements especially the first leg pair shows small and even negative stride amplitudes. This finding indicates that the frontal legs sometimes cover less distance than the distance of the mean body displacement. Hence, it seems that the front legs do not contribute to the same extent to the walking speed as the middle and hind legs. Contrary to backward stride amplitudes, the stride amplitudes of forward movements do not differ significantly among different leg pairs.

To further analyze the spatial properties of backward locomotion, we quantified the ants' footfall geometry. During forward locomotion, the anterior extreme position (AEP) is the most anterior footfall position of the leg after a swing phase. At the end of the stance phase, just before the leg is lifted again, a leg is in its posterior extreme position (PEP). The terms 'anterior' and 'posterior' refer to the ant's body orientation. We use these terms also for backward locomotion, but it should be noted that the anterior and posterior position of the legs are reversed within the step cycle. During rearward locomotion, the AEP is at the end of a stance phase, whereas the PEP is reached after a swing phase.

If we compare the AEPs and PEPs of backward and forward walking ants (Fig. 2Ci), we can see that during backward locomotion the tarsal contact is more spread to increase static stability. Further, the frontal legs are positioned more anteriorly. The middle legs are shifted slightly more distally and anteriorly.

The footprint clustering of AEPs and PEPs is shown in Fig. 2Cii. Here we plot the standard deviation of the mean for all AEPs and PEPs. The comparison of the clustering of the AEPs during backward and forward walking reveals a significant statistical difference. The same is true for the PEPs. However, we cannot find a difference of the AEPs and PEPs clustering within one walking direction (backwards as well as forwards).

Stepping pattern and inter-leg coordination

In the following section we quantify the locomotion pattern of backward (25.8 to 65.6 mm s^{-1}) and forward (22.6 to 64.0 mm s^{-1}) moving ants (Fig. 3) and analyze how the inter-leg movements are coordinated temporally.

Although the lower range of walking speed is overrepresented quantitatively in our data set, we are convinced that we covered a natural walking speed distribution in our analysis of backward walking ants. Fast backward walks (>50 mm s^{-1}) are less frequent, while walking speeds between 20 and 50 mm s^{-1} are much more often observed. For comparative reasons we thus adapted the analyzed walking speed range of forward walking ants (which of course can be observed in a much broader scope of walking speeds up to 600 mm s^{-1} and even greater; Wahl et al., 2015). The walking speed of backward dragging ants strongly depends on the ants' individual performance and mostly on the size and weight of the food item. If the food morsel is too lightweight, the ants would not reliably drag it backwards but try to push and carry it forwards (see Movie 3).

Fig. 3A gives an exemplary demonstration of a typical backward and forward walk within a temporal context. The podograms shown visualize the durations of stance and swing phases for each leg (Fig. 3Ai). Further, we assigned each frame of the video a colour index (Fig. 3Aii) and a number index (Fig. 3Aiii), according to the current gait pattern, as indicated in the key. In Fig. S1, a more detailed list of different leg combinations assigned to a particular gait type is shown; those that did not match with these ideal leg combinations were classified as 'undefined gait' (listed and quantified in Fig. S2). The examples show that during backward walks no regular repetition of leg combinations can be found, while in forward locomotion tripod coordination is the predominant coordination pattern.

Frame-by-frame indexing was also used for a quantitative analysis. The percentage distribution (Fig. 3Bi) of the different leg combinations is illustrated as a bar chart, where every frame of the video was taken into account. For a more specific idea of the individual's walk, we calculated the averaged number index for each video (Fig. 3Bii). During backward locomotion there is no preferred gait type; rather, wavegait (one leg in swing phase) and undefined leg combinations make up the larger part of the quantitative analysis. In contrast, forward walks show a high proportion of the tripod pattern, while the fraction of non-tripod coordination is small and can be related to the transition between one tripod group (L1, R2, L3) and the next one (R1, L2, R3). With increasing walking speed, the percentage of tripod coordination increases while the proportion of the hexa support phase (all six legs with ground contact) decreases in backward as well as in forward walks (see also Wahl et al., 2015).

During backward locomotion, a quantification of the undefined leg combinations reveals a wide range of different leg combinations, where no pattern has a clear majority. We show that 74% of the undefined leg combinations recorded during backward locomotion do not follow Cruse's rule 1 (ipsilaterally or contralaterally); this constitutes 24% of all analyzed frames. In these frames we find a simultaneous stepping of adjacent legs and therefore statically unstable leg combinations (Cruse et al., 2007). During forward walking 20% of the undefined stepping patterns also show unstable combinations in which Cruse's rule 1 is disregarded (ipsilaterally or contralaterally). However, they make up only 2% of all analyzed frames. Most undefined frames (80%) during forward locomotion can be attributed to the transition of one tripod group to the next (see Fig. S2).

RESEARCH ARTICLE Journal of Experimental Biology (2016) 219, 2110-2118 doi:10.1242/jeb.137778

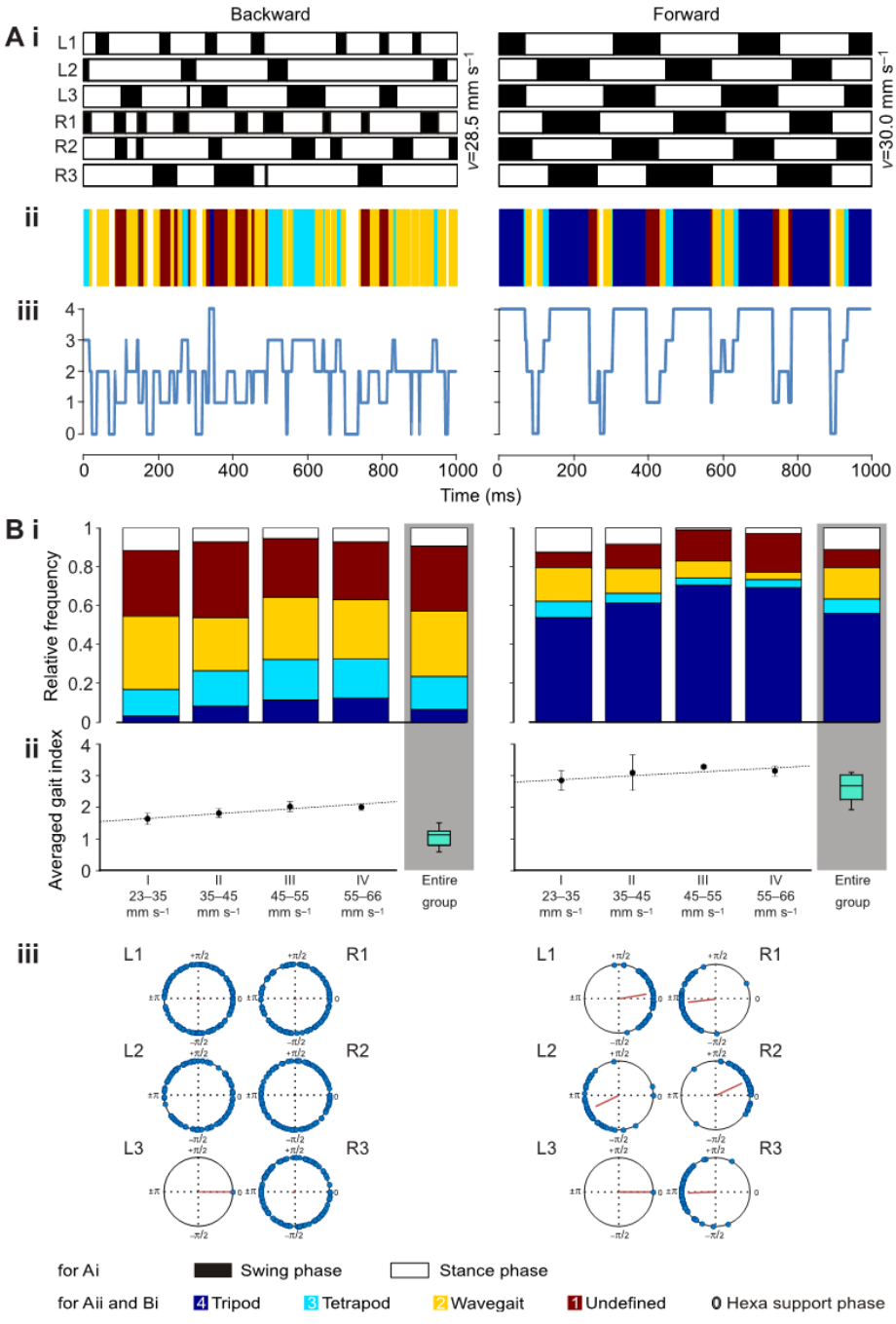

Fig. 3. Stepping pattern and inter-leg coordination. (A) Example of backward and forward locomotion. The podograms (Ai) illustrate the footfall patterns of all six legs at 28.5 mm s^{-1} for the backward and 30.0 mm s^{-1} for the forward example. White bars represent the stance phase, black bars represent the swing phase. L, left; R, right; 1, 2 and 3, front, middle and hind leg. Each frame of our examples was classified according to the prevailing gait pattern [colour (Aii) and number (Aiii) indices are indicated in the key at the bottom of the figure]. (B) Quantitative indexing analysis of each of *n*=20 backward and forward walking ants. Each frame was indexed with a colour and number code as in A. The summarized results for colour index analysis (Bi) were categorized according to the ants' walking speed (I–IV). For exact values, see Table S3. The averaged number index (Bii) for each video was grouped according to walking speed categories (I–IV). The data points represent the means; error bars show the s.d. Averaged number indices of the entire groups differ significantly (*t*-test, $P \leq 0.001$). Box plots give the 10th, 25th, 50th, 75th and 90th percentile distributions. (Biii) Phase plots as the swing phase onset of all legs in relation to L3 (reference leg). Blue circles symbolize the onset of each cycle. The mean vector is represented by the red line, with its length indicating the variance. Backward walking ants show no regular repetition of leg coordination, whereas forward walking ants show clear tripod coordination.

Journal of Experimental Biology

RESEARCH ARTICLE Journal of Experimental Biology (2016) 219, 2110-2118 doi:10.1242/jeb.137778

Because swing and stance phases are repetitive events, we can also use a circular illustration. Phase plots are a useful tool with which to analyze the variability of the inter-leg coordination. The phase plots (Fig. 3Biii) of the backward walks show a short length of the mean vector with no clear tendency towards phase coupling. There is a high variability of the blue dots, symbolizing the swing phase onsets with respect to the left hind leg (L3). This is due to the irregular leg coordination without leg synchronization. In contrast, forward runs display strong antiphase swinging of the tripods.

General walking parameters

We further analyzed the relationship between walking speed and important walking parameters (Fig. 4), where we found interesting differences between backward and forward walking.

First, during backward locomotion, walking speed is increased by longer stride lengths (Fig. 4Ai) and higher stride frequencies (Fig. 4Aii). In contrast, the forward walking ants increase only stride frequency for increasing speed (Fig. 4Bii), while the stride length (Fig. 4Bi) is kept more or less constant within the analyzed walking speed range.

Second, as opposed to forward walking ants (with almost superposed correlation lines), in backward walking ants the correlation lines tend to be distinctly separated. This is most notable in Fig. 4Ai,ii and 4Bi,ii, which might indicate a certain degree of leg specialization: during rearward locomotion, front legs tend to make small and frequent strides, whereas hind legs make large but fewer strides. At the end of the swing phase, the flexed front legs are often put close to the ant's thorax, seemingly to push the body in the direction of movement. The hind legs, however, seem to be placed far backwards and cling to the ground to pull the body (and the load) in the direction of movement.

Third, the backward swing speeds (Fig. 4Aiii) are faster than the forward swing speeds (Fig. 4Biii). The backward swing phase (Fig. 4Aiv) is short compared with the forward swing phase (Fig. 4Biv). These aspects reduce the time that the legs are in air and thus do not contribute to the stability of walking. The backward stance phases, especially those of the first leg pair, are also shortened compared with the forward stance phases.

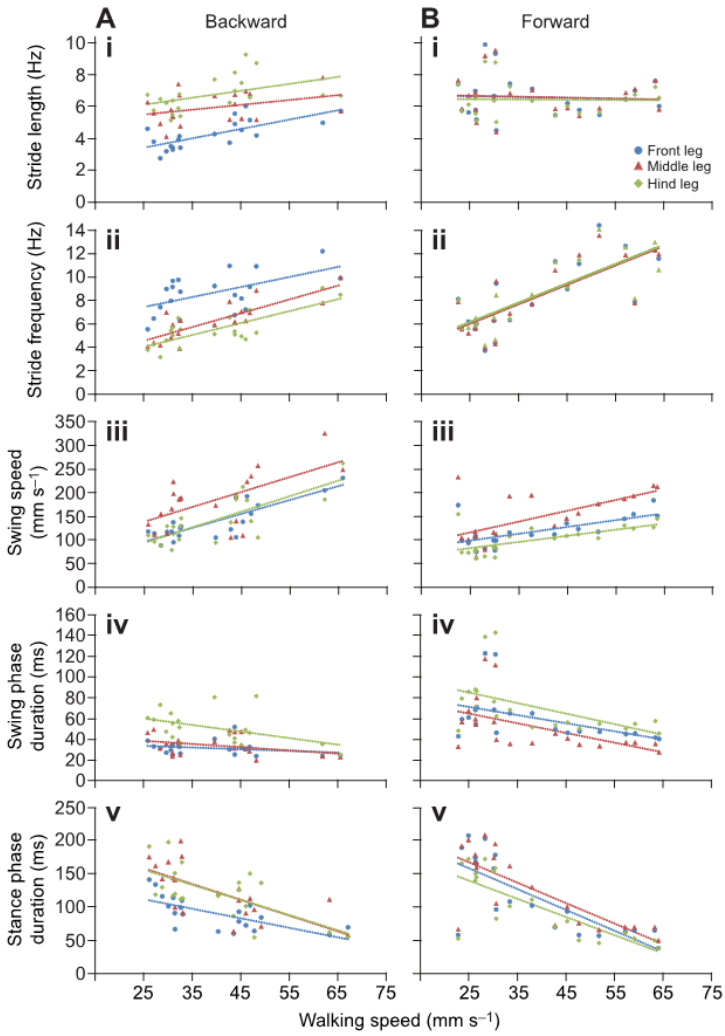

Fig. 4. General walking parameters. Front, middle and hind legs are plotted separately in each diagram. The same videos were analyzed as in Fig. 2. The linear regressions were used to analyze the general walking parameters and their relationships. For the linear regression formula and the coefficient of determination (R^2), see Table S1.

RESEARCH ARTICLE Journal of Experimental Biology (2016) 219, 2110-2118 doi:10.1242/jeb.137778

DISCUSSION

Backward walking is not an uncommon situation in an ant's life, in particular if large and heavy food items need to be transported. Interestingly, it has rarely been investigated how legs are coordinated during backward locomotion. To elucidate this fundamental question in ants, we compared the performance of backward and forward walking.

Stepping pattern of backward walking ants

Tripod, tetrapod and wavegait patterns are known to describe the inter-leg coordination in hexapods during forward locomotion. These different gait types are ideal forms of leg coordination patterns that are quite useful for classification. However, it is not possible to execute a distinct gait type in an absolute manner, which also becomes clear in our results. During forward walking, the transition from one to the next tripod group (L1, R2, L3 to R1, L2, R3 and vice versa) does not occur simultaneously for all three legs, because this would lead to an abrupt and jerky locomotion. Rather, the transitional change from one ideal leg combination to the next is discontinuous with regard to the stepping pattern and requires intermediate combinations to maintain a smooth sequence of movement.

The locomotion pattern of forward walking is well examined in ants, which show a remarkable robustness of tripod coordination over almost the entire range of walking speeds (Wahl et al., 2015), during leg loss (Wittlinger and Wolf, 2013) and even during swimming (Bohn et al., 2012). However, locomotion and inter-leg coordination during backward walking has never been studied in ants. We know that stick insects (*Carausius morosus* and *Aretaon asperrimus*) walk backwards when they try to escape. This behaviour can be elicited if the antennae are stimulated. Rearward walking lasts for 5–30 s (Graham and Epstein, 1985). In rare cases, stick insects can also walk backwards spontaneously over a few step cycles (Jeck and Cruse, 2007). These studies show that although during rearward walking the stepping pattern is irregular, the ipsilateral legs still swing in a typical sequence from front to middle to hind leg (metachronal wave). A similar picture emerges in backward walking *Drosophila* (Bidaye et al., 2014, see their supplementary material). Transgenically modified 'moonwalker flies' walk backwards at certain temperatures. They only rarely use tripod or tetrapod combinations during backward walks. Rather, their locomotion follows a non-rigid and loosely coordinated leg pattern. As in escaping stick insects, a reversed metachronal wave of leg swings on the ipsilateral side is maintained.

Contrary to the studies mentioned above, we present a naturally occurring backward locomotion that is performed voluntarily and is persistent over a long time period. Backward dragging ants do not show a periodically emerging gait pattern. Further, the metachronal wave of the ipsilateral leg swings is only visible to some extent. The wave from front to middle to hind leg is often interrupted. That means that during the backward walks we find deviations from the coordination rules of Cruse (1990). Previous experiments with *Carausius morosus* that performed straight and curved walks on a spherical treadmill already suggest that the strength and efficacy of these coordination rules are context dependent (Dürr, 2005).

The coordination rules suitably describe walking during forward locomotion, where they coherently display the coupling and alternating activity of several leg groups. In particular, rules 1–4, which presume inter-leg coordination, seem to become less important and are partly ignored during the backward walks in our study. In these rules the current state of one leg influences the motor behaviour of its neighbouring leg in several ways. It might be that rule 5, dealing with load distribution, outcompetes the other rules during the behaviour of backward dragging. Because of the dragging of the heavy food, the ants' rearward walk becomes unstable. The maxim of coordination is now not to fall, while the performance of an ideal stepping pattern retreats into the background. That means that in our case the leg coordination might especially be determined by sensory feedback, while a regular inter-leg coordination is widely ignored. Backward dragging thus reveals the extensive flexibility of leg coordination and emphasizes the remarkable adaptability of motor programs as a result of the integration of sensory feedback. Unfortunately, in our data set we cannot assess whether rule 6, the TOT reflex, is present in *C. fortis* during backward walking.

Although our data especially show irregular locomotion behaviour, it should be mentioned that backward tripod-like coordination is possible per se (see Movie 4). This has been observed over several consecutive step cycles; nonetheless, we never observed an ant exclusively using a tripod-like pattern during backward locomotion. Because of the fast backward leg movements, there is not much temporal overlap, and the tripod coordination pattern seems to be distorted and less exact.

Specializations of leg pairs

Although no repetitive leg coordination can be found over a longer period of time, some kind of specialization seems to occur. The front legs make frequent but small strides, putting the flexed front leg close to the thorax and pushing the body and the load into the moving direction until the front leg is extended again. In contrast, the middle and especially the hind legs make less frequent but long strides (Fig. 4). The legs are reaching far backwards in order to find some grip to cling to the ground and to pull the body and the load into the direction of movement. Note that these specializations are often present but are not mandatory. They are neither periodically repeated in a temporal context nor do they force an obligatory inter-leg coordination.

Interestingly, similar specializations of certain leg pairs have also been described in the few studied examples of backward walking insects. Rearward walking stick insects show a reversed specialization: here the front legs make larger steps at a corresponding lower frequency than the middle and hind legs (Graham and Epstein, 1985). A similar tendency can be found in the fruit flies' hind legs, which step significantly more often than the front and middle legs during backward walking (Bidaye et al., 2014). However, specialized leg pair coordination is not exclusively found during backward locomotion. In other challenging walking situations, such as forward walks on an inclined surface, a particular modification of common stepping patterns is revealed. In stick insects, the front legs become uncoupled from normal locomotion, showing multiple stepping, while the middle and hind leg coordination remains regular (Grabowska et al., 2012).

Food dragging and stability of backward walking

Our results show that the movements of ants during backward dragging become unstable, thus it can be suggested that the ant's centre of mass has to be balanced more than during forward walking. One reason for this is that backward walking ants move slowly and, hence, the support provided by dynamic stability is low (Ting et al., 1994). Further, it can be assumed that by grasping the food item with the mandibles and dragging it backwards, the ant's centre of mass is shifted to the anterior (probably even outside the tripod triangle), as is indicated in the more anterior footfall position of the front and middle legs. Therefore, the limits of a stable tripod

Journal of Experimental Biology

RESEARCH ARTICLE Journal of Experimental Biology (2016) 219, 2110-2118 doi:10.1242/jeb.137778

walk are exceeded in rearward locomotion and the ants change to a more flexible and stable leg pattern. The influence of load on locomotion was previously investigated in *C. fortis* (Zollikofer, 1994b). Compared with the present study, the load was less and the ants maintained tripod coordination. Nevertheless, carrying load led to slight deformations of the tripod triangle.

To maintain a stable walk, the tarsal positions are spatially more spread during backward than during forward locomotion. This probably increases the ants' static stability. Besides, the ants dragging the weight possess an additional support point – the mandibles clamping to the food – which might facilitate unstable gait conformations and increase static stability. This might explain why backward dragging ants are able to disregard Cruse's rule 1 to a much higher extent than during forward locomotion. Backward dragging ants could more easily compensate for unstable movements such as the simultaneous stepping of ipsilateral or contralateral legs. Further, rearward food dragging ants increased their contact with the substrate. This becomes conspicuous in our results. First, backward walks have relatively fast swing phases. This reduces the time that legs are in air and are not supporting the ant. Second, during rearward walking, leg pattern combinations are used where often more than three legs have ground contact. The proportion of tetrapod and wavegait combinations is higher in backward walks, as are 'undefined combinations', a majority of which have at least three legs on the ground simultaneously to support the ant.

Interestingly, a similar outcome was shown in experiments with *Drosophila*, where a load with twice the body mass was glued onto the flies' notum (Mendes et al., 2014). The authors report an increase in swing speed compared with unloaded flies. Further, the flies had more contact with the substrate as walking via tripod and tetrapod gaits become less frequent and wavegait and hexa support phases increased.

Final remarks

Although ants are known to be very robust tripod walkers, their leg coordination is less coupled during backward walking, demonstrating the flexibility of ant locomotion. We have to keep in mind that we examined backward dragging behaviour under idealized conditions. This means that not all food items found in an ant's natural environment have an elongated shape and can easily be grasped with the mandibles. We also tried to avoid bulky food. It might be that under natural conditions the front legs are especially hampered and therefore limited in their range of movements. Furthermore, the mass of the food load is often not as symmetrical as in our study, which might give leg and body movements a biased direction. Additionally, the natural substrate is more uneven than our sanded, plain aluminium floor (even the desert ground, see movie 1 in Pfeffer and Wittlinger, 2016). One can easily assume, therefore, that we would find even more flexibility of locomotion under natural conditions with even less coupled leg coordination and more unsteady leg and body movements. But as we know, ants actually cope well with their natural environment. That fact that the stability could be maintained during backward dragging indicates a strong influence of sensory feedback overriding the seeming rigidity of the tripod leg pattern. Here, the exciting question arises of if and how a challenging task such as odometry is accomplished with such a flexibility of the walking apparatus (Pfeffer and Wittlinger, 2016). This might also be an interesting aspect for the implementation of insect walking in robotics. Through further biomechanical measurements in backward walking ants, for example, ground reaction forces and further kinematic parameters, important information could be provided for a more precise understanding of legged locomotion and its neuronal control.

Acknowledgements

We express our gratitude to Harald Wolf for encouragement during the fieldwork, discussing the data and financial advice. We would like to thank Ursula Seifert for her valuable help in organizing the field excursions and for editing the text. Jörg Henninger deserves special thanks for providing a helpful script for our analysis in the Python environment. We are much indebted to two anonymous referees for their valuable comments on an earlier version of the manuscript.

Competing interests

The authors declare no competing or financial interests.

Author contributions

The experiments were planned by S.E.P. and M.W., and carried out by S.E.P., V.L.W. and M.W. The data were analyzed by S.E.P. and V.L.W. The paper was written by S.E.P. and M.W.

Funding

The University of Ulm provided basic financial support and infrastructure.

Data availability

Data are available from the authors on request. Videos are available from the Dryad Digital Repository at http://dx.doi.org/10.5061/dryad.7k82t.

Supplementary information

Supplementary information available online at
http://jeb.biologists.org/lookup/suppl/doi:10.1242/jeb.137778/-/DC1

References

Batschelet, E. (1981). *Circular Statistics in Biology*. London: Academic Press.
Bender, J. A., Simpson, E. M., Tietz, B. R., Daltoria, K. A., Quinn, R. D. and Ritzmann, R. E. (2011). Kinematic and behavioral evidence for a distinction between trotting and ambling gaits in the cockroach *Blaberus discoidalis*. *J. Exp. Biol.* **214**, 2057-2064.
Berens, P. (2009). CircStat: a MATLAB toolbox for circular statistics. *J. Stat. Softw.* **31**, 1-21.
Bidaye, S. S., Machacek, C., Wu, Y. and Dickson, B. J. (2014). Neuronal control of *Drosophila* walking direction. *Science* **344**, 97-101.
Bohn, H. F., Thornham, D. G. and Federle, W. (2012). Ants swimming in pitcher plants: kinematics of aquatic and terrestrial locomotion in *Camponotus schmitzi*. *J. Comp. Physiol. A* **198**, 465-476.
Bowerman, R. F. (1981). Arachnid locomotion. In *Locomotion and Energetics in Arthropods* (ed. C. F. Herreid and C. R. Fourtner), pp. 73-102. New York: Plenum.
Byrne, M., Dacke, M., Nordström, P., Scholtz, C. and Warrant, E. (2003). Visual cues used by ball-rolling dung beetles for orientation. *J. Comp. Physiol. A Sens. Neural Behav. Physiol.* **189**, 411-418.
Clarac, F. and Chasserat, C. (1983). Quantitative analysis of walking in a decapod crustacean, the rock lobster *Jasus lalandii*: I. Comparative study of free and driven walking. *J. Exp. Biol.* **107**, 189-217.
Cruse, H. (1990). What mechanisms coordinate leg movement in walking arthropods? *Trends Neurosci* **13**, 15-21.
Cruse, H., Dürr, V. and Schmitz, J. (2007). Insect walking is based on a decentralized architecture revealing a simple and robust controller. *Philos. Trans. R. Soc. A Math. Phys. Eng. Sci.* **365**, 221-250.
Delcomyn, F. (1971). The locomotion of the cockroach *Periplaneta americana*. *J. Exp. Biol.* **54**, 443-452.
Dürr, V. (2005). Context-dependent changes in strength and efficacy of leg coordination mechanisms. *J. Exp. Biol.* **208**, 2253-2267.
Grabowska, M., Godlewska, E., Schmidt, J. and Daun-Gruhn, S. (2012). Quadrupedal gaits in hexapod animals – inter-leg coordination in free-walking adult stick insects. *J. Exp. Biol.* **215**, 4255-4266.
Graham, D. (1972). A behavioural analysis of the temporal organisation of walking movements in the 1st instar and adult stick insect (*Carausius morosus*). *J. Comp. Physiol.* **81**, 23-52.
Graham, D. and Epstein, S. (1985). Behaviour and motor output for an insect walking on a slippery surface: II. Backward walking. *J. Exp. Biol.* **118**, 287-296.
Hanski, I. and Cambefort, Y. (2014). *Dung Beetle Ecology*. Princeton, NJ: Princeton University Press.
Hughes, G. M. (1952). The co-ordination of insect movements in the walking movements of insects. *J. Exp. Biol.* **29**, 267-285.
Jeck, T. and Cruse, H. (2007). Walking in *Aretaon asperrimus*. *J. Insect Physiol.* **53**, 724-733.
Marshall, N. J. and Diebel, C. (1995). 'Deep-sea spiders' that walk through the water. *J. Exp. Biol.* **198**, 1371-1379.

Journal of Experimental Biology (2016) 219, 2110-2118 doi:10.1242/jeb.137778

Mendes, C. S., Bartos, I., Akay, T., Márka, S. and Mann, R. S. (2013). Quantification of gait parameters in freely walking wild type and sensory deprived *Drosophila melanogaster*. *eLife* **2**, e00231.
Mendes, C. S., Rajendren, S. V., Bartos, I., Márka, S. and Mann, R. S. (2014). Kinematic responses to changes in walking orientation and gravitational load in *Drosophila melanogaster*. *PLoS ONE* **9**, e109204.
Pfeffer, E. S. and Wittlinger, M. (2016). How to find home backwards? Navigation during rearward homing of *Cataglyphis fortis* desert ants. *J. Exp. Biol.* **219**, 2119-2126.
Reinhardt, L. and Blickhan, R. (2014). Level locomotion in wood ants: evidence for grounded running. *J. Exp. Biol.* **217**, 2358-2370.
Ritzmann, R. and Zill, S. N. (2013). Neuroethology of insect walking. *Scholarpedia* **8**, 30879.
Schilling, M., Hoinville, T., Schmitz, J. and Cruse, H. (2013). Walknet, a bio-inspired controller for hexapod walking. *Biol. Cybern.* **107**, 397-419.
Seidl, T. and Wehner, R. (2008). Walking on inclines: how do desert ants monitor slope and step length. *Front. Zool.* **5**, 8.
Sleinis, S. and Silvey, G. E. (1980). Locomotion in a forward walking crab. *J. Comp. Physiol. A* **136**, 301-312.
Ting, L. H., Blickhan, R. and Full, R. J. (1994). Dynamic and static stability in hexapedal runners. *J. Exp. Biol.* **197**, 251-269.
Wahl, V., Pfeffer, S. E. and Wittlinger, M. (2015). Walking and running in the desert ant *Cataglyphis fortis*. *J. Comp. Physiol. A* **201**, 645-656.
Wilson, D. M. (1966). Insect walking. *Annu. Rev. Entomol.* **11**, 103-122.
Wittlinger, M. and Wolf, H. (2013). Homing distance in desert ants, *Cataglyphis fortis*, remains unaffected by disturbance of walking behaviour and visual input. *J. Physiol.* **107**, 130-136.
Wosnitza, A., Bockemühl, T., Dübbert, M., Scholz, H. and Büschges, A. (2013). Inter-leg coordination in the control of walking speed in *Drosophila*. *J. Exp. Biol.* **216**, 480-491.
Zollikofer, C. (1994a). Stepping patterns in ants – influence of speed and curvature. *J. Exp. Biol.* **192**, 95-106.
Zollikofer, C. (1994b). Stepping patterns in ants – influence of load. *J. Exp. Biol.* **192**, 119-127.

Journal of Experimental Biology 219: doi:10.1242/jeb.137778: Supplementary information

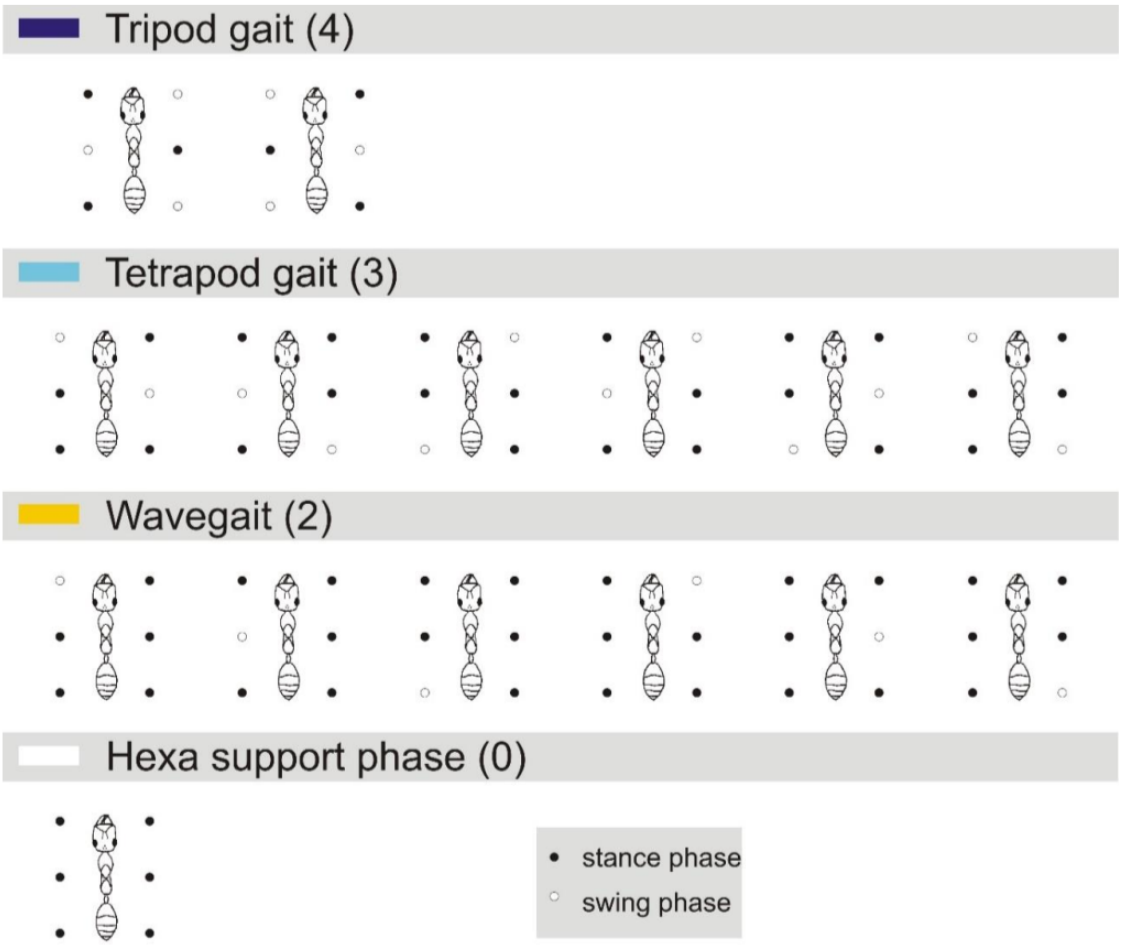

Fig. S1. Different leg combinations assigned to different gait patterns.

In hexapods, several leg coordination patterns (gaits) are known that rhythmically emerge during locomotion. The current understanding is that the different gait patterns are part of a continuum with a continuous transition from tripod to tetrapod to wavegait coordination with decreasing walking speed (Wilson 1966, Schilling et al. 2013). Further, it is plausible that also within one gait type during the transition between one coupled leg group to the next, deviant leg combinations emerge to avoid jerky and abrupt movements. This also means that the different gaits are sometimes difficult to distinguish. Nevertheless, the classification of distinct gaits is a very helpful concept for the analysis of locomotion. In simple terms, we can define a tripod gait where three legs, a tetrapod gait where four legs, and a wavegait where five legs

Journal of Experimental Biology • Supplementary information

Journal of Experimental Biology 219: doi:10.1242/jeb.137778: Supplementary information

engage simultaneously in stance phase, while the other legs are in swing. We analysed the stepping within a temporal context by assigning each frame a number and a colour according to the present leg combination as it is shown in this figure. If none of the listed leg combinations could be found, the frame was classified as 'undefined' and respectively the leg pattern is shown in the next figure (S2). This method is useful to illustrate leg combinations over time, but as well to quantify the different gait patterns and to further evaluate the ants' stepping behaviour.

Journal of Experimental Biology • Supplementary information

Journal of Experimental Biology 219: doi:10.1242/jeb.137778: Supplementary information

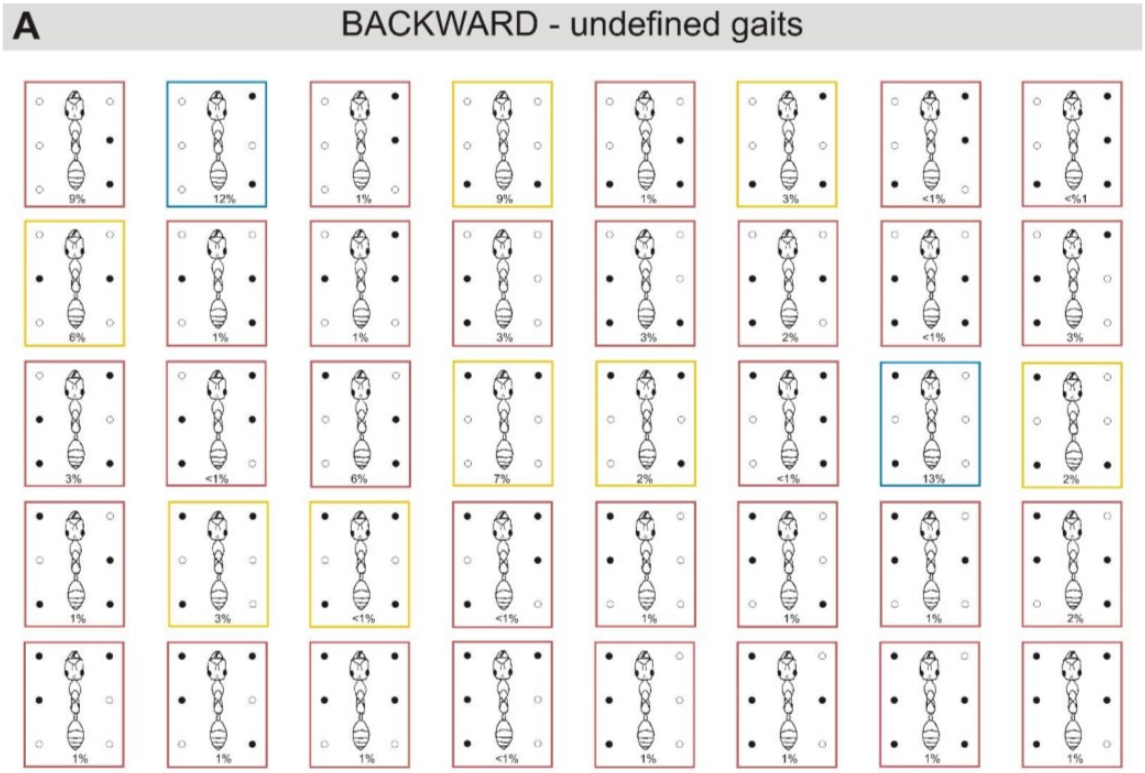

C VALIDITY OF RULE 1

		Invalidity of rule 1 *ipsilateral*	Invalidity of rule 1 *contralateral*	Validity of rule 1 *ipsi- and contralateral*
BACKWARD	Proportion of *undefined* frames	44 %	30 %	26 %
	Proportion of *all* frames	14 %	10 %	8 %
FORWARD	Proportion of *undefined* frames	9 %	11 %	80 %
	Proportion of *all* frames	1 %	1 %	6 %

Journal of Experimental Biology • Supplementary information

Journal of Experimental Biology 219: doi:10.1242/jeb.137778: Supplementary information

Fig. S2. Undefined leg combinations.

Leg combinations that did not match with one of the ideal gait patterns as shown in figure S1 were classified as 'undefined' and are illustrated in this graph. The different leg combinations that occur during backward (Fig S2 A) and forward (Fig S2 B) locomotion are listed and quantified. The corresponding relative occurrence of each leg combination is indicated as percentage information below each ant.

We further analysed theses undefined leg combinations whether they are in conformance with Cruse's rule 1. This rule states that as long as a leg is in swing phase, it has an inhibitory influence on the anterior leg of the ipsilateral side. If one of the listed undefined leg combinations deviates from this rule we marked it with a *red frame*. Further studies suggests that Cruse's rule 1 might also be applicable to the contralateral leg (Dean and Wendler 1983). If an inhibitory effect to the contralateral leg was disregarded, we marked the respective leg combination with *a yellow frame*. A disregard of these rules (ipsilaterally or contralaterally) means an overlapping of swing movements of two adjacent legs and therefore a statically unstable leg combination. If rule 1 is fulfilled (ipsilaterally as well as contralaterally) the respective leg combination is indicated with a *blue frame*.

Most leg combinations that have been classified as 'undefined' deviate from either one of these rules (red and yellow frames), but their quantities differ noteworthy depending on the walking direction (Fig S2 C). Rearward walking can be characterized by a wide range of different types of leg combinations, where none is occurring in a clear majority. The undefined combinations that contradicts rule 1 either ipsilaterally or contralaterally (red and yellow frames) make up a percentage of 24% of all analysed frames, while during forward locomotion they account for only 2%. Nevertheless, the two leg combinations that do not contradict rule 1 (ipsilaterally and contralaterally, blue frames) make up 26% of the undefined combinations during backward locomotion. These two leg combinations are also found during forward locomotion, with a large proportion of 80% of all undefined leg combinations. These two combinations are representing an inchoate tripod coordination, missing the respective middle leg. They emerge during the transition between one tripod group (L1, R2, L3) to the next one (R1, L2, R3), where the middle legs are the last legs touching the ground (see phase plot analysis, Fig 3 B iii).

It should be noted that we applied the rule for this analysis in a deterministic manner. This means, for example, if one leg is in swing and its anterior or contralateral neighbour is also in

Journal of Experimental Biology • Supplementary information

Journal of Experimental Biology 219: doi:10.1242/jeb.137778: Supplementary information

swing phase we marked the respective leg combination as violation to Cruse's rule 1. The rules generally should not be considered as deterministic but rather stochastic (Dürr 2005). Hence, rule 1 does not strictly prevent, the lift-off of the anterior and contralateral neighbour. Rather it affects the likelihood of a stance-swing transition.

Journal of Experimental Biology • Supplementary information

Journal of Experimental Biology 219: doi:10.1242/jeb.137778: Supplementary information

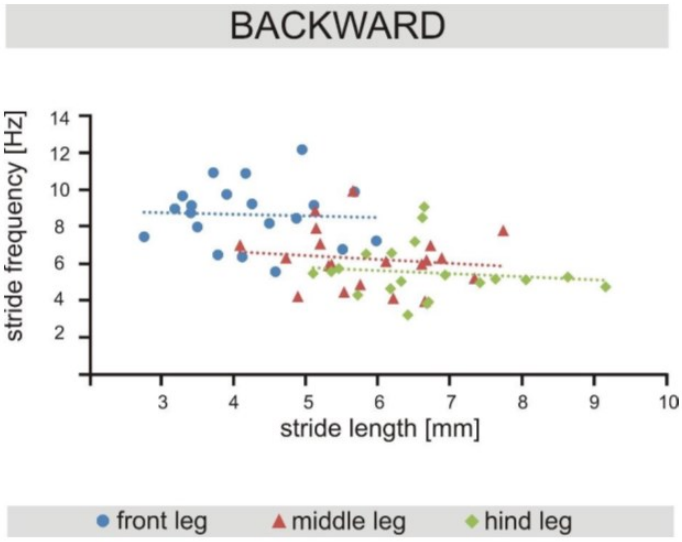

Fig. S3. Stride length versus stride frequency during backward and forward walking.

During backward walking stride length and stride frequency show no correlation. Note that the regression lines of the three leg pairs are separated in backward walks. This indicates a leg pair specific stepping specialisation, as already shown and discussed in our work.

The linear regression lines of front, middle and hind leg do not differ significantly in a multiple comparison regarding the slope and y-intercept (t-test for regression coefficient, $p<0.05$). Linear regressions for backward walking: front legs ($y=-0.09x +9.05$; $R^2=0.0023$), middle legs ($y=-0.21x + 7.48$; $R^2=0.0157$), hind legs ($y=-0.17 + 6.63$; $R^2=0.0148$).

Journal of Experimental Biology • Supplementary information

Journal of Experimental Biology 219: doi:10.1242/jeb.137778: Supplementary information

Video 1: Backward walking

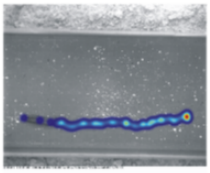

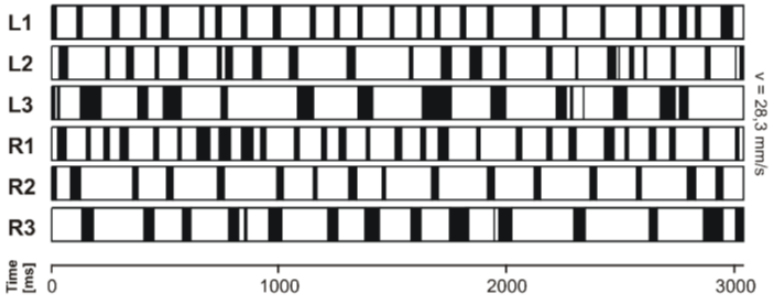

Video 2: Forward walking

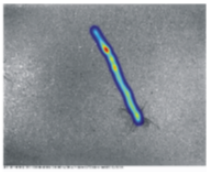

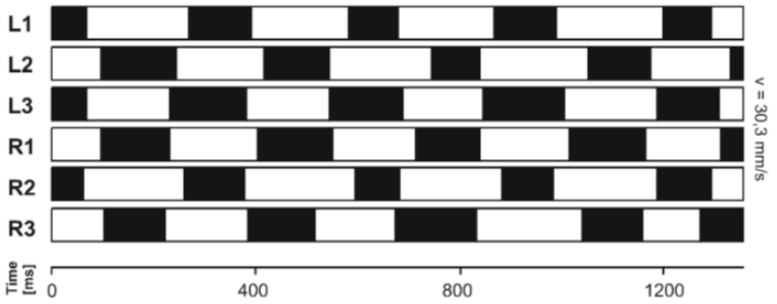

Video 3: Forward pulling

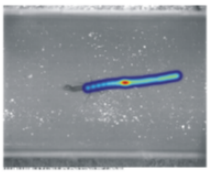

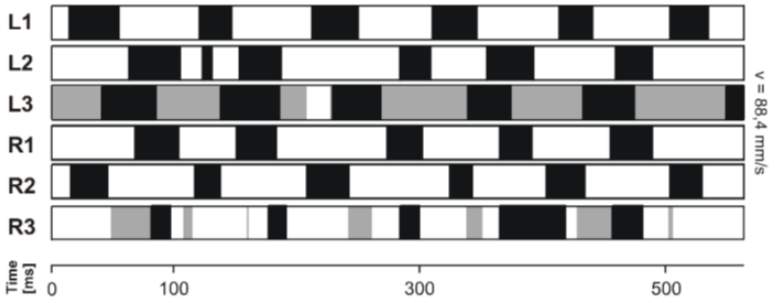

Video 4: Backward tripod-like coordination

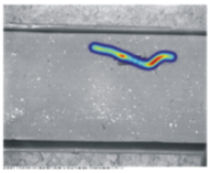

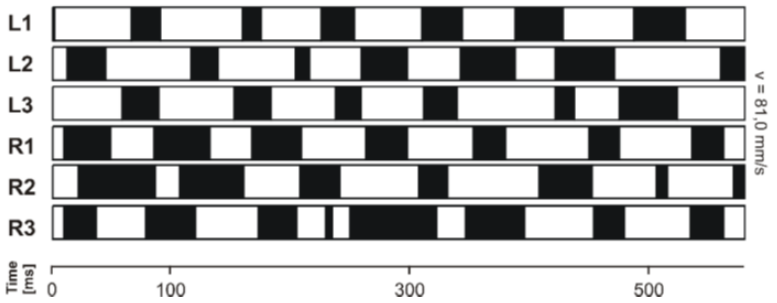

Journal of Experimental Biology • Supplementary information

Journal of Experimental Biology 219: doi:10.1242/jeb.137778: Supplementary information

Fig. S4. Overview of supplementary movies.

Heatmaps are shown on the left side, while the corresponding podograms are shown on the right side for each video. Heatmaps give an impression about the walking speed of the ant. The warmer the colour (from dark blue to dark red), the slower the motion. Dark blue shows highest walking speeds. Podograms give an overview of inter-leg coordination. Black bars represent swing phases, white bars stance phases and grey bars leg dragging (tarsus moving along the floor without lifting off). L, left; R, right; 1, 2, 3, front leg, middle and hind leg. The videos are shown with 16.7 times slow motion.

Journal of Experimental Biology • Supplementary information

Journal of Experimental Biology 219: doi:10.1242/jeb.137778: Supplementary information

Supplementary table 1. Linear regression functions and coefficients of determination (compare Fig. 4).

			Backward locomotion		Forward locomotion	
			linear regression formula	coefficient of determination	linear regression formula	coefficient of determination
A	stride length vs. walking speed	front	y = 0.0583x + 1.9617	R^2 = 0.5173	y = -0.0059x + 6.7386	R^2 = 0.0041
		middle	y = 0.0301x + 4.7375	R^2 = 0.1236	y = -0.0057x + 6.7401	R^2 = 0.0042
		hind	y = 0.0433x + 5.0196	R^2 = 0.2035	y = -0.0016x + 6.4333	R^2 = 0.0005
B	frequency vs. walking speed	front	y = 0.0855x + 5.3113	R^2 = 0.3127	y = 0.1217x + 1.331	R^2 = 0.6016
		middle	y = 0.1175x + 1.6271	R^2 = 0.6743	y = 0.1181x + 1.4614	R^2 = 0.617
		hind	y = 0.1015x + 1.5161	R^2 = 0.5877	y = 0.12x + 1.4469;	R^2 = 0.6314
C	swing speed vs. walking speed	front	y = 3.042x + 20.724	R^2 = 0.689	y = 1.4316x + 60.717	R^2 = 0.4376
		middle	y = 3.2678x + 58.231	R^2 = 0.3783	y = 2.2782x + 56.744	R^2 = 0.4003
		hind	y = 3.409x + 8.8227	R^2 = 0.5865	y = 1.289x + 48.329	R^2 = 0.4148
D	swing phase duration vs. walking speed	front	y = -0.0002x + 0.0378	R^2 = 0.0701	y = -0.0008x + 0.0903	R^2 = 0.2275
		middle	y = -0.0003x + 0.0465	R^2 = 0.1302	y = -0.0009x + 0.0877	R^2 = 0.2762
		hind	y = -0.0006x + 0.0765	R^2 = 0.0119	y = -0.001x + 0.1099	R^2 = 0.2753
E	stance phase duration vs. walking speed	front	y = -0.0015x + 0.1472	R^2 = 0.2075	y = -0.0032x + 0.2384	R^2 = 0.5892
		middle	y = -0.0024x + 0.2171	R^2 = 0.4691	y = -0.0031x + 0.2462	R^2 = 0.6011
		hind	y = -0.0023x + 0.2123	R^2 = 0.4438	y = -0.0028x + 0.2098	R^2 = 0.6098
F	cycle period duration vs. walking speed	front	y = -0.0017x + 0.187	R^2 = 0.55	y = -0.0039x + 0.3287	R^2 = 0.5342
		middle	y = -0.0025x + 0.2435	R^2 = 0.3178	y = -0.004x + 0.3339	R^2 = 0.5433
		hind	y = -0.0031x + 0.2919	R^2 = 0.5561	y = -0.0038x + 0.3197	R^2 = 0.5321

Journal of Experimental Biology • Supplementary information

Journal of Experimental Biology 219: doi:10.1242/jeb.137778: Supplementary information

Supplementary table 2. Modified index of straightness for stance- and swing envelopes shown in Fig. 2 A.

The table shows the values of the modified index of straightness (Batschelet, 1981) describing the tortuousness of each stance- and swing envelope illustrated in figure 2. The median at the end of the table includes all legs of the respective column.

	Backward locomotion		Forward locomotion	
	stance phase	swing phase	stance phase	swing phase
L1	0.85	0.49	0.90	0.75
L2	0.65	0.80	0.93	0.60
L3	0.87	0.14	0.88	0.58
L1	0.86	0.57	0.94	0.48
L2	0.48	0.11	0.89	0.46
L3	0.80	0.48	0.94	0.79
median	**0.82**	**0.49**	**0.92**	**0.59**

Supplementary table 3. Exact percentage values of the walking speed groups (I-V) shown in Fig. 3.

The summarized results for the colour index analysis (Fig 3 Bi) were categorized according to the ants' walking speed I. 23-35 mm/s; II. 35-45 mm/s; III. 45-55 mm/s; IV. 55-66 mm/s; E, Entire group. The values are rounded percentage information.

	Backward locomotion					Forward locomotion				
	I	II	III	IV	E	I	II	III	IV	E
Number of videos	10	4	4	2	20	11	2	3	4	20
Tripod	3	8	12	12	7	54	61	70	69	56
Tetrapod	14	19	21	21	18	10	6	4	5	9
Wavegait	38	27	32	30	34	17	13	9	3	16
Undefined gait	33	39	30	30	32	7	12	16	20	8
Hexa support phase	12	7	5	7	9	12	8	1	3	11

Journal of Experimental Biology 219: doi:10.1242/jeb.137778: Supplementary information

References

Batschelet, E. (1981). Circular Statistics in Biology. London: Academic Press.

Dean, J. and Wendler, G. (1983). Stick insect locomotion on a walking wheel: interleg coordination of leg position. *J. Exp. Biol.* **103**, 75-94.

Dürr, V. (2005). Context-dependent changes in strength and efficacy of leg coordination mechanisms. *J. Exp. Biol.* **208**, 2253-2267.

Schilling, M., Hoinville, T., Schmitz, J. and Cruse, H. (2013). Walknet, a bioinspired controller for hexapod walking. *Biol. Cybern.* **107**, 397-419.

Wilson, D. M. (1966). Insect walking. *Annu. Rev. Entomol*. **11**, 103-122.

Journal of Experimental Biology • Supplementary information

Journal of Experimental Biology 219: doi:10.1242/jeb.137778: Supplementary information

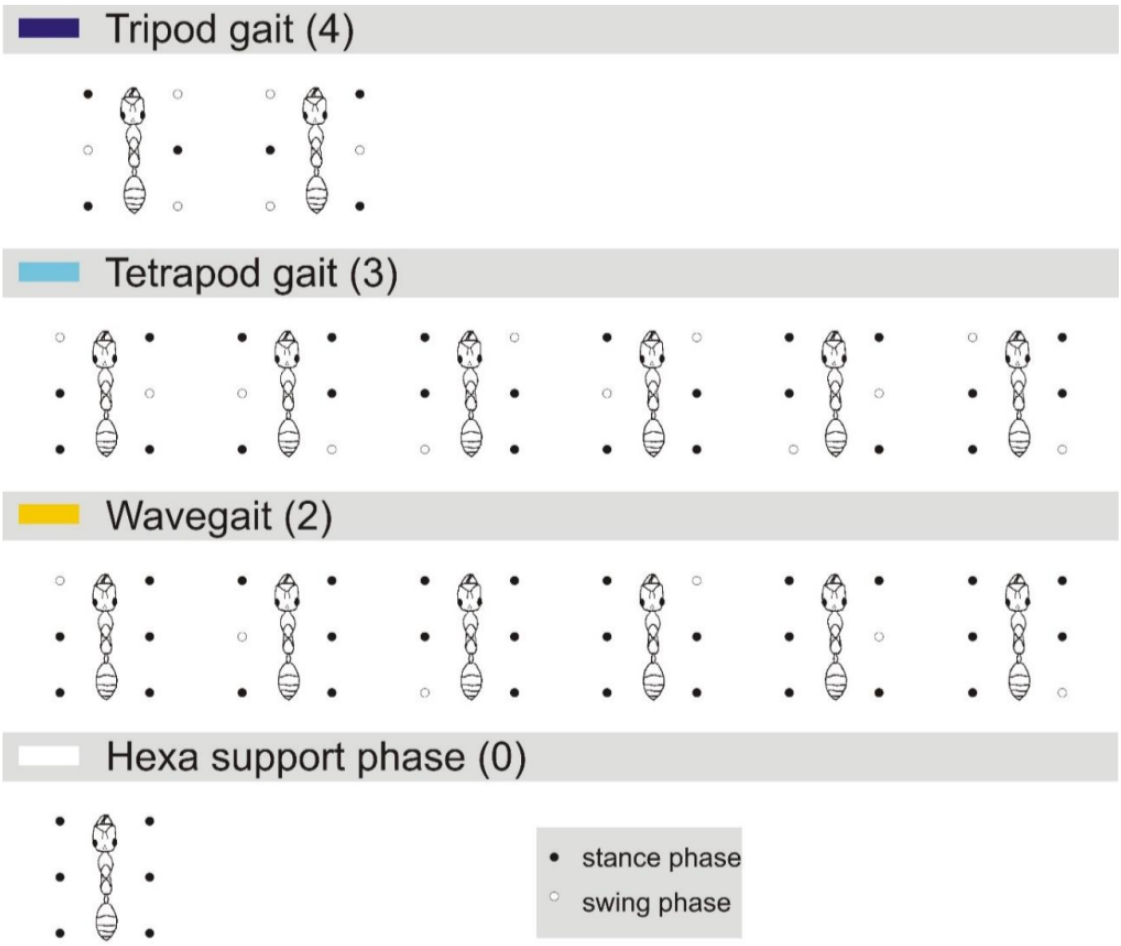

Fig. S1. Different leg combinations assigned to different gait patterns.

In hexapods, several leg coordination patterns (gaits) are known that rhythmically emerge during locomotion. The current understanding is that the different gait patterns are part of a continuum with a continuous transition from tripod to tetrapod to wavegait coordination with decreasing walking speed (Wilson 1966, Schilling et al. 2013). Further, it is plausible that also within one gait type during the transition between one coupled leg group to the next, deviant leg combinations emerge to avoid jerky and abrupt movements. This also means that the different gaits are sometimes difficult to distinguish. Nevertheless, the classification of distinct gaits is a very helpful concept for the analysis of locomotion. In simple terms, we can define a tripod gait where three legs, a tetrapod gait where four legs, and a wavegait where five legs

Journal of Experimental Biology • Supplementary information

Journal of Experimental Biology 219: doi:10.1242/jeb.137778: Supplementary information

engage simultaneously in stance phase, while the other legs are in swing. We analysed the stepping within a temporal context by assigning each frame a number and a colour according to the present leg combination as it is shown in this figure. If none of the listed leg combinations could be found, the frame was classified as 'undefined' and respectively the leg pattern is shown in the next figure (S2). This method is useful to illustrate leg combinations over time, but as well to quantify the different gait patterns and to further evaluate the ants' stepping behaviour.

Journal of Experimental Biology • Supplementary information

Journal of Experimental Biology 219: doi:10.1242/jeb.137778: Supplementary information

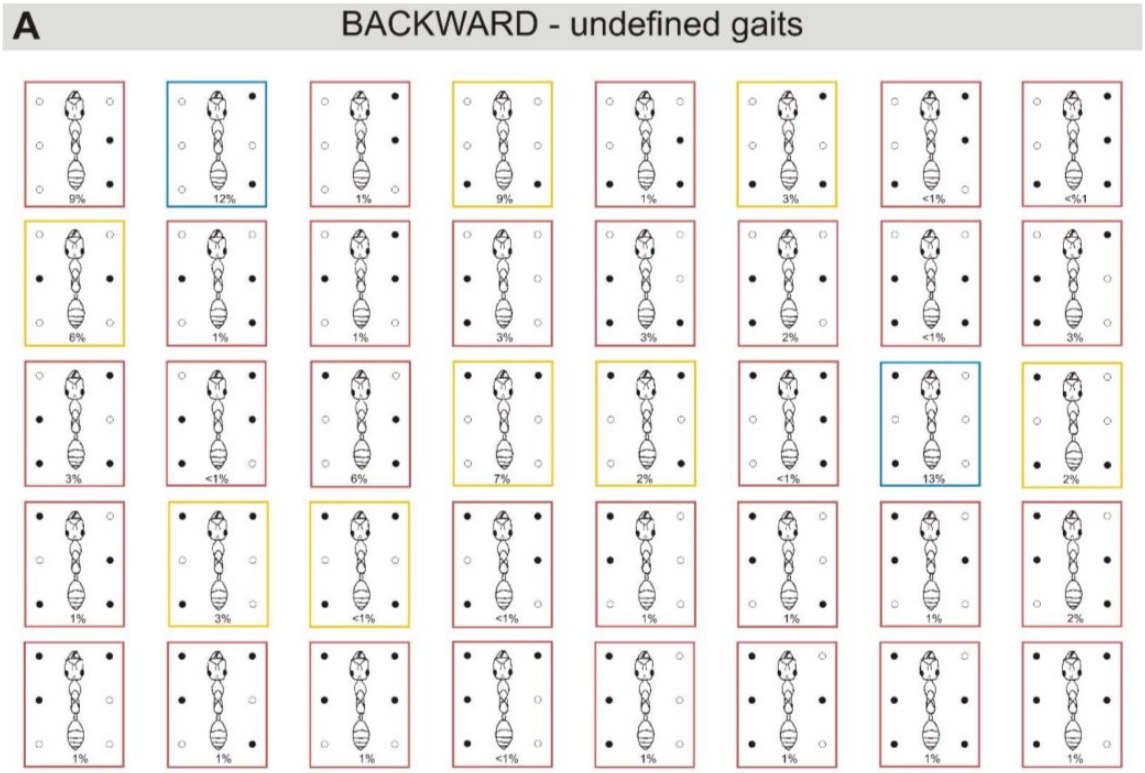

C VALIDITY OF RULE 1

		Invalidity of rule 1 *ipsilateral*	Invalidity of rule 1 *contralateral*	Validity of rule 1 *ipsi- and contralateral*
BACKWARD	Proportion of *undefined* frames	44 %	30 %	26 %
	Proportion of *all* frames	14 %	10 %	8 %
FORWARD	Proportion of *undefined* frames	9 %	11 %	80 %
	Proportion of *all* frames	1 %	1 %	6 %

Journal of Experimental Biology • Supplementary information

Journal of Experimental Biology 219: doi:10.1242/jeb.137778: Supplementary information

Fig. S2. Undefined leg combinations.

Leg combinations that did not match with one of the ideal gait patterns as shown in figure S1 were classified as 'undefined' and are illustrated in this graph. The different leg combinations that occur during backward (Fig S2 A) and forward (Fig S2 B) locomotion are listed and quantified. The corresponding relative occurrence of each leg combination is indicated as percentage information below each ant.

We further analysed theses undefined leg combinations whether they are in conformance with Cruse's rule 1. This rule states that as long as a leg is in swing phase, it has an inhibitory influence on the anterior leg of the ipsilateral side. If one of the listed undefined leg combinations deviates from this rule we marked it with a *red frame*. Further studies suggests that Cruse's rule 1 might also be applicable to the contralateral leg (Dean and Wendler 1983). If an inhibitory effect to the contralateral leg was disregarded, we marked the respective leg combination with *a yellow frame*. A disregard of these rules (ipsilaterally or contralaterally) means an overlapping of swing movements of two adjacent legs and therefore a statically unstable leg combination. If rule 1 is fulfilled (ipsilaterally as well as contralaterally) the respective leg combination is indicated with a *blue frame*.

Most leg combinations that have been classified as 'undefined' deviate from either one of these rules (red and yellow frames), but their quantities differ noteworthy depending on the walking direction (Fig S2 C). Rearward walking can be characterized by a wide range of different types of leg combinations, where none is occurring in a clear majority. The undefined combinations that contradicts rule 1 either ipsilaterally or contralaterally (red and yellow frames) make up a percentage of 24% of all analysed frames, while during forward locomotion they account for only 2%. Nevertheless, the two leg combinations that do not contradict rule 1 (ipsilaterally and contralaterally, blue frames) make up 26% of the undefined combinations during backward locomotion. These two leg combinations are also found during forward locomotion, with a large proportion of 80% of all undefined leg combinations. These two combinations are representing an inchoate tripod coordination, missing the respective middle leg. They emerge during the transition between one tripod group (L1, R2, L3) to the next one (R1, L2, R3), where the middle legs are the last legs touching the ground (see phase plot analysis, Fig 3 B iii).

It should be noted that we applied the rule for this analysis in a deterministic manner. This means, for example, if one leg is in swing and its anterior or contralateral neighbour is also in

Journal of Experimental Biology • Supplementary information

Journal of Experimental Biology 219: doi:10.1242/jeb.137778: Supplementary information

swing phase we marked the respective leg combination as violation to Cruse's rule 1. The rules generally should not be considered as deterministic but rather stochastic (Dürr 2005). Hence, rule 1 does not strictly prevent, the lift-off of the anterior and contralateral neighbour. Rather it affects the likelihood of a stance-swing transition.

Journal of Experimental Biology • Supplementary information

Journal of Experimental Biology 219: doi:10.1242/jeb.137778: Supplementary information

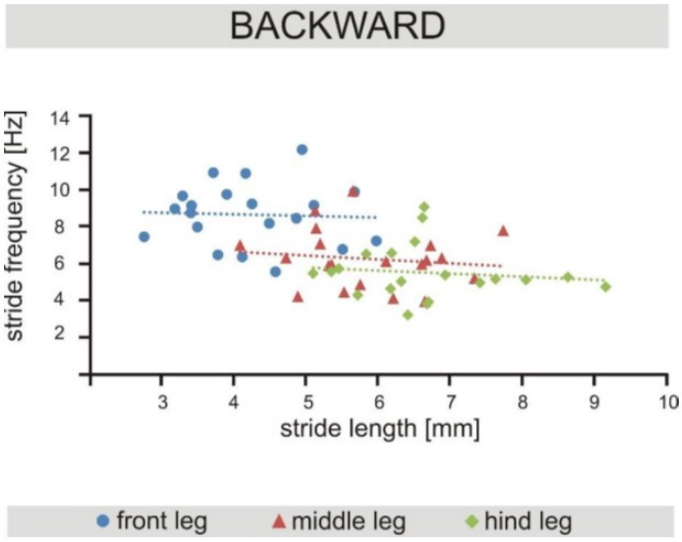

Fig. S3. Stride length versus stride frequency during backward and forward walking.

During backward walking stride length and stride frequency show no correlation. Note that the regression lines of the three leg pairs are separated in backward walks. This indicates a leg pair specific stepping specialisation, as already shown and discussed in our work.

The linear regression lines of front, middle and hind leg do not differ significantly in a multiple comparison regarding the slope and y-intercept (t-test for regression coefficient, $p<0.05$). Linear regressions for backward walking: front legs ($y=-0.09x +9.05$; $R^2=0.0023$), middle legs ($y=-0.21x + 7.48$; $R^2=0.0157$), hind legs ($y=-0.17 + 6.63$; $R^2=0.0148$).

Journal of Experimental Biology • Supplementary information

Journal of Experimental Biology 219: doi:10.1242/jeb.137778: Supplementary information

Video 1: Backward walking

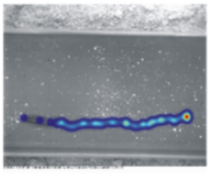

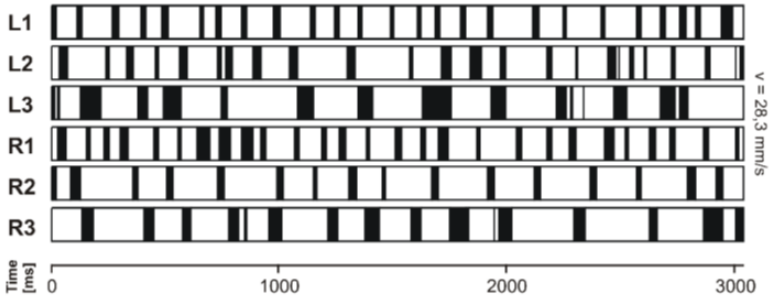

Video 2: Forward walking

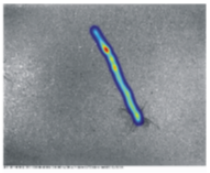

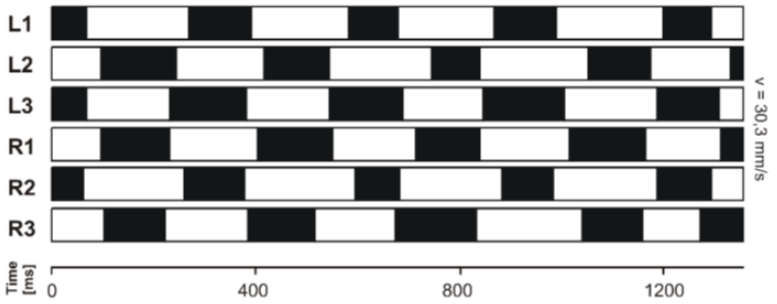

Video 3: Forward pulling

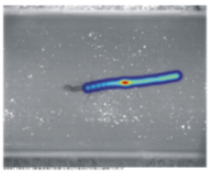

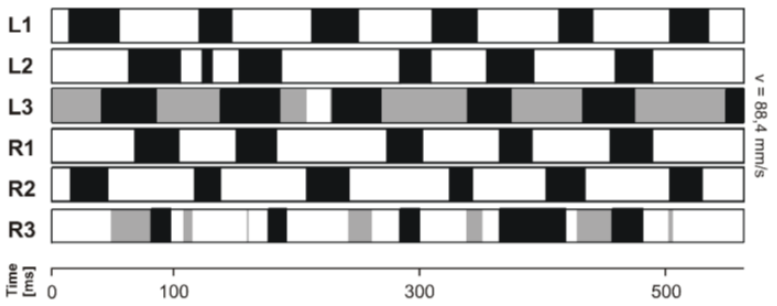

Video 4: Backward tripod-like coordination

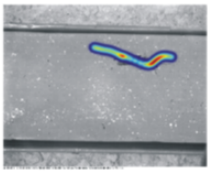

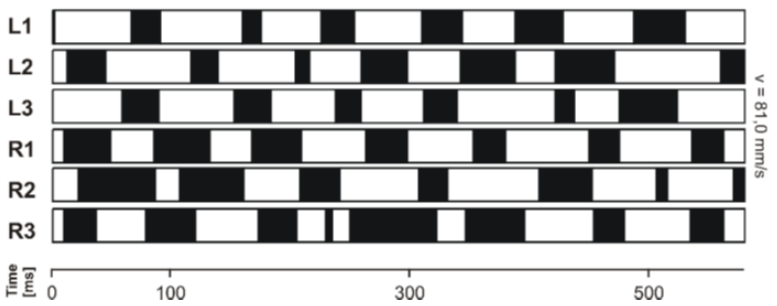

Journal of Experimental Biology • Supplementary information

Journal of Experimental Biology 219: doi:10.1242/jeb.137778: Supplementary information

Fig. S4. Overview of supplementary movies.

Heatmaps are shown on the left side, while the corresponding podograms are shown on the right side for each video. Heatmaps give an impression about the walking speed of the ant. The warmer the colour (from dark blue to dark red), the slower the motion. Dark blue shows highest walking speeds. Podograms give an overview of inter-leg coordination. Black bars represent swing phases, white bars stance phases and grey bars leg dragging (tarsus moving along the floor without lifting off). L, left; R, right; 1, 2, 3, front leg, middle and hind leg. The videos are shown with 16.7 times slow motion.

Journal of Experimental Biology • Supplementary information

Journal of Experimental Biology 219: doi:10.1242/jeb.137778: Supplementary information

Supplementary table 1. Linear regression functions and coefficients of determination
(compare Fig. 4).

			Backward locomotion		Forward locomotion	
			linear regression formula	coefficient of determination	linear regression formula	coefficient of determination
A	stride length vs. walking speed	front	y = 0.0583x + 1.9617	R^2 = 0.5173	y = -0.0059x + 6.7386	R^2 = 0.0041
		middle	y = 0.0301x + 4.7375	R^2 = 0.1236	y = -0.0057x + 6.7401	R^2 = 0.0042
		hind	y = 0.0433x + 5.0196	R^2 = 0.2035	y = -0.0016x + 6.4333	R^2 = 0.0005
B	frequency vs. walking speed	front	y = 0.0855x + 5.3113	R^2 = 0.3127	y = 0.1217x + 1.331	R^2 = 0.6016
		middle	y = 0.1175x + 1.6271	R^2 = 0.6743	y = 0.1181x + 1.4614	R^2 = 0.617
		hind	y = 0.1015x + 1.5161	R^2 = 0.5877	y = 0.12x + 1.4469;	R^2 = 0.6314
C	swing speed vs. walking speed	front	y = 3.042x + 20.724	R^2 = 0.689	y = 1.4316x + 60.717	R^2 = 0.4376
		middle	y = 3.2678x + 58.231	R^2 = 0.3783	y = 2.2782x + 56.744	R^2 = 0.4003
		hind	y = 3.409x + 8.8227	R^2 = 0.5865	y = 1.289x + 48.329	R^2 = 0.4148
D	swing phase duration vs. walking speed	front	y = -0.0002x + 0.0378	R^2 = 0.0701	y = -0.0008x + 0.0903	R^2 = 0.2275
		middle	y = -0.0003x + 0.0465	R^2 = 0.1302	y = -0.0009x + 0.0877	R^2 = 0.2762
		hind	y = -0.0006x + 0.0765	R^2 = 0.0119	y = -0.001x + 0.1099	R^2 = 0.2753
E	stance phase duration vs. walking speed	front	y = -0.0015x + 0.1472	R^2 = 0.2075	y = -0.0032x + 0.2384	R^2 = 0.5892
		middle	y = -0.0024x + 0.2171	R^2 = 0.4691	y = -0.0031x + 0.2462	R^2 = 0.6011
		hind	y = -0.0023x + 0.2123	R^2 = 0.4438	y = -0.0028x + 0.2098	R^2 = 0.6098
F	cycle period duration vs. walking speed	front	y = -0.0017x + 0.187	R^2 = 0.55	y = -0.0039x + 0.3287	R^2 = 0.5342
		middle	y = -0.0025x + 0.2435	R^2 = 0.3178	y = -0.004x + 0.3339	R^2 = 0.5433
		hind	y = -0.0031x + 0.2919	R^2 = 0.5561	y = -0.0038x + 0.3197	R^2 = 0.5321

Journal of Experimental Biology • Supplementary information

Journal of Experimental Biology 219: doi:10.1242/jeb.137778: Supplementary information

Supplementary table 2. Modified index of straightness for stance- and swing envelopes shown in Fig. 2 A.

The table shows the values of the modified index of straightness (Batschelet, 1981) describing the tortuousness of each stance- and swing envelope illustrated in figure 2. The median at the end of the table includes all legs of the respective column.

	Backward locomotion		Forward locomotion	
	stance phase	swing phase	stance phase	swing phase
L1	0.85	0.49	0.90	0.75
L2	0.65	0.80	0.93	0.60
L3	0.87	0.14	0.88	0.58
L1	0.86	0.57	0.94	0.48
L2	0.48	0.11	0.89	0.46
L3	0.80	0.48	0.94	0.79
median	**0.82**	**0.49**	**0.92**	**0.59**

Supplementary table 3. Exact percentage values of the walking speed groups (I-V) shown in Fig. 3.

The summarized results for the colour index analysis (Fig 3 Bi) were categorized according to the ants' walking speed I. 23-35 mm/s; II. 35-45 mm/s; III. 45-55 mm/s; IV. 55-66 mm/s; E, Entire group. The values are rounded percentage information.

	Backward locomotion					Forward locomotion				
	I	II	III	IV	E	I	II	III	IV	E
Number of videos	10	4	4	2	20	11	2	3	4	20
Tripod	3	8	12	12	7	54	61	70	69	56
Tetrapod	14	19	21	21	18	10	6	4	5	9
Wavegait	38	27	32	30	34	17	13	9	3	16
Undefined gait	33	39	30	30	32	7	12	16	20	8
Hexa support phase	12	7	5	7	9	12	8	1	3	11

Journal of Experimental Biology 219: doi:10.1242/jeb.137778: Supplementary information

References

Batschelet, E. (1981). Circular Statistics in Biology. London: Academic Press.

Dean, J. and Wendler, G. (1983). Stick insect locomotion on a walking wheel: interleg coordination of leg position. *J. Exp. Biol.* **103**, 75-94.

Dürr, V. (2005). Context-dependent changes in strength and efficacy of leg coordination mechanisms. *J. Exp. Biol.* **208**, 2253-2267.

Schilling, M., Hoinville, T., Schmitz, J. and Cruse, H. (2013). Walknet, a bioinspired controller for hexapod walking. *Biol. Cybern.* **107**, 397-419.

Wilson, D. M. (1966). Insect walking. *Annu. Rev. Entomol*. **11**, 103-122.

Journal of Experimental Biology • Supplementary information

Kapitel 6

6. Manuscript 4

High speed and high frequency locomotion in the Saharan silver ant Cataglyphis bombycina

Verena Luisa Wahl[1], Sarah Elisabeth Pfeffer[1] and Matthias Wittlinger[1,2]

[1] Institute of Neurobiology, Ulm University, Helmholtzstraße 10/1, 89081 Ulm, Germany

[2] Institute of Biology I, University of Freiburg, Hauptstr. 1, 79104 Freiburg, Germany

This pre-manuscript is prepared for Submission. To avoid infringements of copyrights, the manuscript is not reprinted in this electronic version.

ABSTRACT

The diurnal, thermophilic Saharan silver ant, *Cataglyphis bombycina*, known as the fastest of all *Cataglyphis* desert ant species, is, with respect to body size, probably one of the fastest running animals on the planet. These highly mobile and swiftly manoeuvring ants challenge the extreme temperatures of the sand dune environment that they inhabit with outstanding morphological (Shi et al. 2016) and behavioural adaptations (Wehner et al. 1992). Although *C. bombycina* lives in a similar hot and dry habitat as its well-studied sister species, the navigational model organism *Cataglyphis fortis*, it has comparatively shorter legs. In this account we show, how, although equipped with relatively short legs, *C. bombycina* employs a different strategy in reaching high running speeds that even outperform the fastest known runs of *C. fortis* ants. Here we present a detailed analysis of walking kinematics across a large range of walking and running speeds. Stride length and stride amplitude increase linearly with walking speed, whereas the stride frequency levels off at a maximum of around 40 Hz. In contrast to *C. fortis* with increasing walking speed the duty factor falls below 0.5 even before the appearance of a frequency plateau. From speeds of 120 mms^{-1} on the stance phase is reduced to a minimum of 7 ms and the ants show aerial phases. *C. bombycina* ants lift up all three legs of one tripod from the ground in synchrony and show a consistent tripod coordination, with a TCS of around 0.8, over the entire walking speed range.

KEY WORDS *Cataglyphis* desert ant, stepping pattern, Inter-leg coordination, gait, aerial phases

Danksagung

Da die vorliegende Doktorarbeit ohne die Unterstützung zahlreicher Personen nicht möglich gewesen wäre, möchte ich hier die Gelegenheit nutzen, mich bei einigen Personen zu bedanken.

Ein besonderer Dank gilt Prof. Dr. Harald Wolf für die Ermöglichung dieser Doktorarbeit in der Neurobiologie der Universität Ulm. Ich danke Dir für die ständige Hilfs- und Diskussionsbereitschaft während der gesamten Zeit. Du hattest immer ein offenes Ohr für Fragen und Anregungen und warst ein großartiger Chef. Ich danke Dir auch herzlich für das Vertrauen, zusammen mit Sarah das Projekt in Tunesien in unserem letzten Jahr selbstständig planen und leiten zu dürfen.

Mein ganz besonderer Dank gilt Dr. Matthias Wittlinger für die Betreuung dieser Doktorarbeit. Mit Deiner Begeisterung für die Wüstenameisen und deren Navigationskünste hast Du mich angesteckt. Durch meine Abschlussarbeit und den darauffolgenden Tunesien-Exkursionen durfte auch ich Teil der Ameisenforschung werden. Die tolle Zusammenarbeit, die unschätzbare Hilfe und die vielen anregenden Diskussionen haben maßgeblich zum Gelingen dieser Doktorarbeit beigetragen.

Außerdem gilt mein großer Dank Prof. Dr. Manfred Ayasse für die Übernahme des Zweitgutachtens meiner Doktorarbeit.

Ein herzlicher Dank geht an Sarah Pfeffer für die vielen hilfreichen Gespräche und Diskussionen. Ich danke Dir für die tolle Zeit, die wir gemeinsam erleben durften auf dem Dach der Uni, in Tunesien oder in Ulm in unserem gemeinsamen Büro. Ohne Dich wäre die Zeit nur halb so schön gewesen.

Ich danke Dr. Hansjürgen Dahmen für die tolle und beeindruckende Zusammenarbeit. Du hast mich in zahlreichen Diskussionen an Deiner großen Erfahrung, Deinem umfangreichen Wissen und vor allem Deiner großen Begeisterung für die Kugelapparaturen teilhaben lassen.

Ein großer Dank geht an Ursula Seifert, die Sekretärin und die ‚Gute Seele' des Institutes, für die Hilfe bei der Organisation der Auslandsreisen, für das Korrekturlesen vieler Manuskripte und für so viele Kleinigkeiten, die ich gar nicht alle aufzählen kann. Danke Dir, ohne Dich wäre die Neurobio nicht das, was sie ist.

Ich danke allen Abteilungsmitgliedern der Neurobiologie für die familiäre Atmosphäre und die tolle Stimmung bei den Mittagessen. Mein besonderer Dank gilt Dr. Andrea Wirmer für die Hilfe in statistischen Fragen und Alexander Lindt, Andrea Kubitz, PD Dr. Stefan Jarau und Dr. Wolfgang Mader für hilfreiches Feedback und die Hilfe bei vielen kleinen Problemen.

Außerdem bedanke ich mich bei allen Mitgliedern der Arbeitsgruppen von Jena, Berlin, Würzburg und Sussex für die fachlichen Diskussionen und aber auch für die vielen Grillabende, die wir in Tunesien gemeinsam verbringen durften. Auch den Helfern gilt mein großer Dank.

Auch möchte ich der Tunesischen Republik für die Möglichkeit danken, unsere Feldarbeit in der tollen Landschaft des Landes durchführen zu dürfen. Ich danke auch den Bewohnern von Maharès und Douz für jegliche Gastfreundschaft und die tollen Erfahrungen bei Hochzeiten oder Abendessen.

Ich möchte mich bei Lisa Haug und Silvia Wahl nicht nur fürs Korrekturlesen, sondern auch für den Rückhalt und die Verlässlichkeit bedanken. Danke, dass es Euch gibt.

Und natürlich gilt nicht zuletzt mein herzlicher Dank meiner Familie und meinen Freunden für jegliche Unterstützung und den unerschütterlichen Glauben an mich.

Lebenslauf

Der Lebenslauf wurde aus Gründen des Datenschutzes entfernt.

Der Lebenslauf wurde aus Gründen des Datenschutzes entfernt.

Teile dieser Dissertation wurden bereits in folgenden Fachzeitschriften veröffentlicht:

Dahmen, H., Wahl, V. L., Pfeffer, S. E., Mallot, H. A., & Wittlinger, M. **(2017).**
Naturalistic path integration of Cataglyphis desert ants on an air-cushioned lightweight spherical treadmill.
Journal of Experimental Biology, 220(4), 634-644.
doi: 10.1242/jeb.148213
http://jeb.biologists.org/content/220/4/634

Pfeffer, S. E., Wahl, V.L. & Wittlinger, M**. (2016).**
How to find home backwards? Locomotion and inter-leg coordination during rearward walking of Cataglyphis fortis desert ants
Journal of Experimental Biology, 219(14), 2110-2118
doi: 10.1242/jeb.137778
http://jeb.biologists.org/lookup/doi/10.1242/jeb.137778

Wahl, V., Pfeffer, S. E., & Wittlinger, M. **(2015).**
Walking and running in the desert ant Cataglyphis fortis
Journal of Comparative Physiology A, 201(6), 645-656
doi: 10.1007/s00359-015-0999-2
http://link.springer.com/article/10.1007/s00359-015-0999-2

WISSENSCHAFTLICHE VORTRÄGE

Wolf H, Wahl V, Wittlinger M **(2013).**
Gait parameters at different walking speeds in the desert ant, *Cataglyphis fortis*
106th Annual Meeting of the German Zoological Society, 13.09.-16.09.13, München, Germany

Wahl VL, Dahmen H, Pfeffer SE, Wittlinger M **(2016).**
Virtual navigation in *Cataglyphis* desert ants – path integration on an air suspended spherical treadmill.
XII International Congress of Neuroethology, 30.03.-03.04.16, Montevideo, Uruguay

Eidesstattliche Erklärung

Ich versichere hiermit, dass ich die Arbeit selbstständig angefertigt habe und keine anderen als die angegebenen Quellen und Hilfsmittel benutz sowie die wörtlich oder inhaltlich übernommenen Stellen als solche kenntlich gemacht habe und die Satzung der Universität Ulm zur Sicherung guter wissenschaftlicher Praxis in der jeweils gültigen Fassung beachtet habe.

Ulm,

……

(Verena Luisa Wahl)